APPENDICES

Technical Memorandum: Puget Sound Nutrient Source Reduction Project Phase II - Optimization Scenarios (Year 1)

Table of Contents

Appendix A – Updates to Freshwater Inputs and Limitations 1
Appendix B – Watershed Flow Assessment 17
Appendix C – Changes to Reference Organic Carbon 26
Appendix D – HYCOM Ocean Boundary 28
Appendix E – Scenario 4 Methods 40
Appendix F – DO Assessment of Water Quality Standard 48
Appendix G – Additional Results Tables and Figures 51
Appendix H – Water Quality Binders 67
References 68
Acronyms 71

Appendix A – Updates to Freshwater Inputs and Limitations

The following updates were made to the freshwater inflows to the Salish Sea Model (SSM) for the Optimization Scenarios.

Water quality regression updates for watersheds

- For Optimization Scenarios involving model year 2014 runs, we used updated regressions (based on an expanded 2006–2018 dataset downloaded from Ecology's Environmental Information Management database) to estimate daily concentrations for water quality parameters. Table A1 lists these updates, including a comparison of the date range and number of data points available for the original regressions and for the updated regressions. Due to the low number of available data for certain parameters, regressions were fit using the full range of available data in lieu of setting aside a portion of data for testing how well the regressions generalize to years in which it has not been trained on. For model year 2014, the new regressions generally were able to explain a greater proportion of variance in the data for different parameters than the previously used regressions (Table A2.)
- Several watersheds, particularly in South Sound, did not have newer data. However, the USGS flow values used in the original 2006-2007 water quality regressions were at that time preliminary in nature for some locations, including Chambers Creek, Goldsborough Creek, McAllister Creek, McLane Creek, and Woodard Creek. Flow for these locations were updated with quality-assured flow values from EIM. In a few instances, previously used flow values were rejected in the subsequent QA process, and in those cases, the gaps were filled by scaling nearby USGS gauged flow to the sample location. When we updated regressions for model year 2014, revisions to flows for several non-long term monitoring stations resulted in changes to the regressions for these locations.

- Changes to regressions for all stations includes: retention of outliers for DOC which were previously dropped and removal of data now flagged as rejected in EIM, the latter of which rarely occurred. Additionally, variables such as POC were calculated by taking the difference of TOC and DOC, which in some cases resulted in negative values. Previously negative POC values were replaced with the detection limit (0.001 mg/L), however, in the updated regressions negative POC values were replaced with the minimum non-negative value for the given station (generally 0.1 mg/L).
- The updated regressions were used to modify reference DOC and POC concentrations for many US inflows except lakes. For more details on changes to organic carbon reference conditions, refer to Appendix C.
- For Optimization Scenarios involving model year 2006, we still used the original regressions centered on data collected during 2006 and 2007 except for organic carbon, in some cases, as described below. In the original datasets, many rivers did not have any organic carbon data and were characterized in the model by constant year-round concentrations of DOC and POC based on the median of data collected in other Puget Sound rivers (Mohamedali et al., 2011). Since then, sufficient organic carbon data were collected at the following rivers: Duckabush, Nooksack, Samish, Snohomish and Stillaguamish. For these rivers, the updated WQ regressions for DOC and POC developed for year 2014 scenarios were also applied to model year 2006 scenarios in place of constant year-round concentrations. Table A3 lists these rivers as well as all the watersheds that are associated with the WQ regressions for these rivers which now all have time-varying DOC and POC concentrations.
- Previously constant values meant that existing organic carbon loads were equal to reference organic carbon loads for the inflows in Table A3 (which are calculated as the 10^{th} percentile or 50^{th} percentile of the existing time-series, depending on the region). These updates mean that these rivers now do have an estimated anthropogenic organic carbon load.
- In general, unmonitored freshwater inflows that do not have water quality data are associated with regressions developed for neighboring or adjacent watersheds. For Optimization Scenarios, we updated some of these associations (i.e., we changed which watershed regression was applied to unmonitored inflows for all parameters or just for DOC and POC). These changes are listed in Table A4.
- Previously, the Lake Cushman inflow to Hood Canal (downstream of the hydroelectric dam) had an estimated reference condition. For the Optimization Scenarios, reference concentrations for the Lake Cushman inflow were set to equal existing concentrations in order to consistently apply reference conditions to water bodies with significant hydraulic modifications for which explicit reference condition determinations have not been made. For the same reason, Lake Washington's reference inflow concentrations are also set equal to existing.

Table A1. Comparison of date range and number of samples used to fit new and old regressions.

Stations without additional data following the initial regression timeline (2006-2007) were not included in this table but are listed in (Mohamedali et al. 2011).

River Regression	Variable	Old Regression - Date Range of Data Used	Old Regression -N	New Regression - Date Range of Data Used	New Regression – N
Big Beef Creek	NH4	08/2006-10/2007	15	08/2006 -9/2011	62
Big Beef Creek	NO23	08/2006-10/2007	15	08/2006 -9/2011	62
Big Beef Creek	OP	08/2006-10/2007	15	08/2006 -9/2011	62
Big Beef Creek	TP	08/2006-10/2007	15	08/2006 -9/2011	62
Big Beef Creek	TPN	08/2006-10/2007	15	08/2006 -9/2011	62
Vancouver Island S.	NH4	*	*	11/2007-12/2018	232
Vancouver Island S.	DOC	*	*	05/2012-12/2018	171
Vancouver Island S.	NO23	*	*	09/2006-12/2018	276
Vancouver Island S.	DTP	8/2006-10/2007	33	8/2006-12/2018	323
Vancouver Island S.	TP	8/2006-10/2007	33	8/2006-12/2018	315
Vancouver Island S.	TPN	*	*	09/2007-12/2018	261
Vancouver Island S.	DTPN	9/2006-10/2007	30	9/2006-10/2018	320
Deschutes R.	NH4	8/2006-10/2007	15	08/2006-12/2018	149
Deschutes R.	DOC	8/2006-10/2007	15	08/2006-10/2007, 2010(2 mo), 2011(4 mo), 10/2017-12/2018	36
Deschutes R.	POC[2]	8/2006-10/2007	15	08/2006-10/2007, 2010(2 mo), 2011(4 mo), 10/2017-12/2018	33
Deschutes R.	NO23	8/2006-10/2007	15	08/2006-12/2018	475
Deschutes R.	OP	8/2006-10/2007	15	08/2006-12/2018	148
Deschutes R.	DTP	8/2006-10/2007	15	08/2006-10/2007	15
Deschutes R.	TP	8/2006-10/2007	15	08/2006-12/2018	149
Deschutes R.	DTPN	8/2006-10/2007	15	08/2006-10/2007, 07/2009-10/2009	19
Deschutes R.	TPN	8/2006-10/2007	15	08/2006-12/2018	150
Duckabush R.	NH4	8/2006-10/2007	15	08/2006-12/2018	147
Duckabush R.	DOC	*	*	2010(2 mo), 2011(4 mo), 10/2017-12/2018	22
Duckabush R.	POC[2]	*	*	2010(2 mo), 2011(4 mo), 10/2017-12/2018	19
Duckabush R.	NO23	8/2006-10/2007	15	08/2006-12/2018	146
Duckabush R.	OP	8/2006-10/2007	15	08/2006-12/2018	145
Duckabush R.	TP	8/2006-10/2007	15	08/2006-12/2018	145
Duckabush R.	TPN	8/2006-10/2007	15	08/2006-12/2018	144
Elwha R.	NH4	8/2006-10/2007	15	08/2006-12/2018	147

River Regression	Variable	Old Regression - Date Range of Data Used	Old Regression -N	New Regression - Date Range of Data Used	New Regression – N
Elwha R.	DOC	1977-1981	12	2010(2 mo), 2011(4 mo), 10/2017-12/2018	21
Elwha R.	POC[2]	1977-1981	12	2010(2 mo), 2011(4 mo), 10/2017-12/2018	18
Elwha R.	NO23	8/2006-10/2007	15	08/2006-12/2018	146
Elwha R.	OP	8/2006-10/2007	15	08/2006-12/2018	146
Elwha R.	TP	8/2006-10/2007	14	08/2006-12/2018	145
Elwha R.	TPN	8/2006-10/2007	14	08/2006-12/2018	147
Vancouver Island C.	DOC	8/2006-10/2007	33	08/2006-12/2018	325
Vancouver Island C.	NO23	8/2006-10/2007	33	08/2006-12/2018	326
Vancouver Island C.	DTP	8/2006-10/2007	33	08/2006-12/2018	320
Vancouver Island C.	TP	8/2006-10/2007	33	08/2006-12/2018	311
Vancouver Island C.	TPN	*	*	09/2007-12/2018	256
Vancouver Island C.	DTPN	10/2006-10/2007	28	10/2006-12/2018	316
Fraser R.	DOC	08/2006-10/2007	21	08/2006-12/2018	258
Fraser R.	NO23	09/2006-10/2007	3 (Not used[1])	09/2006-12/2018	235
Fraser R.	DTP	08/2006-10/2007	22	08/2006-12/2018	257
Fraser R.	TP	08/2006-10/2007	21	08/2006-12/2018	251
Fraser R.	DTPN	09/2006-10/2007	20	09/2006-12/2018	253
Fraser R.	TPN	*	*	09/2007-12/2018	211
Green R.	NH4	08/2006-10/2007	15	08/2006-12/2018	147
Green R.	DOC	08/2006-10/2007	15	2010(3 mo), 2011(4 mo), 10/2017-12/2018	37
Green R.	POC[2]	08/2006-10/2007	15	2010(3 mo), 2011(4 mo), 10/2017-12/2018	34
Green R.	NO23	08/2006-10/2007	15	08/2006-12/2018	149
Green R.	OP	08/2006-10/2007	15	08/2006-12/2018	147
Green R.	DTP	08/2006-10/2007	15	08/2006-10/2007	15
Green R.	TP	08/2006-10/2007	15	08/2006-12/2018	148
Green R.	DTPN	08/2006-10/2007	15	08/2006-09/2009	19
Green R.	TPN	08/2006-10/2007	15	08/2006-12/2018	149
Howe Sound	NH4	08/2006-10/2007	22 (Not used)	08/2006-10/2011	133
Howe Sound	DOC	08/2006-10/2007	33	08/2006-10/2011	145
Howe Sound	NO23	08/2006-10/2007	3 (Not used[1])	09/2006-10/2011	98
Howe Sound	OP	08/2006-10/2007	33	08/2006-10/2011	145
Howe Sound	DTP	08/2006-10/2007	33	08/2006-10/2011	145
Howe Sound	TP	08/2006-10/2007	32	08/2006-10/2011	138

River Regression	Variable	Old Regression - Date Range of Data Used	Old Regression -N	New Regression - Date Range of Data Used	New Regression – N
Howe Sound	DTPN	08/2006-10/2007	34	08/2006-10/2011	143
Howe Sound	TPN	*	*	09/2007-10/2011	78
Nisqually R.	NH4	08/2006-10/2007	15	08/2006-12/2018	147
Nisqually R.	DOC	08/2006-10/2007	14	2010(2 mo), 2011(4 mo), 10/2017-12/2018	35
Nisqually R.	POC[2]	08/2006-10/2007	14	2010(2 mo), 2011(4 mo), 10/2017-12/2018	35
Nisqually R.	NO23	08/2006-10/2007	15	08/2006-12/2018	147
Nisqually R.	OP	08/2006-10/2007	14	08/2006-12/2018	145
Nisqually R.	DTP	08/2006-10/2007	15	08/2006-10/2007	15
Nisqually R.	TP	08/2006-10/2007	15	08/2006-12/2018	146
Nisqually R.	DTPN	08/2006-10/2007	15	08/2006-10/2009	19
Nisqually R.	TPN	08/2006-10/2007	15	08/2006-12/2018	148
Nooksack R.	NH4	09/2006-10/2007	14	08/2006-12/2018	147
Nooksack R.	DOC	*	*	2010(3 mo), 2011(4 mo), 10/2017-12/2018	22
Nooksack R.	POC[2]	*	*	2010(3 mo), 2011(4 mo), 10/2017-12/2018	22
Nooksack R.	NO23	09/2006-10/2007	14	09/2006-12/2018	147
Nooksack R.	OP	09/2006-10/2007	14	09/2006-12/2018	146
Nooksack R.	TP	09/2006-10/2007	14	09/2006-12/2018	141
Nooksack R.	TPN	09/2006-10/2007	14	09/2006-12/2018	147
Puyallup R.	NH4	08/2006-10/2007	15	08/2006-12/2018	149
Puyallup R.	DOC	08/2006-10/2007	15	2010(2 mo), 2011(4 mo), 10/2017-12/2018	36
Puyallup R.	POC[2]	08/2006-10/2007	15	2010(2 mo), 2011(4 mo), 10/2017-12/2018	36
Puyallup R.	NO23	08/2006-10/2007	15	08/2006-12/2018	148
Puyallup R.	OP	08/2006-10/2007	15	08/2006-12/2018	148
Puyallup R.	DTP	08/2006-10/2007	15	08/2006-10/2007	15
Puyallup R.	TP	08/2006-10/2007	15	08/2006-12/2018	148
Puyallup R.	DTPN	08/2006-10/2007	15	08/2006-10/2009	19
Puyallup R.	TPN	08/2006-10/2007	15	08/2006-12/2018	148
Samish R.	NH4	08/2006-10/2007	15	08/2006-12/2018	148
Samish R.	NO23	08/2006-10/2007	15	08/2006-12/2018	148
Samish R.	OP	08/2006-10/2007	15	08/2006-12/2018	147
Samish R.	TP	08/2006-10/2007	15	08/2006-12/2018	148
Samish R.	TPN	08/2006-10/2007	15	08/2006-12/2018	147

River Regression	Variable	Old Regression - Date Range of Data Used	Old Regression -N	New Regression - Date Range of Data Used	New Regression – N
Samish R.	DOC	*	*	2010(3 mo), 2011(4 mo), 10/2017-12/2018	22
Samish R.	POC[2]	*	*	2010(3 mo), 2011(4 mo), 10/2017-12/2018	19
Skagit R.	NH4	08/2006-10/2007	15	08/2006-12/2018	145
Skagit R.	NO23	08/2006-10/2007	15	08/2006-12/2018	148
Skagit R.	OP	08/2006-10/2007	15	08/2006-12/2018	147
Skagit R.	TP	08/2006-10/2007	15	08/2006-12/2018	145
Skagit R.	TPN	08/2006-10/2007	15	08/2006-12/2018	148
Skagit R.	DOC	1977-1981	14	2010(3 mo), 2011(4 mo), 10/2017-12/2018	22
Skagit R.	POC[2]	1977-1981	14	2010(3 mo), 2011(4 mo), 10/2017-12/2018	22
Skokomish R.	NH4	08/2006-10/2007	14	08/2006-10/2018	140
Skokomish R.	NO23	08/2006-10/2007	14	08/2006-10/2018	139
Skokomish R.	OP	08/2006-10/2007	14	08/2006-10/2018	140
Skokomish R.	TP	08/2006-10/2007	14	08/2006-10/2018	140
Skokomish R.	TPN	08/2006-10/2007	14	08/2006-10/2018	140
Skokomish R.	DOC	1996-1998, 2004	36	2010(3 mo), 2011(4 mo), 10/2017-12/2018	19
Skokomish R.	POC[2]	*	*	2010(3 mo), 2011(4 mo), 10/2017-12/2018	19
Snohomish R.	NH4	08/2006-10/2007	15	08/2006-12/2018	148
Snohomish R.	NO23	08/2006-10/2007	15	08/2006-12/2018	148
Snohomish R.	OP	08/2006-10/2007	15	08/2006-12/2018	145
Snohomish R.	TP	08/2006-10/2007	15	08/2006-12/2018	146
Snohomish R.	TPN	08/2006-10/2007	15	08/2006-12/2018	148
Snohomish R.	DOC	*	*	2010(3 mo), 2011(4 mo), 10/2017-12/2018	22
Snohomish R.	POC[2]	*	*	2010(3 mo), 2011(4 mo), 10/2017-12/2018	22
Stillaguamish R.	NH4	08/2006-10/2007	15	08/2006-12/2018	148
Stillaguamish R.	NO23	08/2006-10/2007	15	08/2006-12/2018	149
Stillaguamish R.	OP	08/2006-10/2007	15	08/2006-12/2018	148
Stillaguamish R.	TP	08/2006-10/2007	15	08/2006-12/2018	146
Stillaguamish R.	TPN	08/2006-10/2007	15	08/2006-12/2018	149

River Regression	Variable	Old Regression - Date Range of Data Used	Old Regression -N	New Regression - Date Range of Data Used	New Regression – N
Stillaguamish R.	DOC	*	*	2010(3 mo), 2011(4 mo), 10/2017-12/2018	22
Stillaguamish R.	POC[2]	*	*	2010(3 mo), 2011(4 mo), 10/2017-12/2018	22
Vancouver Island N.	NH4	*	*	11/2008-12/2018	255
Vancouver Island N.	DOC	08/2006-10/2007	15	02/2006-12/2018	284
Vancouver Island N.	NO23	09/2006-10/2007	13	09/2006-12/2018	276
Vancouver Island N.	DTP	09/2006-09/2007	2 (Not used[1])	09/2006-12/2018	253
Vancouver Island N.	TP	09/2006-09/2007	2 (Not used[1])	09/2006-12/2018	251
Vancouver Island N.	DTPN	09/2006-09/2007	1 (Not used[1])	09/2006-12/2018	255
Vancouver Island N.	TPN	10/2006-10/2007	12	10/2006-12/2018	274
Victoria SJDF	NH4	08/2006-10/2007	21 (Not used)	08/2006-08/2009	62
Victoria SJDF	DOC	08/2006-10/2007	37	08/2006-08/2009	78
Victoria SJDF	NO23	08/2006-10/2007	37	08/2006-08/2009	78
Victoria SJDF	DTP	08/2006-10/2007	37	08/2006-08/2009	78
Victoria SJDF	TP	08/2006-10/2007	37	08/2006-08/2009	75
Victoria SJDF	DTPN	08/2006-10/2007	37	08/2006-08/2009	78
Victoria SJDF	TPN	08/2006-10/2007	37	08/2006-08/2009	78

*no data available

[1]Data points not used in previous regression due to insufficient dynamic range in the data to develop a regression.

[2]Value was calculated not measured

NH4=ammonium; DOC=dissolved organic carbon; NO23=nitrite +nitrate; DTP= dissolved total phosphorus; TP=total phosphorus; DTPN=dissolved total persulfate nitrogen; TPN=total persulfate nitrogen.

Table A2. Model goodness of fit (R^2) for 2014 using old and new regressions.

Old and new regressions were used to predict water quality parameters for 2014; the fit of these predictions against observations were evaluated using R^2.

River Regression	Variable	N	Old Regression –R^2	New Regression –R^2
Vancouver Island S.	NH4	26	*	0.96
Vancouver Island S.	DOC	26	*	0.03
Vancouver Island S.	NO23	26	*	0.92
Vancouver Island S.	DTP	26	0.48	0.59
Vancouver Island S.	TP	26	0.07	0.66
Vancouver Island S.	DTPN	26	0.83	0.94
Vancouver Island S.	TPN	26	*	0.88
Deschutes R.	NH4	12	0.37	0.64
Deschutes R.	NO23	12	0.30	0.58
Deschutes R.	OP	12	0.64	0.83
Deschutes R.	TP	12	0.67	0.83
Deschutes R.	TPN	12	0.31	0.55
Duckabush R.	NH4	12	0.01	0.17
Duckabush R.	NO23	11	0.29	0.58
Duckabush R.	OP	11	0.67	0.67
Duckabush R.	TP	12	0.88	0.76
Duckabush R.	TPN	10	0.48	0.42
Elwha R.	NH4	10	0.42	0.07
Elwha R.	NO23	10	0.53	0.40
Elwha R.	OP	11	0.01	0.02
Elwha R.	TP	10	0.29	0.48
Elwha R.	TPN	10	0.50	0.37
Vancouver Island C.	DOC	26	0.66	0.72
Vancouver Island C.	NO23	26	0.41	0.74
Vancouver Island C.	DTP	26	0.42	0.40
Vancouver Island C.	TP	26	0.85	0.77
Vancouver Island C.	DTPN	25	0.50	0.71
Vancouver Island C.	TPN	26	*	0.58
Fraser R.	DOC	23	0.38	0.52
Fraser R.	NO23	23	*	0.92
Fraser R.	DTP	23	0.01	0.01
Fraser R.	TP	23	0.58	0.85
Fraser R.	DTPN	23	0.72	0.83
Fraser R.	TPN	23	*	0.74
Green R	NH4	12	0.46	0.64
Green R	NO23	12	0.61	0.58
Green R	OP	12	0.18	0.36

River Regression	Variable	N	Old Regression $-R^2$	New Regression $-R^2$
Green R	TP	12	0.03	0.61
Green R	TPN	12	0.37	0.42
Nisqually R	NH4	12	0.00	0.00
Nisqually R	NO23	12	0.81	0.85
Nisqually R	OP	12	0.59	0.55
Nisqually R	TP	12	0.27	0.71
Nisqually R	TPN	12	0.76	0.77
Nooksack R.	NH4	12	0.25	0.69
Nooksack R.	NO23	12	0.45	0.83
Nooksack R.	OP	12	0.41	0.00
Nooksack R.	TP	9	0.58	0.76
Nooksack R.	TPN	12	0.42	0.79
Puyallup R.	NH4	12	0.30	0.26
Puyallup R.	NO23	12	0.72	0.88
Puyallup R.	OP	12	0.00	0.04
Puyallup R.	TP	12	0.46	0.79
Puyallup R.	TPN	12	0.69	0.90
Samish R.	NH4	11	0.09	0.45
Samish R.	NO23	12	0.48	0.59
Samish R.	OP	12	0.67	0.62
Samish R.	TP	12	0.79	0.76
Samish R.	TPN	11	0.40	0.55
Skagit R.	NH4	12	0.03	0.56
Skagit R.	NO23	12	0.52	0.85
Skagit R.	OP	12	0.00	0.10
Skagit R.	TP	12	0.31	0.36
Skagit R.	TPN	12	0.46	0.79
Skokomish R.	NH4	12	0.59	0.85
Skokomish R.	NO23	11	0.74	0.86
Skokomish R.	OP	12	0.53	0.72
Skokomish R.	TP	12	0.69	0.61
Skokomish R.	TPN	12	0.71	0.85
Snohomish R.	NH4	12	0.00	0.00
Snohomish R.	NO23	12	0.64	0.86
Snohomish R.	OP	12	0.25	0.52
Snohomish R.	TP	12	0.58	0.90
Snohomish R.	TPN	12	0.45	0.79
Stillaguamish R.	NH4	12	0.07	0.05
Stillaguamish R.	NO23	12	0.72	0.76
Stillaguamish R.	OP	12	0.67	0.55

River Regression	Variable	N	Old Regression $-R^2$	New Regression $-R^2$
Stillaguamish R.	TP	12	0.64	0.71
Stillaguamish R.	TPN	12	0.61	0.64
Vancouver Island N.	NH4	25	*	0.03
Vancouver Island N.	DOC	25	0.29	0.55
Vancouver Island N.	NO23	25	0.14	0.53
Vancouver Island N.	DTP	25	*	0.16
Vancouver Island N.	TP	25	*	0.44
Vancouver Island N.	DTPN	25	*	0.59
Vancouver Island N.	TPN	25	0.21	0.62

*No prediction due to lack of data for regression fit.
NH4=ammonium; DOC=dissolved organic carbon; NO23=nitrite +nitrate;
DTP= dissolved total phosphorus; TP=total phosphorus;
DTPN=dissolved total persulfate nitrogen; TPN=total persulfate nitrogen.

Table A3. List of freshwater inflows that now have updated dissolved and particulate organic carbon (DOC and POC) regressions.

Freshwater inflow name	WQ regression association
Duckabush R	Duckabush River
Dabob Bay	Duckabush River
Dosewallips R	Duckabush River
Quilcene	Duckabush River
Nooksack R	Nooksack River
Birch Bay	Nooksack River
Samish_Bell south	Samish River
Whidbey east	Samish River
Whidbey west	Samish River
Lopez Island	Samish River
Orcas Island	Samish River
San Juan Island	Samish River
Whatcom_Bell north	Samish River
Snohomish R	Snohomish River
South Snohomish	Snohomish River
Stillaguamish R	Stillaguamish River

Table A4. Summary of changes made to regression associations used to estimate water quality concentrations at select unmonitored freshwater inflows.

Freshwater inflow name	Original WQ regression association	Updated WQ regression association	Reason for change – see Notes below table
Kitsap Hood	Big Beef Creek for all parameters	Sinclair-Dyes for DOC and POC, Big Beef Creek for all other parameters	Note 1
Kitsap NE	Big Beef Creek for all parameters	Sinclair-Dyes for DOC and POC, Big Beef Creek for all other parameters	Note 1
Port Gamble	Big Beef Creek for all parameters	Sinclair-Dyes for DOC and POC, Big Beef Creek for all other parameters	Note 1
NW Hood	Big Beef Creek for all parameters	Duckabush River	Note 2
Hamma Hamma River	Skokomish River for all parameters	Duckabush River for all parameters	Note 3
Skokomish River	Skokomish River for all parameters	Skookum Creek for POC only, Skokomish River for all other parameters	Note 4

Notes - Reason for changes:

1. Due to lack of organic carbon data in Big Beef Creek, these inflows previously had no regressions for DOC and POC, and instead were specified with constant year-round concentrations of DOC and POC. This meant that the reference and existing concentrations for these inflows were set equal to each other in the Bounding Scenarios report. This update means they now have time-varying DOC and POC concentrations, based on the regressions developed for Sinclair-Dyes inlet, which is also located on the Kitsap Peninsula.

2. NW Hood drains into Hood Canal on the same side as the Duckabush River, while Big Beef Creek is located on the opposite side of the canal. The Duckabush River now also has DOC and POC data and site-specific regressions.

3. The Hamma Hamma River watershed adjacent to the Duckabush River, and the Skokomish River water quality data may be influenced by the presence of an upstream dam. The Duckabush River now also has DOC and POC data and site-specific regressions.

4. We still do not have POC data for the Skokomish River. The reference and existing concentrations for this river were set equal to each other in the Bounding Scenarios report. This update means that for 2006, we assigned the Skookum Creek POC regression to the Skokomish River. Alternatively, we could also have applied the Duckabush River regression (which now has DOC and POC data). We will evaluate these alternatives more closely for the next phase of this project. Also, we will use the same approach for all model years since this update was applied only to year 2006.

River Temperature

Observed temperature time series for most river and streams are not available. We used observed Cedar River temperatures to characterize Puget Sound rivers in PSM (Khangaonkar et al. 2012), and that practice has so far carried over to SSM. Because surface Puget Sound marine water temperatures are more strongly influenced by solar radiation than the heat load of rivers, except areas adjacent to river mouths, using representative temperature profiles is acceptable (Khangaonkar et al. 2012). As the SSM domain has expanded, we have continued to use a representative (Cedar River) temperature for the Puget Sound rivers, and used the Fraser River temperature time series to represent Canadian rivers in the domain. In 2018, the domain was expanded to include the larger rivers that discharge into the Pacific Ocean of Washington State.

Since salinity differences between freshwater inflows and receiving marine waters are the most significant drivers in estuarine density stratification, refinement of freshwater inflow temperatures has not been prioritized to date. As we continue to explore potential avenues to improve model performance, we may explore options for using modeled surface water temperatures instead of the representative temperature profiles used to date.

During this optimization phase, we updated the time series for several boundary condition freshwater inputs that were previously categorized incorrectly. The temperature times series that were updated include: Cushman Powerhouse No. 2, Lake Washington, Fraser, Chehalis, Willapa, Columbia, and Willamette inflows. The updated river temperature time series model performance statistics are shown in Table A5. These updates resulted in slight changes to predicted noncompliant areas and number of days in certain locations. Since the updated temperature profiles were used for Scenario 5, but not for Scenarios 1-4, we use the term "baseline" when referring to the existing hindcast year runs corresponding to each set of scenarios.

Table A5. Model performance statistics (RMSE and bias) with and without temperature updates.

Year	Parameters	RMSE w/out updates	Bias w/out updates	RMSE w/ updates	Bias w/ updates
2006	Temperature	0.71	0.41	0.69	0.38
2006	Salinity	0.74	-0.48	0.74	-0.47
2006	Oxygen	1.09	-0.58	1.13	-0.62
2014	Temperature	0.78	-0.23	0.78	-0.23
2014	Salinity	0.84	-0.44	0.84	-0.44
2014	Oxygen	0.99	-0.43	0.98	-0.43

Limitations and uncertainty of watershed estimates

Watershed estimate methods were described in Mohamedali et al. 2011, Pelletier et al. 2017 and Ahmed et al. 2019. This section focuses on inherent limitations with the methodology employed. We expect that some watersheds have larger degree of uncertainty in loading estimates compared to others, as described below.

Watershed regression used in SSM are based on available monthly water quality data and daily guaged flows at river mouths where that information is available. Loading estimates for 81% and 79% of the drainage area flowing into the marine waters within the SSM domain are based on site-specific guaged flows or water-quality measurements, respectively. As a result of observational data limitations, about 19% and 21% of the drainage area flowing into the US portion of the SSM domain are based on estimates using neighboring guaged flows and/ or stream water quality, respectively. The cream-colored areas in maps shown in Figures A1 and A2 correspond with drainage areas for which loading estimates for either flows or water quality are based on neighboring catchments. Most of the catchments that fall into this category are relatively small. The TN and TOC load watersheds with site-specific WQ regression represent 83% and 77% of the total load from US watersheds, respectively, while the TN and TOC load with watershed-specific flow gages represent 84% and 85% of the total load from US watersheds, respectively.

Sackmann (2011), using a bootstrapping approach, compared a monthly sampling strategy to a continuous observational dataset obtained close to the Deschutes River mouth, at a location upstream of the dam, during the 2009-2010 water year. Sackmann (2011) concluded that the total annual nitrate load estimated from a regression using monthly data was within 10% of the observed value based on continuous observations.

The Sackmann (2011) results, when interpreted more broadly, provide a basis to the assumption that regressions for larger watersheds within the Puget Sound domain based on monthly observations and available gauged flows could generally fall within ten percent of annual estimates that could be derived from continuous measurements. An exception to that assumption is for watershed inflows influenced by a dam, which can result in predicted increases in organic carbon concentrations as well as changes to the mix of nitrogen species discharged into marine waters (Roberts et al. 2015). A comparison between regression-predicted daily loads and observations showed much greater observed daily loads potentially due to dam release or storm events not characterized by the regression (Figueroa-Kaminsky, 2018).

In 2017 to make improvements to the loading estimates for the largest rivers in the Washington portion of the domain, we requested continuous monitoring at seven large river mouths. While funding for this work has been secured, due to multiple unavoidable delays it is likely that data collection will not begin until 2022 (Hopkins, 2021). Given that timeline, we may not be able to incorporate any of that new watershed data into the final PSNSRP report.

McCarthy (2019) compared annual nitrogen SSM input watershed estimates computed from the regression-based SSM inputs with 2002 Pacific Northwest application of the SPARROW (Spatially Referenced Regression on Watershed Attributes) model (Wise and Johnson, 2013). That particular SPARROW application estimated higher total nitrogen loads in large, mixed land use watersheds (Skagit, Stillaguamish, and Snohomish watersheds) than SSM nutrient load inputs. Based on the McCarthy (2019) comparison, we expect that regressions based on monthly observations used in SSM may generally under-predict watershed loads.

We compared the total nitrogen load from a single small catchment using a regression based on observations from neighboring catchment with newly accessed in-situ observations. This limited analysis shows that small catchment load estimates can be currently largely under-predicted (average of 3.5 times lower daily total nitrogen for Judd Creek in 2007) when using regressions from neighboring watersheds.

Loads from catchments that are ungauged or do not have site-specific water quality data constitute up to 16% or 23%, respectively, of the domain-wide water quality loads. Load estimates for these catchments, and their greater degree of uncertainty, can influence marine water predictions in small, sheltered embayments. For instance, Discovery Bay is a small embayment connected to the Strait of Juan de Fuca. It is modeled with freshwater inputs based on loading regression estimates that use neighboring watershed observations to estimate both flow and water quality.

Discovery Bay freshwater inflows are based on the Dungeness gauge, which is used to estimate flow via the drainage ratio method, and water quality observations from the Elwha River used to estimate water quality parameters. We are not aware of any observations available to compare to the regression estimates, and a comparison with SPARROW annual load estimates indicates that SSM inputs for Discovery Bay may be under-predicted by a factor of five. We are actively pursuing refinements to the SPARROW model to improve its temporal resolution as well as searching for any available observational data that might lead to improvements and updates of the watershed estimates including a more robust quantification of their error, particularly at these small catchments. Consequently, we urge caution in interpreting results for small embayments, such as Discovery Bay, that have estimated watershed inflows based solely on regressions from observations in neighboring catchments.

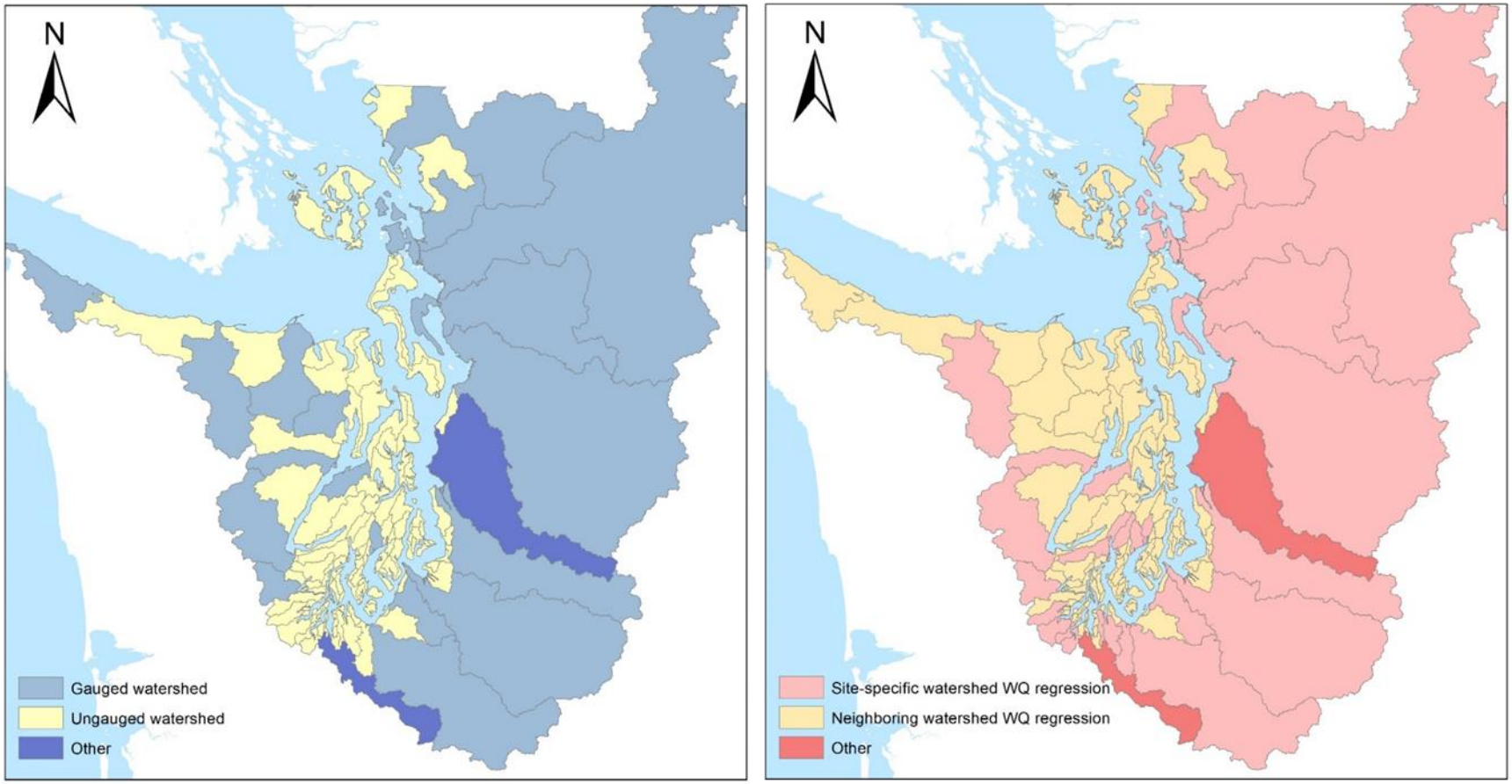

Figure A1. Map of watershed drainage areas within the US SSM domain.

The left map shows watersheds with watershed-specific flow gauges and watersheds that are ungauged.
The right map shows watersheds with watershed-specific water quality regressions and watersheds that use a neighboring watershed regression.
"Other" represents watersheds with a hybrid flow calculation approach due to the influence of dams, Lake Washington, and Deschutes River/Capitol Lake.

Appendix B – Watershed Flow Assessment

Flows to the Salish Sea Model (SSM) aggregated to different geographic regions

The 'Salish Sea' is geographically defined as the inland marine waterways of Washington State and British Columbia, and extends from the north end of the Strait of Georgia to the south end of Puget Sound and the west end of the Strait of Juan de Fuca. The Salish Sea is connected to the Pacific Ocean primarily via the Strait of Juan de Fuca, but there is also some tidal influence from the north through Johnstone Strait.

Puget Sound, which is within the Salish Sea, begins at Admiralty Inlet in the north and extends through all inlets and basins south of this point. WA waters of the Salish Sea, which is a geographic definition specific to this document, includes Puget Sound as well the waters to the north of Puget Sound but still within US waters, including the US parts of the Strait of Juan de Fuca and Strait of Georgia, and Bellingham, Samish and Padilla Bays (together referred to, sometimes, as the 'northern bays' in this report).

To better illustrate how much freshwater flow enters different areas of the SSM domain, we aggregated these flows to different geographic marine areas and regions. These cumulative flows are illustrated in Figures B1 through B3. In addition, Figure B4 provides maps to complement each figure (using the same color scheme), showing the location of the individual watershed inflows included in the different groups.

Figures B1 through B4 provide more comparisons of the cumulative flows entering the SSM, but are aggregated into different geographic marine areas and regions.

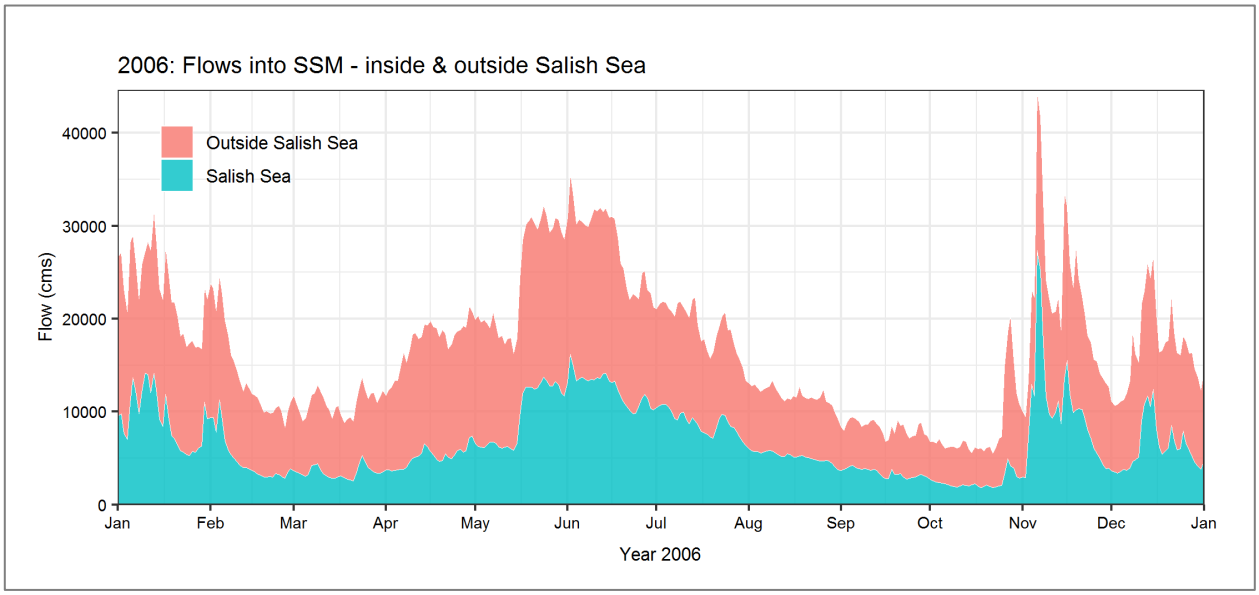

Figure B1. Stacked area plot comparing freshwater flows for year 2006 entering the Salish Sea Model (SSM) both '*inside*' the Salish Sea (inland waterways of Puget Sound, Strait of Georgia, and Strait of Juan de Fuca) and '*outside*' Salish Sea (flows into the open Pacific Ocean and/or Johnstone Strait).
Also see maps in Figure B4 that illustrate the location of these inflows using the same color scheme.

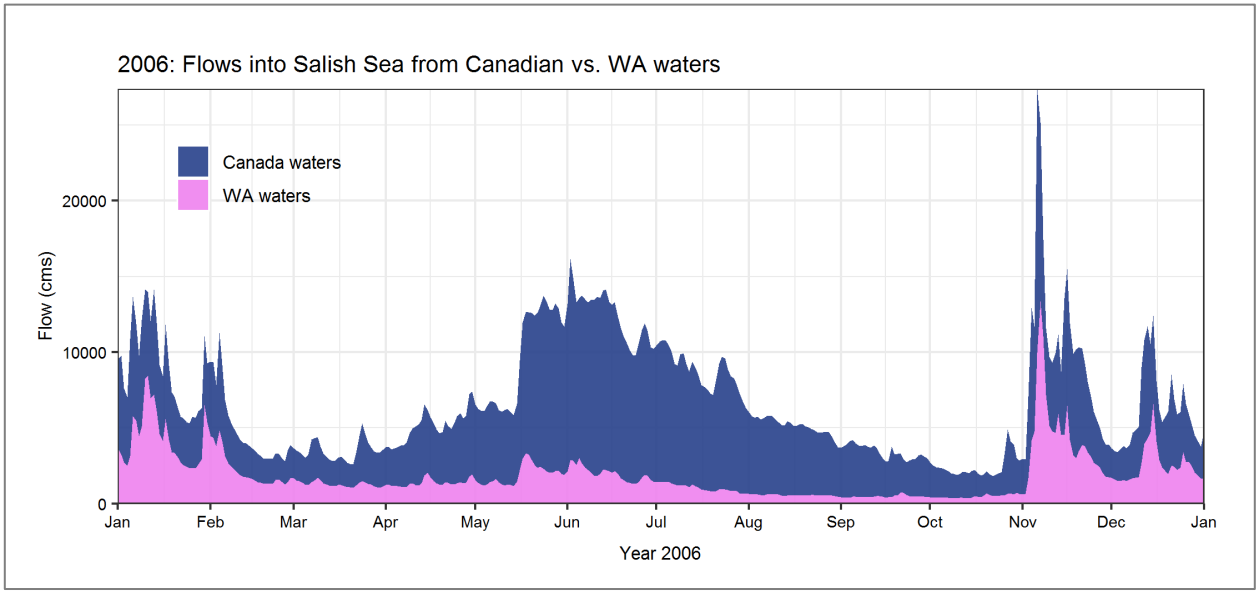

Figure B2. Stacked area plot comparing freshwater flows entering the Salish Sea from Canada vs. WA waters during 2006.

This plot does not include other flows in the SSM domain that enter the model outside the Salish Sea geographic boundary (e.g. flows entering the Pacific Ocean or Johnston Strait). Also see maps in Figure B4 that illustrate the location of these inflows using the same color scheme.

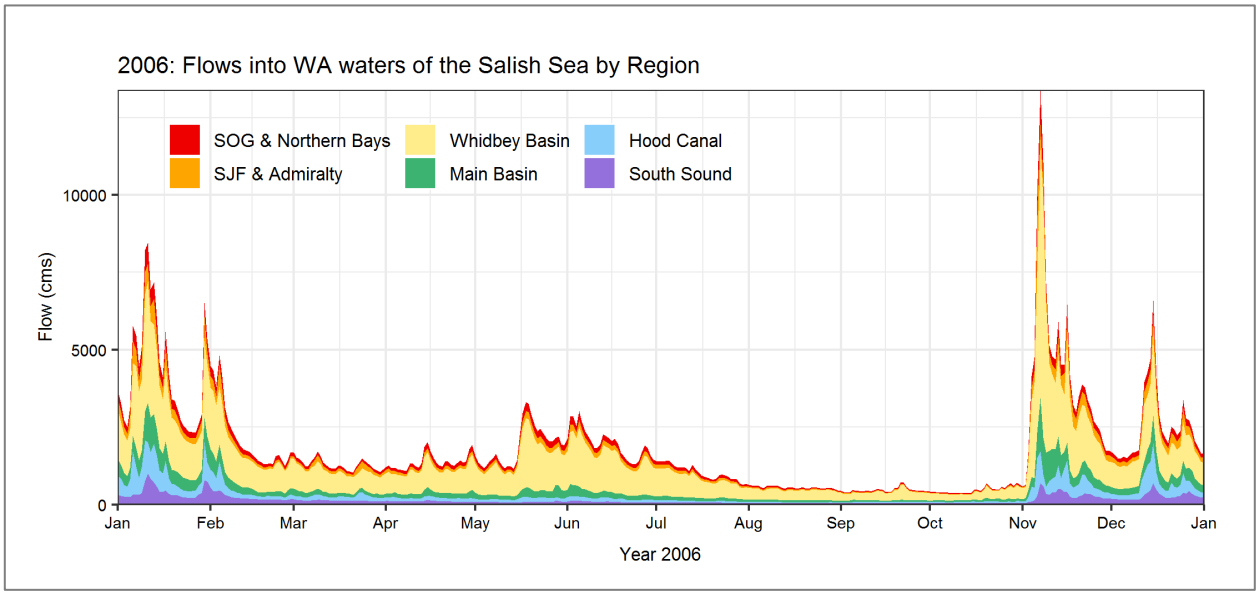

Figure B3. Stacked area plot comparing freshwater flows from different regions entering WA waters of the Salish Sea during 2006.

Note that a very small amount of flow enters SJF & Admiralty Inlet (in orange), so that color is barely visible. Also see maps in Figure B4 that illustrate the location of these inflows using the same color scheme.

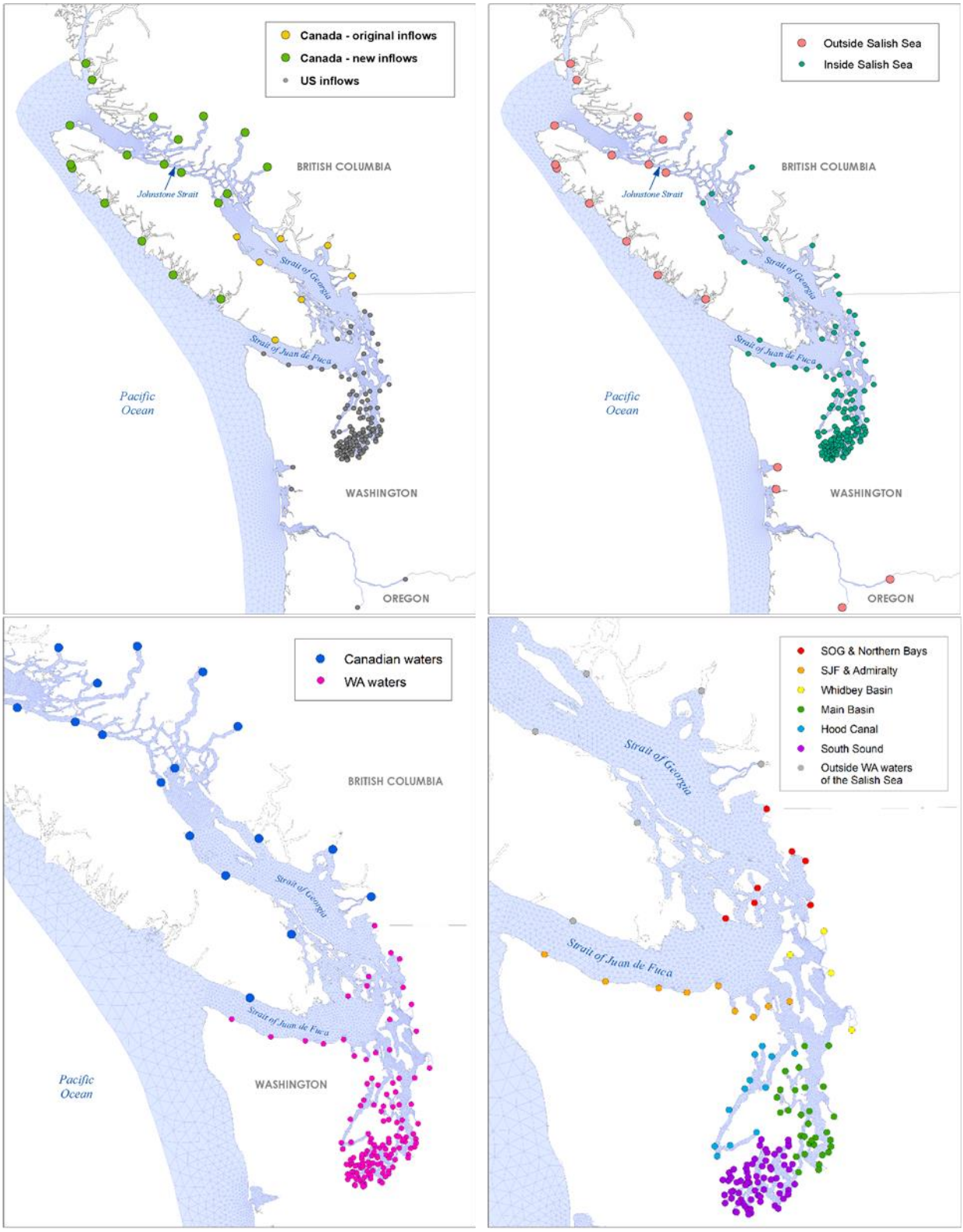

Figure B4. Maps illustrating the location of freshwater inflows included in the Salish Sea Model (SSM) domain, grouped by different geographic boundaries.

Each map has a different color scheme to show the aggregation/grouping of these freshwater flows at different levels to match the color scheme in Figures B1 through B3.

Watershed flows from British Columbia, Canada

The original model (Puget Sound Model, or PSM) domain extended from the mouth of the Strait of Juan de Fuca to South Puget Sound. The northern boundary was set at the entrance to Johnstone Straits past the Fraser River north of Vancouver B.C. Khangaonkar et al. (2017) expanded the model domain to include the continental shelf, and it now includes Discovery Islands, Johnstone Strait, Broughton Archipelago, and the associated waterways, along with major rivers along the Pacific Coast (Chehalis, Columbia, Willamette, and Willapa Rivers). This new model was labelled the Salish Sea Model or SSM.

Ahmed et al. (2019) incorporated freshwater inputs to the expanded model domain. Updates to SSM watersheds in the Canadian portion of the model domain were briefly summarized in Appendix B in Ahmed et al. 2019. However, this previous documentation placed emphasis on discussing methods for predicting flow for ungauged or poorly gauged watersheds. Here, we supplement the previous work by providing greater detail regarding the significance of the watershed flow updates and will briefly explore the performance of flow prediction methods used in Appendix B of Ahmed et al. (2019).

The addition of 19 British Columbia (BC) watersheds to the SSM domain (Appendix B Ahmed et al. 2019) substantially increased the amount of streamflow entering the model domain in this region. For model year 2006, total simulated BC flows were, on average, about twice the magnitude of PSM flows (Figure B5). While the expanded domain BC watersheds account for roughly 32% of the drainage area of the Fraser River, the cumulative daily flow for these watersheds exceed Fraser River flows throughout most of the year during 1999 through 2017 (Figure B6). However, many of these new flows from BC do not directly enter the geographic boundary of the Salish Sea. Instead, they contribute flows to the Pacific Ocean, Johnstone Strait, or northern areas of BC marine waters.

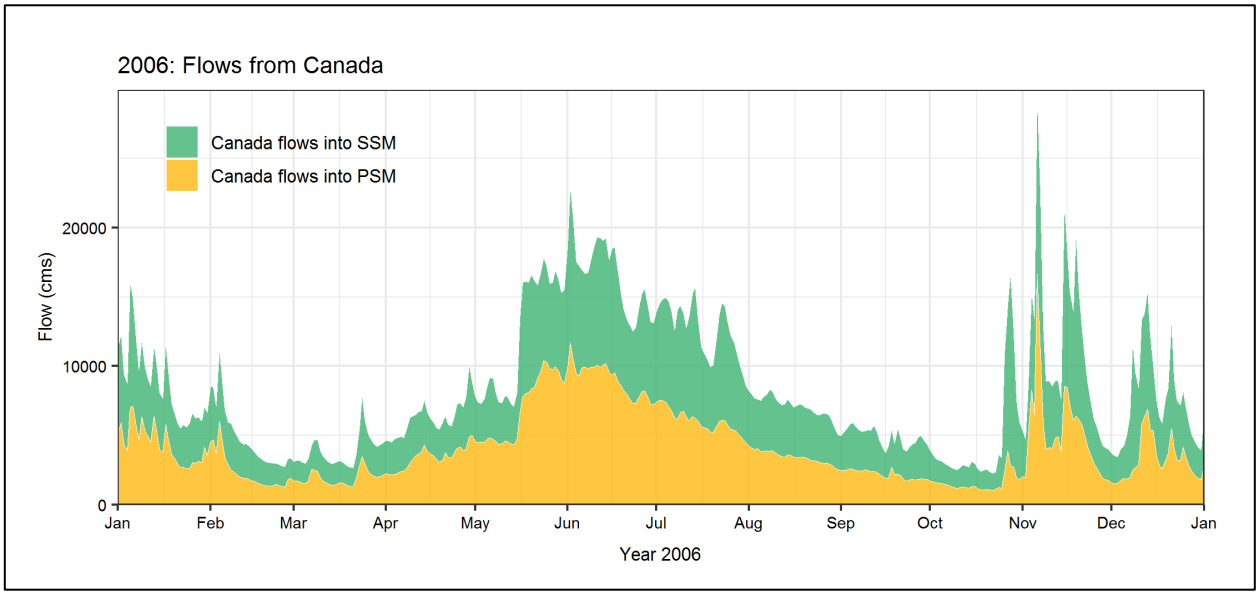

Figure B5. Stacked area plot comparing freshwater flows from British Columbia (Canada) included in the PSM vs. SSM during 2006.

Also see maps in Figure B4 that illustrate the location of these inflows using the same color scheme.

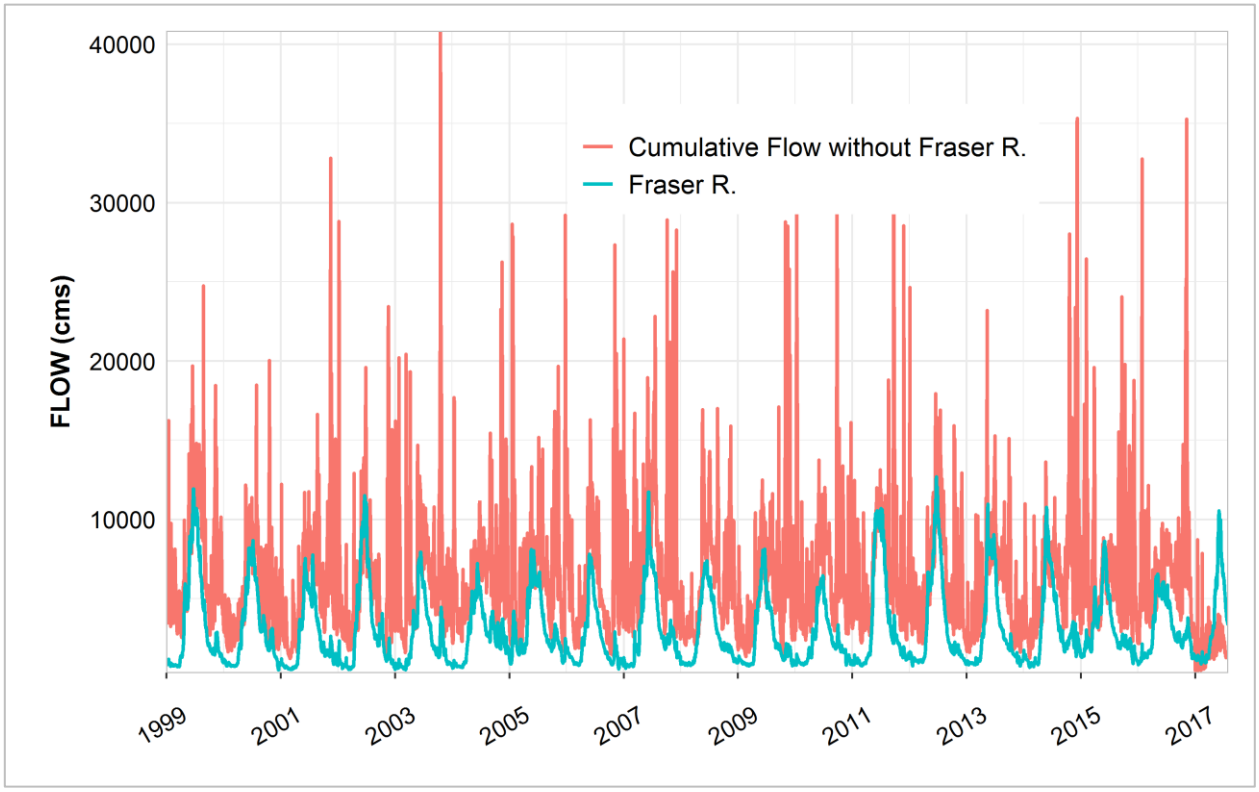

Figure B6. Time series comparison of 1999-2017 flows for the Fraser River and cumulative flows for the other rivers in British Columbia.

Flows were scaled from stream gauge to the mouth of each river using the ratio of the total drainage area to that of the gaged area.

We specified the additional BC flows in the model (green dots in Figure B4(a), and green dots in Figure B5) with nutrient concentrations that match the ambient marine water quality concentrations at the location where they enter. While this is a simplification, these Canadian flows are relatively far from our Puget Sound, several of them flow into the Pacific Ocean, and at this time, we do not have concentration data to characterize these freshwater inputs more accurately.

Despite a lack of complete understanding of watershed characteristics, there is enough climate and physiographic data available to develop a basic understanding of the driving factors regarding flow in these more recent BC streamflow additions to SSM. The remainder of this sub-section compares factors influencing flow from the Fraser River and flow from coastal watersheds west of Fraser River.

The Fraser River is largely influenced by snow and glacial melt from the northern and mountainous regions of the basin (Déry et al., 2012). The dominance of snowmelt as a driving factor for flow in the Fraser River can be easily identified by the single, but long-lasting, peak in the hydrograph, which typically lasts from May-August (Figure B6).

While the hydrology of the Fraser River has been assessed at great lengths, literature for the remaining watersheds in this study is limited. Soil survey data from the Government of Canada[1]

[1] http://sis.agr.gc.ca/cansis/nsdb/slc/index.html

covered only 2% of the drainage area of the coastal BC watersheds in SSM, and impervious surface data were unavailable. Relief (Figure B3) and climate data (Kang et al., 2014) for the region indicate that the coastal BC watersheds in SSM, comprised of Vancouver Island and coastal watersheds west of the Fraser River, are influenced primarily by storm run-off events. With the exception of the lower Fraser River Basin and the Columbia Mountain Range, the terrain of the new BC watersheds has much steeper inclines (Figure B7). In general, terrain with steep inclines tend to reduce the infiltration of precipitation during storm events in favor of surface run-off, leading to surges in streamflow (Mays, 2010).

Vancouver Island and coastal watersheds west of the Fraser River receive 1-4 times more precipitation than the Fraser River Basin, with maximum rainfall intensity in West Vancouver Island and progressively lower intensity with increasing latitude north of 52 degrees (Kang et al., 2014). These findings, although hampered by sparse data availability, provide some insight regarding the factors influencing the hydrology of the coastal BC watersheds in SSM.

Figure B7. Relief map of new British Columbia watersheds added to the Salish Sea Model domain and the Fraser River Basin (outlined in red).

Comparison of flow estimates for Coastal BC watersheds in SSM

We sought to compare other published values with flow estimates published in Ahmed et al. (2019) for the coastal BC watersheds. However, published values that exactly match the areas of interest are not available. Only a limited comparison with observations was possible due to the paucity of gauge data, as explained below.

For the years 1999-2018, flow data records for coastal BC watersheds in SSM are incomplete. As mentioned in Appendix B of Ahmed et al. (2019), many of the BC watersheds are missing flow data in the range of days to years.

Through a literature review, we found that in addition to the statistical methods used in Appendix B of Ahmed et al. (2019), conceptual and physically based rainfall-runoff models are useful methods for predicting flow in ungauged or poorly gauged BC watersheds.

The University of British Columbia Watershed Model (UBCWSM) is a conceptual rainfall run-off model which was originally developed for the Fraser River, and it is a widely used model for the region (Loukas et al. 2014). Despite its heavy use, UBCWSM is not open source and is difficult to employ. An open source alternative to the UBCWSM is the GR4J (Loukas et al. 2014) conceptual rainfall-runoff model for predicting streamflow. The GR4J model balances empirically based regression methods we previously used and physically based models, which can be inherently complex and time-consuming to calibrate.

The GR6J model (Lavtar et al. 2020), a variation of the GR4J model with two additional parameters, was selected for this comparison due to its low data requirements and ease of use. The GR6J model requires only four input parameters for calibration: precipitation, evapotranspiration, streamflow, and drainage area. These parameters are used as input for the station of interest as the model is a non-spatially varying, lumped model. Given limited published flow estimates within watersheds for this portion of the domain, we conducted a comparison between flows predicted for this region between GR6J and the regression approaches used in Ahmed et al. (2019).

The GR6J model uses precipitation and evaporation data to determine the amount of infiltrative storage of precipitation as well as the quantity of run-off that will be routed to the stream channel for a given storm event. Once the model has been calibrated, streamflow can be predicted exclusively using precipitation and evapotranspiration data. Precipitation and temperature data were obtained from the Government of Canada[2]. Evapotranspiration data were derived from precipitation, temperature, and latitude using the methods described in (Oudin et al. 2005). Weather stations in the study region were generally non-existent or were too far from flow gages of interest. As a result, only one flow station (Comox, 08HB006) was available to evaluate the performance of previously used regression methods against the GR6J conceptual rainfall run-off model.

[2] https://climate.weather.gc.ca/climate_data/daily_data_e.html?StationID=162

With the exception of 1999, which was used as a model spin-up year, the GR6J model was calibrated with the same flow data as the regression model to minimize bias in the comparison. For the evaluation period, 2018 was selected to help assess how well each model could generalize to data that was not used for calibration. The goodness of fit (GOF) of each model to the observed flow data was evaluated using the five statistical indices analogous to those used in Loukas et al. (2014) including: Nash-Sutcliffe Model Efficiency Criteria (NSE), Correlation (CORR), root mean square error (RMSE), bias, and percent maximum annual flow error (%MAFE) (Table B1).

Table B1. 2018 Goodness of fit statistics for two different streamflow prediction models at Comox flow gauge near Courtenay.

Model	Calibration Date Range	NSE	CORR	RMSE (cms)	Bias (cms)	% MAFE
Regression	1999-2016	0.47	0.70	26	-0.97	-51.6
GR6J	2000-2016	0.72	0.85	19	1.14	-17.5

NSE = Nash-Sutcliffe model efficiency coefficient (score of 1 is perfect fit); CORR= correlation, also known as 'R'; RMSE= root mean square error; %MAFE = percent maximum annual flow error.

Both the regressions described in Ahmed et al. (2019) Appendix B and GR6J methods showed strong correlations (0.7 and above) with observed data (Table B1) at the station where data are available in the Comox River. This limited comparison may not be representative of the performance in the entire region and must be viewed within that context.

The GR6J model displayed greater accuracy than the regression model in predicting peak flow events (Figure B8). The regression model on average under-predicted peak flow events by about 52% while the GR6J model under-predicted the same events by 18% on average (Table B1). The inability of the regression model to capture peak flow events in late January and mid-December (Figure B4) resulted in an overall tendency to under-predict (negative bias) with a higher RMSE, despite reasonable performance for the rest of the year. Conversely, the GR6J model, with exception of one peak event in mid-May, performed very well during peak flow events but tended to over-predict during low flow events from July to September (Figure B8), resulting in a positive bias (Table B1).

The NSE values for both models were both greater than zero, revealing that each model performed better than using the mean value for all predictions. However, NSE values of 0.5 and above are generally considered acceptable (Moriasi et al., 2007). NSE values of 0.47 and 0.72 for the regression and GR6J model, respectively, indicate that the regression model is performing within an acceptable range and that the GR6J model is performing relatively well. These findings indicate that the currently employed regression methods are reasonable in their predictive power for streamflow. Further investigation and implementation of potentially more robust methods such as GR6J could result in more accurate improvements, particularly during peak flow conditions. However, without more flow data for the region, it is not possible to ascertain this.

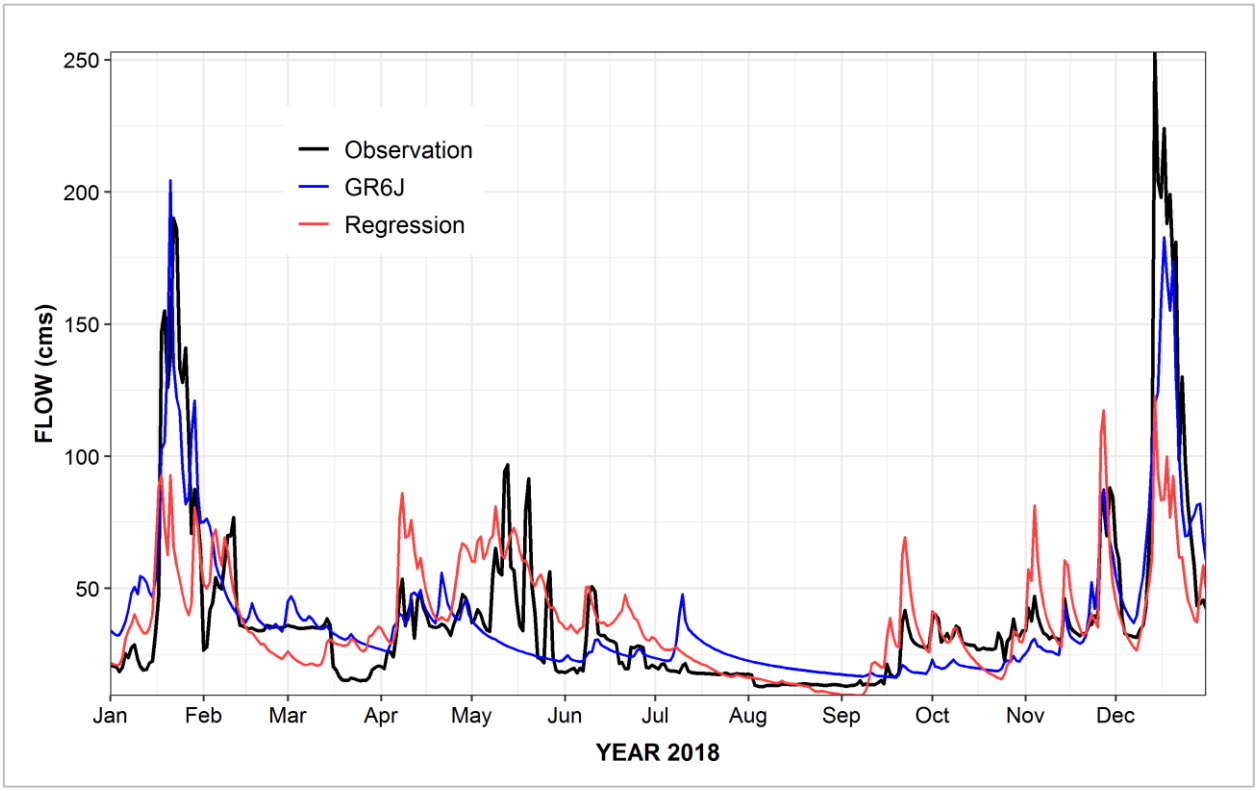

Figure B8. Comparison of flow predictions using flow regressions and a GR6J rainfall-runoff model and flow observations at Comox River (Quadra Islands).

Appendix C – Changes to Reference Organic Carbon

Partitioning of Particulate Organic Carbon

In the Salish Sea Model (SSM), particulate organic carbon (POC) in the rivers is split into two fractions: (1) labile (POC_l) with a hydrolysis rate of 0.03 per day and (2) refractory (POC_r). For existing condition runs, POC_l is based on aggregation of two fractions used in Ahmed et al. (2014) (POC_fast with a hydrolysis rate of 0.08 per day and POC_slow with a hydrolysis rate of 0.02 per day) and is considered to be labile (POC_l). The remaining third of the total POC was considered as refractory (POC_r). Ahmed et al. (2019) used the same split for reference condition. However, upon further literature review, we determined to split organic carbon for the reference condition differently, allowing a larger proportion for refractory organic matter. For reference condition, the fraction of POC that was labile is now considered to be equal to the fraction of POC with a higher hydrolysis rate (POC_fast), while the fraction that had a slower hydrolysis rate (POC_slow) and that which was refractory (POC_r) were combined as refractory (POC_r). The basis for this change is explained below.

Allochthonous particulate carbon are terrestrially derived. When anthropogenic sources are present in the watershed, it is expected that labile POC are relatively more abundant than refractory POC. On the other hand, as anthropogenic sources are removed, that is under natural reference conditions, it is expected that the proportion of labile POC would be less abundant compared to refractory POC. For the Puget Sound, studies in Hood Canal offer insights about this (Simenstad et al. 1985).

Arndt et al. (2013) and Hedges et al. (1997) estimated that terrestrial organic matter is relatively more refractory. Riverine discharges of POC in pristine or reference environments are expected to be mostly influenced by forested watersheds. Simenstad et al. (1985) researched organic matter composition from watersheds in Hood Canal, such as the Duckabush, which are relatively free of anthropogenic influences. They found that terrestrial organic matter entering that system could be linked to terrestrial vascular plants, including coniferous and deciduous tree leaves. Additionally, they found that during the time of their study in Hood Canal, marine primary production was responsible for the majority of the labile particulate matter. Terrestrial sources were not found to be the primary source of labile particulate detritus entering marine waters in that relatively pristine system. Therefore, the reference conditions were modified to reflect that POC of terrestrial origin is at least two-thirds refractory in systems with little or no anthropogenic influence.

Other updates to organic carbon reference condition

As indicated in Appendix A, new regressions were developed with updated data, where available, which were used to generate time series of daily water quality concentrations for organic carbon for all SSM inflows from the year 1999-2017. These multi-year time series of organic carbon concentrations are then used to establish site-specific monthly organic carbon reference conditions for each US inflow into the SSM (using calculated monthly 10^{th} or 50^{th} percentiles, depending on the region). The same monthly reference organic carbon concentrations were used for year 2006 and 2014.

Figure C1 compares plots of reference DOC and POC between the Bounding and Optimization Scenarios for each Washington river inflow into the SSM for year 2006. Previously constant values for some rivers meant that existing and reference organic carbon concentrations were the same. The

updated existing and reference conditions mean that these rivers now have an anthropogenic organic carbon load, as would be expected.

In summary, changes to the organic carbon reference condition include updated DOC time series due to new data, POC partitioning, and updated regressions due to other changes described in Appendix A. The cumulative result of all of the updates on reference condition minimum DO was compared with those of the reference condition in the Bounding Scenario Report (Ahmed et al. 2019) as shown in Figure C1 for 2006. The difference in the minimum DO between these two reference condition is also shown in Figure C1.

For the most (99.9%) of the unmasked area, the difference in the predicted minimum DO from the use of the Bounding Scenarios and the Optimization Scenarios reference conditions has the following statistics: median of 0.0017 mg/L, maximum of 0.04 mg/L, minimum of -0.0012 mg/L. A positive difference indicates that the minimum DO was higher under Optimization reference compared with Bounding reference condition, and a negative difference reflects the opposite. Of the 0.1% (14 grid cells) of the unmasked area that showed a larger difference in minimum DO between the two reference conditions, the median difference was 0.07 mg/L, with a maximum and minimum difference of 0.12 mg/L and 0.05 mg/L, respectively.

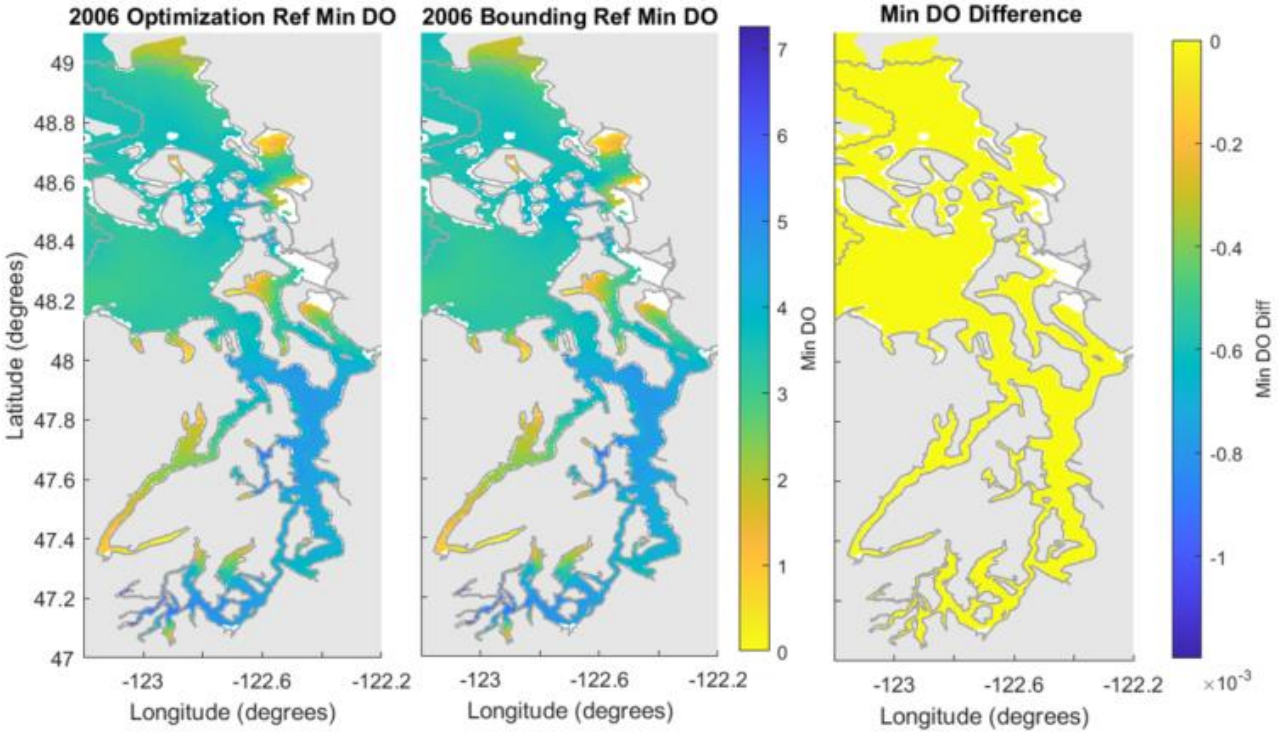

Figure C1. Predicted minimum DO in Optimization Scenarios reference conditions (lower labile POC and other updates) and Bounding Scenarios 2006 reference conditions, and the difference between the two predictions.

Appendix D – HYCOM Ocean Boundary

Introduction

The Hybrid Coordinate Ocean Model (HYCOM) is an eddy resolving, global and basin scale ocean circulation model that emerged out of the Miami Isopycnic-Coordinate Ocean Model (MICOM) (Chassignet et al. 2007). The state of the science model design of HYCOM, including its eddy resolving spatial resolution and three-hour temporal resolution, makes it an attractive choice for coupling with the Salish Sea Model (SSM). Recent updates to SSM have begun using HYCOM outputs to solve open boundary conditions (OBC) for both model hydrodynamics (FVCOM) and water quality (ICM).

Previously, SSM OBC used data from the Department of Fisheries and Oceans Canada (DFO). However, DFO data are collected on a quarterly basis and spatially cover only a small fraction of the 87 SSM boundary nodes. Therefore, to use DFO data for the OBC, interpolation had to be performed both spatially and temporally. Coupling HYCOM to SSM significantly improves the temporal and spatial resolution of data used for the OBC.

HYCOM model outputs consist of either daily or three-hour resolution predictions for water temperature, salinity, water surface elevation, and northward and eastward water velocity. Global HYCOM outputs currently have a horizontal grid resolution of 1/12° (~ 7 km on average for mid latitudes, i.e. Salish Sea) and a hybrid coordinate vertical structure with 41 layers (Metzger et al. 2013).

Traditional ocean circulation models, such as MICOM, use isopycnic (density tracking) coordinates to represent the vertical model structure. Studies conducted in the U.S (Data Assimilation and Model Evaluation Experiment) and Europe (Dynamics of North Atlantic Models) found single coordinate vertical structures were able to capture large-scale circulation patterns reasonably well. However, they were unable to represent the influence of localized processes on water mass distribution and thermohaline circulation (Chassignet et al. 2003). To help resolve vertical discretization limitations of previous circulation models, HYCOM incorporates depth (z-levels), density (isopycnic), and terrain following (sigma) coordinates. The optimal choice of vertical coordinate for a given location is solved for at the end of each baroclinic time step to more appropriately reflect seasonal shifts in water mass distribution. In general, the default configuration is isopycnal in the open stratified ocean, sigma near the coast, and fixed depth/pressure level (z-level) in mixed surface layers and un-stratified regions (Chassignet et al. 2007).

The hybrid coordinate system used by HYCOM allows for representation of localized processes such as coastal upwelling of the California Current (Bakun, 1973) which brings colder, lower DO, high nutrient waters along the continental shelf and into the Strait of Juan de Fuca (PSEMP, 2012). Although coastal upwelling is primarily influenced by the direction and magnitude of winds, along shore bathymetry is another important factor (Pitcher et al. 2010). Steep ridges for example, will result in enhanced vertical entrainment of water masses, leading to a greater amount of mixing than would occur with a gently sloping shelf (Hickey and Banas, 2003). Due to the terrain following sigma coordinates that HYCOM uses near the coast, it is better suited than its' predecessors to

capture the upwelled influence as the total depth shallows near the continental shelf, thus resulting in the correct temperature and salinity for upwelled waters (Metzger, et al 2017).

One approach used to identify the effects of upwelling is differences in localized sea surface temperature (Xu, et al. 2013). For the Pacific Northwest coastal region, model year 2014 seasonally averaged sea surface temperature indicates the occurrence of summer time upwelling along the continental shelf and coast (Figure D1). As shown in Figure D1, average summer sea surface temperature gradually declines from the continental shelf towards the coast, with the coldest temperatures occurring in the Strait of Juan de Fuca. The series of plots in Figure D1 follow the same seasonal sea surface temperature averaging approach that Hickey et al. (2013) employed when applying the Regional Ocean Modeling System in the region. They ascribed the localized differences in sea surface temperature effect to the upwelling of deeper, colder water. The results we obtain with HYCOM for 2014 mirror those of Hickey et al. (2013).

The water properties predicted by HYCOM constitute the boundary conditions for SSM. Consequently, as is expected, upwelled water properties from HYCOM are reflected in SSM. For example, at a location near a reported upwelling index (NOAA, 2021), which in 2014 peaked in August, HYCOM and Global Ocean Data Assimilation System (GODAS) both predict a nearly identical curvilinear temperature-depth relationship. Figure D-2 (upper right plot) shows the temperature-depth profiles at two locations near the continental shelf, a HYCOM/GODAS grid cell and the nearest (35 km) SSM node 42 for August 2014. The adjacent SSM cell reflects colder temperatures near the surface that may be due to the influence of the colder well-mixed surface waters exiting the SJF. As expected, SSM also predicts the curvilinear temperature-depth pattern expected from the influence of the continental shelf boundary based on HYCOM predictions.

Further evidence of the impact of upwelled waters in the coupled HYCOM-SSM boundary comes from comparisons with depth profile patterns in the Strait of Juan de Fuca. Davenne and Masson (2001) analyzed an extensive set of temperature and salinity observations in the Strait of Juan de Fuca. They found and documented that in the Strait of Juan de Fuca the deeper water reaches its maximum temperature in the winter, when the surface water is at its coldest, so the deeper water is colder in the summer (July) than in the winter (January). The SSM shows the same pattern Davenne and Masson (2001) observed, as shown near the entrance of Strait of Juan de Fuca (Figure D2, upper left plot).

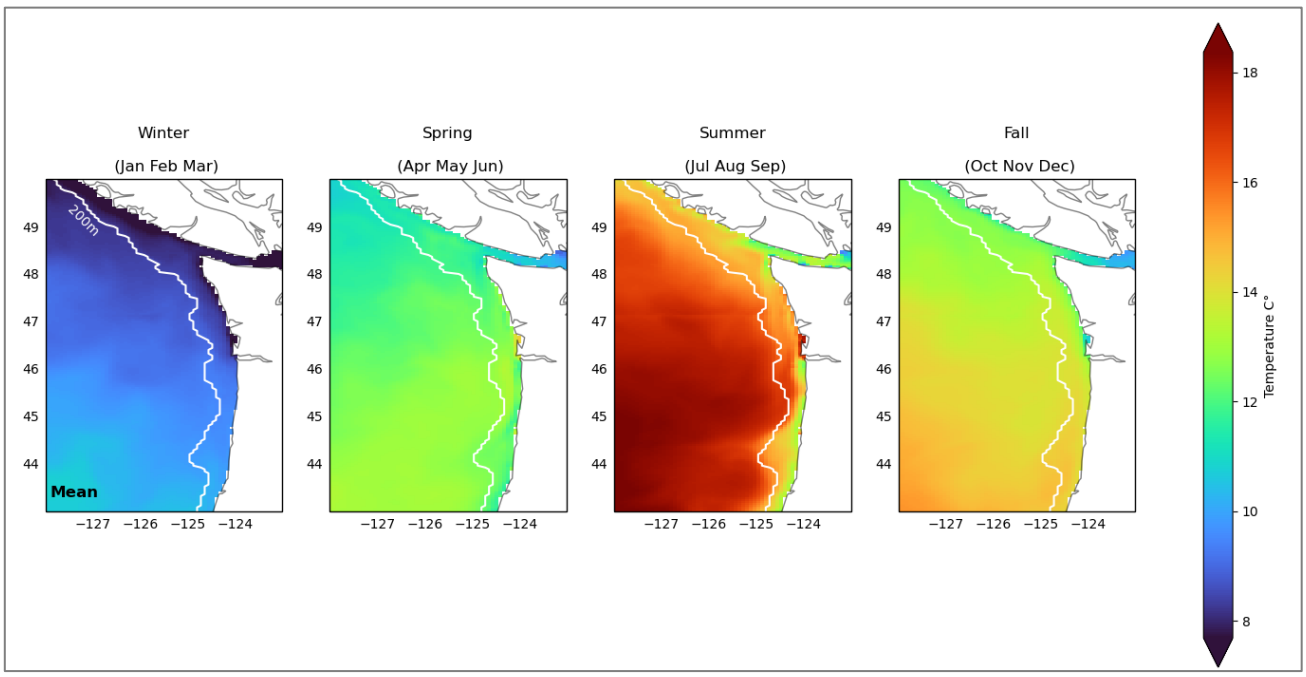

Figure D1. 2014 Seasonally averaged HYCOM sea surface temperature predictions along the Pacific Northwest Coast. 200m contour line represents the continental divide.

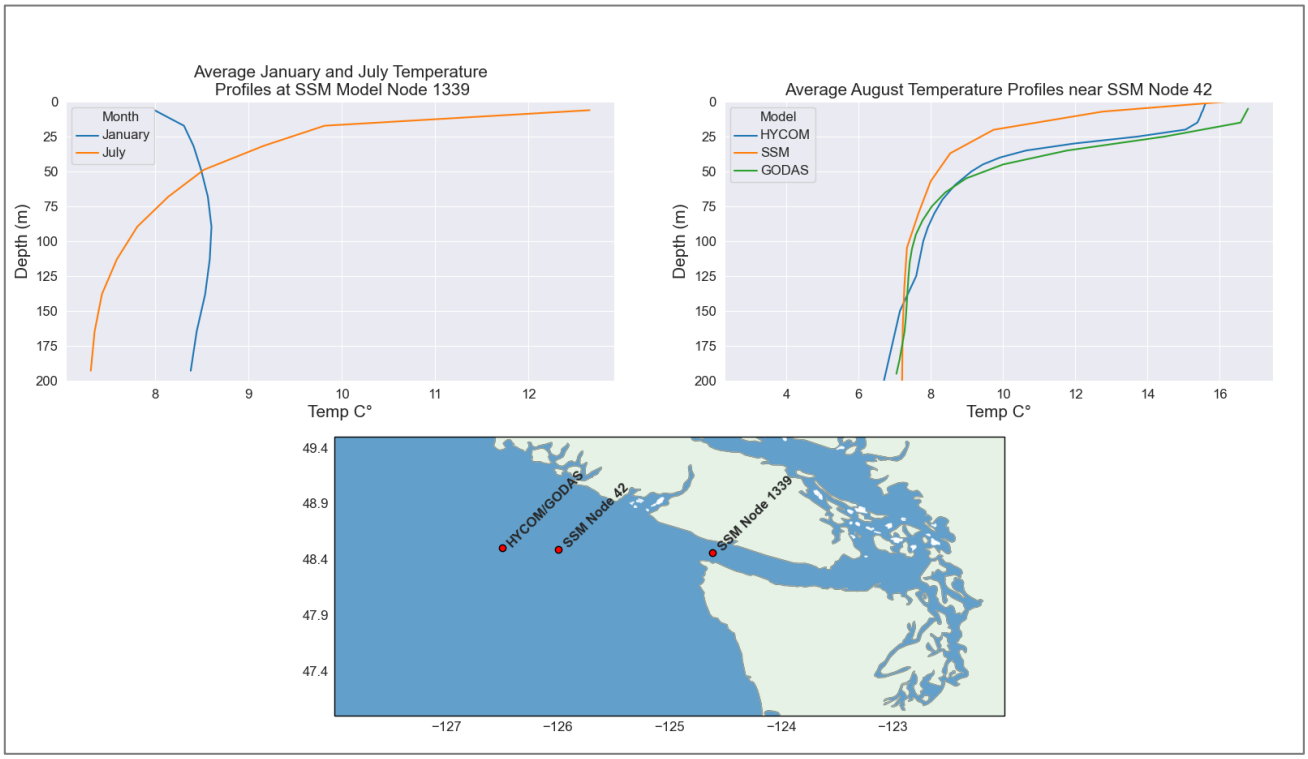

Figure D2. Comparison of SSM summer vs. winter temperature profiles at the entrance of Strait of Juan de Fuca (upper left plot), evaluation of August temperature profiles for different models, near the continental divide (upper right plot), and map of the locations used for assessment (bottom).

HYCOM is operated and maintained through a collaborative effort between the U.S. Navy and NOAA National Centers for Environmental Prediction (NCEP), and is sponsored by the Global Ocean Data Assimilation Experiment (GODAE). HYCOM outputs are available for download at https://www.hycom.org/. These outputs of HYCOM predictions are validated using the U.S Navy Global Ocean Forecast System (GOFS). Among other procedures, GOFS assimilates a network of observational data together, flags and omits data deemed unsuitable, and uses quality assured data to validate and adjust HYCOM predictions of a given variable in a way that is dynamically consistent across variables. (Cummings et al. 2013).

Because HYCOM is a hydrodynamic model and does not predict any water quality variables, regressions using observed salinity data were fitted for select variables. These regressions were used with HYCOM salinity to solve the open boundary conditions for SSM.

Methods

Ocean boundary input files for SSM for the year 2014 were created using the latest operational HYCOM outputs (GOFS 3.1 Reanalysis). Before creating OBC input files for SSM FVCOM and ICM, the following pre-processing steps were required:

- **Time zone adjustment**

  HYCOM outputs, which are referenced to Coordinated Universal Time (UTC), were paired with SSM outputs in Pacific Standard Time (PST) by selecting the nearest time to PST (PST = UTC-8). Due to the three-hour temporal resolution of HYCOM, UTC-9 was used as an approximation for PST.

- **Unpacking encoded values**

  In order to maintain exact precision, HYCOM default values are encoded and require an offset and scale factor to transform them into meaningful data. Offsets and scale factors can be found when accessing HYCOM data from the OpenDap Dataset Access Form located at https://www.hycom.org/.

- **Sub-setting HYCOM to SSM boundary nodes**

  HYCOM grid subset to SSM boundary node point locations, reducing the model dimensions from 4D to 3D.

- **Interpolating missing data in time**

  For missing timestamps, linear interpolation in time was iteratively performed for each given vertical layer at a particular SSM boundary node. A small-scale qualitative assessment of interpolated values for temperature and salinity revealed the interpolation to be adequate, following the general pattern of HYCOM predictions (Figure D3).

- **Holding water quality and hydrodynamics constant for deeper depth**

  Ahmed et al. (2019) found that constant values below a depth of about 150 meters at the open boundary, near the continental shelf, resulted in improved SSM performance. Accordingly, temperature and salinity values were held constant below 125 and 200 meters, respectively.

- **Binning HYCOM layers to SSM**

  Before creating OBC input files for FVCOM, HYCOM layers must be matched to the appropriate SSM layers; a process we refer to as ‘binning’. HYCOM layers were binned to SSM layers using the methods described in Appendix D of Ahmed et al. (2019). Due to large bathymetry

discrepancies between HYCOM and SSM, HYCOM bathymetry was first extended to match SSM.

HYCOM bathymetry is substantially shallower than SSM bathymetry in certain areas where the two model domains overlap. For example, node 35, located just past the continental shelf (Figure D3), is the deepest SSM node. This location is represented with a water column depth of 200 meters in HYCOM but a depth of 600 meters in SSM. Because HYCOM inputs to SSM ultimately are viewed in terms of SSM, initial binning methods tended to reduce stratification. Using node 35 as an example, if the 200 meter HYCOM water column was binned into 10 SSM layers, SSM would view layer 10 temperature and salinity values to be occurring at 600 meters (although the predictions were from 200 meters). Therefore, HYCOM layers were binned *after* they were extended to match SSM bathymetry. To extend HYCOM bathymetry to SSM, the observation from the deepest HYCOM layer was used to represent all depths below the HYCOM depth and up to deepest SSM layer (Figure D4).

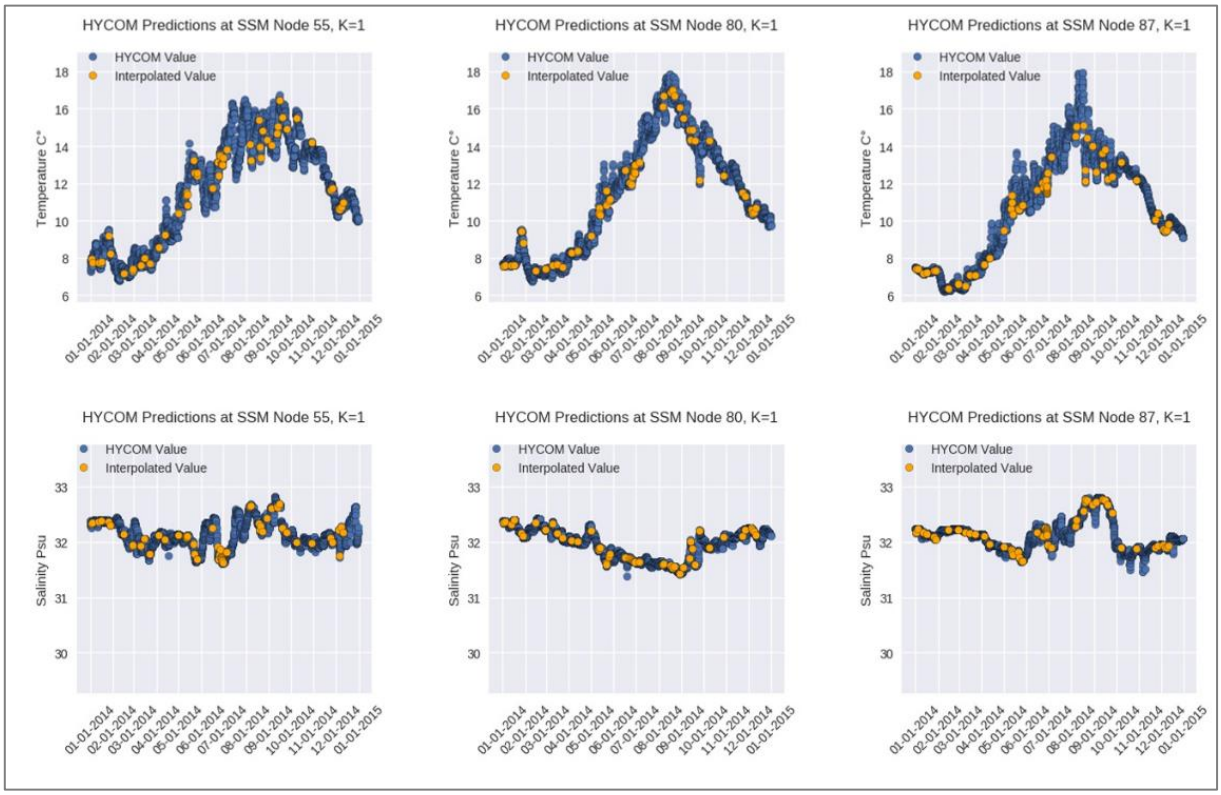

Figure D3. Time series plot of HYCOM interpolated temperature and salinity values for missing timestamps at layer 1 (K=1) for three select SSM boundary nodes.
Although qualitative, these plots show that interpolated values are following the same general pattern as HYCOM predictions.

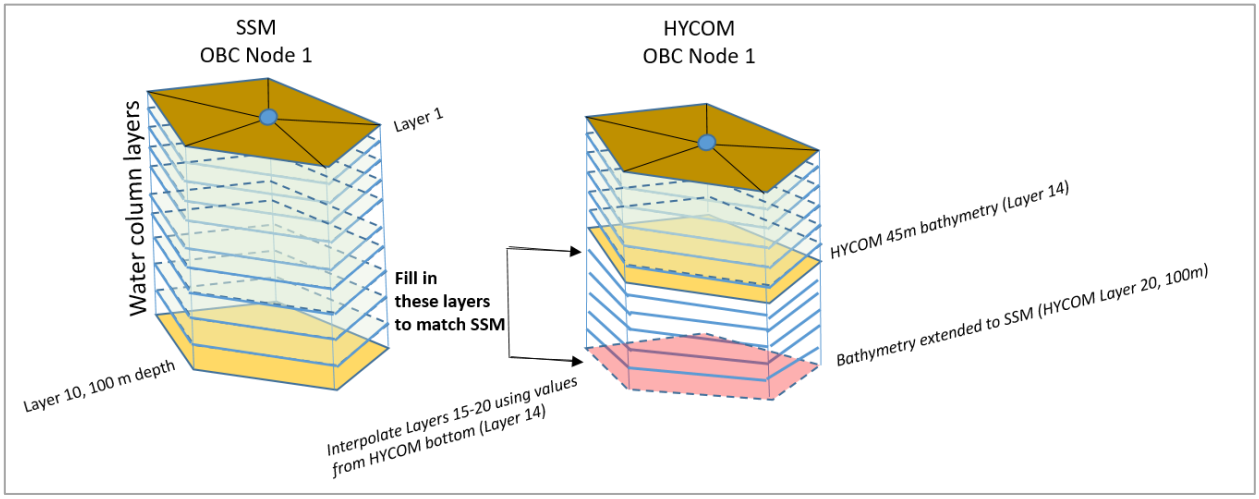

Figure D4. Illustrative example of interpolation scheme used to match HYCOM bathymetry to SSM bathymetry.
HYCOM layer with closest bathymetry to SSM is determined along with the number of layers to be interpolated (six in the figure). Missing values in these new layers are then interpolated using values from the previous HYCOM bottom layer.

As mentioned previously, HYCOM does not simulate all the water quality variables needed by the water quality component of SSM, ICM. Therefore, in order to develop ICM OBC input files, regressions based on salinity were developed to predict water quality parameters. Piecewise regressions provided by Ryan McCabe (personal communication, Oct 3, 2019) of the Joint Institute for Study of the Atmosphere and Ocean (JISAO) were used to predict dissolved oxygen (DO), dissolved inorganic carbon (DIC), alkalinity, and nitrate. Regressions were fit using observed data. However, predictions for different variables were made using HYCOM salinity as inputs to the piecewise regressions. The remaining 28 variables needed by ICM that were not predicted using regressions were developed using DFO data in the same way as has been done in previous SSM work.

Evaluation of HYCOM-based OBC for SSM

To assess the validity of using HYCOM model outputs to solve SSM OBC, an initial validation dataset consisting of NOAA (2011 and 2013) and DFO (2014) cruise data were compiled. The dataset was subset to exclude all but 10 sampling locations that were within an SSM OBC grid cell (Figure D5). Observational time and depth were transformed to match HYCOM SSM OBC input file format (HYCOM binned to 10 SSM vertical layers). This consisted of rounding observed date-times to the nearest 3 hours and binning depths to 10 SSM layers using the methods described in (Ahmed et al. 2019). Observed data were then paired with HYCOM accordingly, based on matching layers and datetimes.

Cross validation of HYCOM and regressed HYCOM predictions using NOAA and DFO observations for the years 2011, 2013, and 2014 generally demonstrated good performance. Model variables for temperature and salinity and the regressed dissolved oxygen (DO) variable displayed strong correlation with observed data (Table D1). The comparison showed acceptable levels of random error (RMSE) for boundary conditions and a tendency to slightly over-predict. The remaining regressed

model parameters displayed a relatively strong degree of correlation with observed data but a slight tendency to over-predict with a relatively high amount of random error. DIC predictions in particular, did not perform as well as other parameters as shown by its relatively high normalized RMSE and lower Pearson's R (Table D1). The global statistics mentioned give a good sense of overall model performance and relative differences between different parameters.

To further assess model performance over time, profile plots of data from stations with more than one sampling period for a given parameter were analyzed. Temporal data availability was limited for the given dataset. None of the stations assessed had more than two time periods of data. DIC and alkalinity data are available for only one collection period for a given station.

Despite limited temporal resolution for each station, profiles indicate that HYCOM captures overall patterns, even during time periods with maximum deviation from observed values, as shown in selected examples in Figure D6.

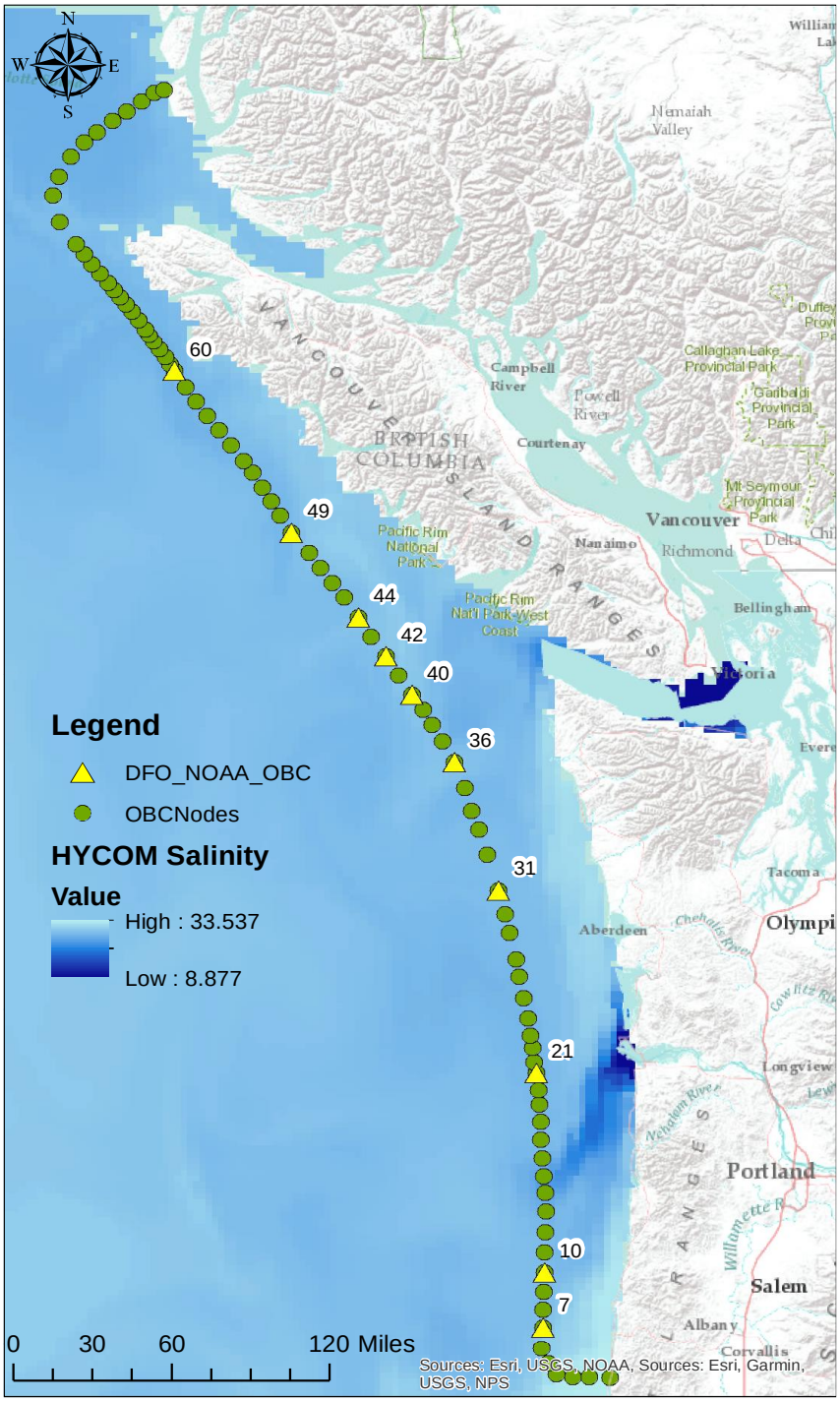

Figure D5. Map of SSM open boundary nodes (OBC) (green circles) and DFO/NOAA stations (yellow triangles).
HYCOM predictions are available at each of the SSM OBC nodes. DFO/NOAA stations coinciding with SSM OBC nodes were used to validate HYCOM model predictions for a given point in time.

Table D1. Summary statistics for cross validation of HYCOM predictions with DFO and NOAA data.

Variable	Years	N	R	RMSE	Bias	NRMSE[1]
Temperature	2011,2013,2014	314	0.86	1.38	0.40	0.54
Salinity	2011,2013,2014	314	0.86	0.49	0.15	0.54
DO	2011 and 2014	218	0.91	1.34	0.27	0.42
NO23	2011,2013,2014	231	0.74	0.13	0.05	0.74
DIC	2011	124	0.70	83.0	34.65	0.79
Alkalinity	2011	118	0.76	26.6	9.84	0.70

[1]Normalized RMSE: RMSE standardized by dividing RMSE by observed standard deviation for a given variable. This allows direct comparison of error performance between different variables.

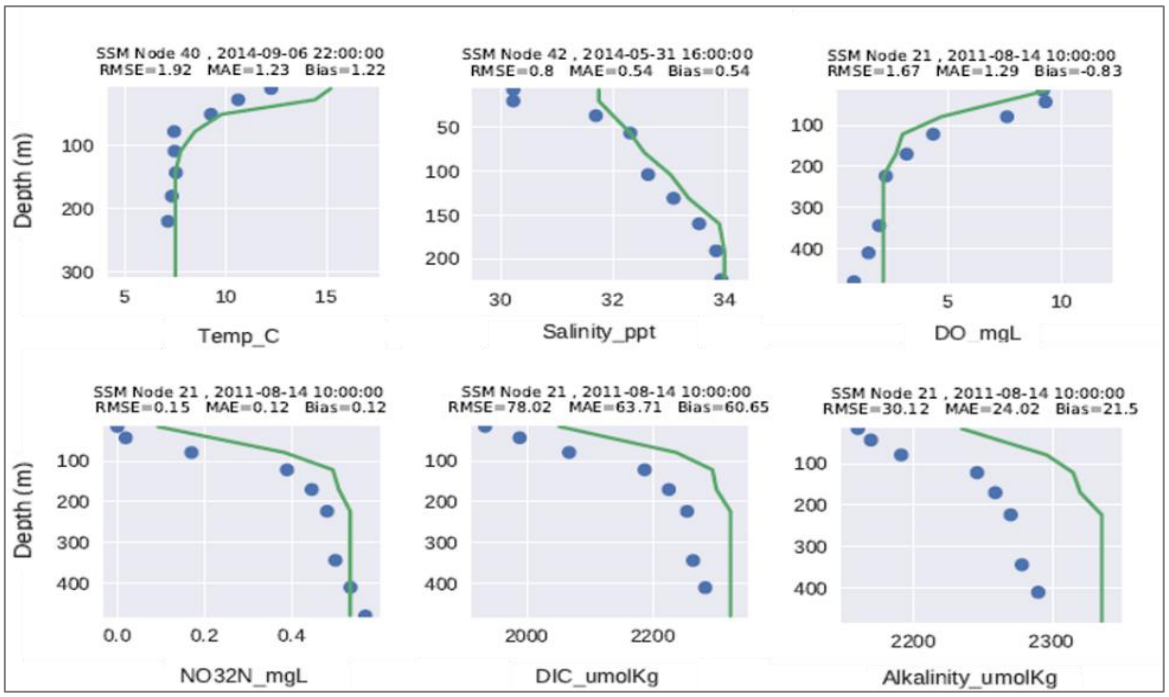

Figure D6. Depth profile plots of HYCOM predictions vs. DFO and NOAA observed data (2011, 2013, and 2014).
Refer to Figure D5 for node locations.

Temperature and salinity predictions generated by HYCOM were nearly perfect in capturing the general characteristics of observed profiles; model error for these parameters occurred almost exclusively in the surface (Figure D7).

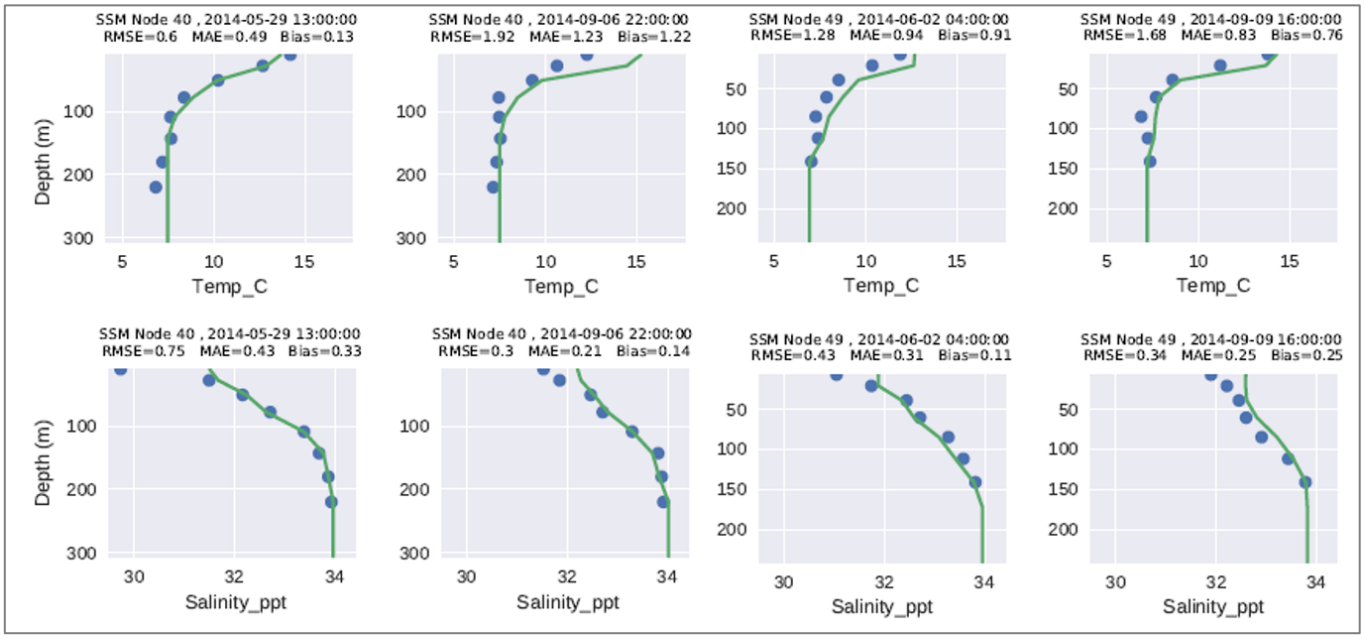

Figure D7. Depth profile plots of HYCOM (green line) predictions vs. DFO and NOAA observed temperature and salinity data at stations where more than one time period of data were available.

Unlike temperature and salinity however, DO prediction errors were not constrained to just surface layers. Performance for DO by contrast exhibited signs of seasonal dependence. Predicted and observed DO profiles coincided nicely in the late spring (May and June) with near zero bias and low RMSE. In the fall however, observed and predicted DO profiles exhibited relatively higher deviations with RMSE values up to three times greater than in the spring (Figure D8).

Nitrate-nitrite performance showed many similarities to DO with regards to error distribution; however, there were no clear spatial-temporal patterns. Higher RMSE (0.13 and 0.11 mg/L) values for nitrate-nitrite at nodes 40 and 49 respectively, (Figure D8) were primarily due to the presence of a few outliers. Overall, HYCOM nitrate-nitrite profiles appear to be an appropriate fit to the observed data (Figure D8).

Alkalinity and DIC predictions were always greater than observed data (Figure D9). Despite this, the model captured the overall characteristics of these profiles. Most of the error for these parameters appear to be associated with a relatively consistent shift of values across all depths, indicating that error could potentially be reduced in the future by applying a simple offset.

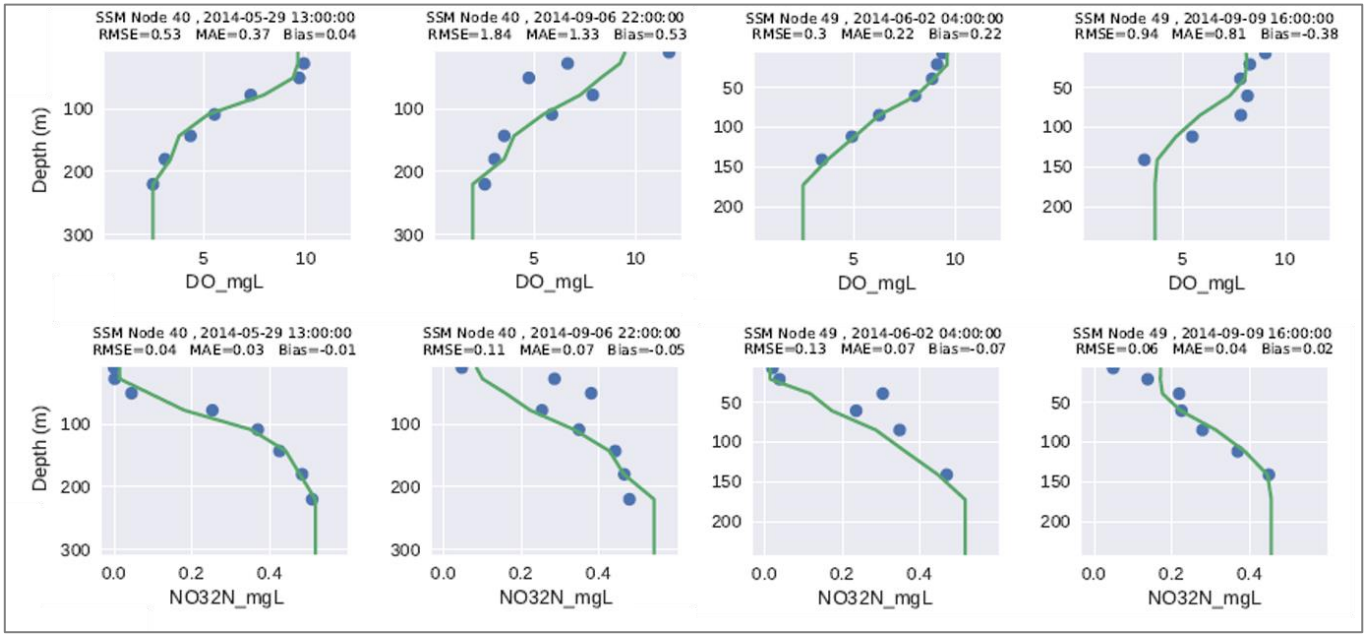

Figure D8. Depth profile plots of HYCOM (green line) predictions vs. DFO and NOAA observed dissolved oxygen (DO) and nitrate-nitrite data at stations where more than one time period of data were available.

Refer to Figure D5 for node locations.

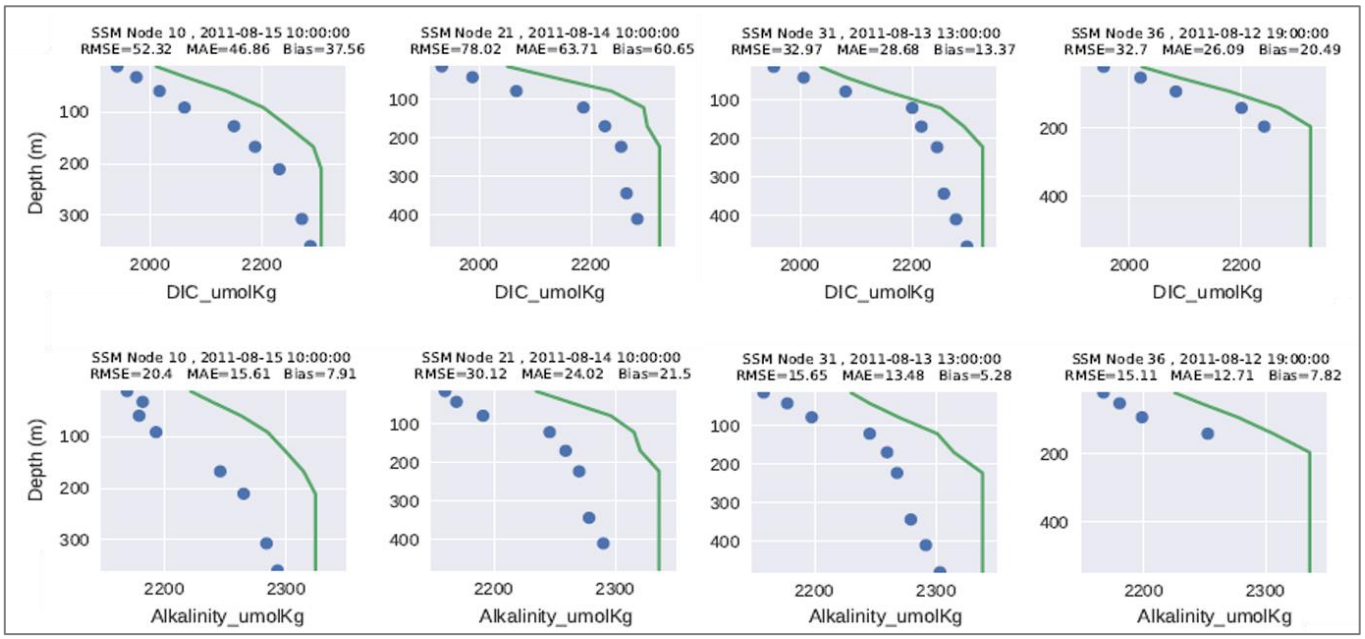

Figure D9. Depth profile plots of HYCOM (green line) predictions vs. NOAA dissolved inorganic carbon and alkalinity data.

Refer to Figure D5 for node locations.

Since the findings of this analysis were hampered by sparse spatial and temporal resolution of the validation dataset, a robust evaluation of the HYCOM-based OBC was not achieved. This assessment will be expanded upon as data becomes available and as time allows for compiling new data. In the future, the validation dataset will be expanded to include DFO data from 1999-2013. Due to post-processing time constraints these data were not incorporated into this analysis. While a more rigorous cross validation will be performed in the future, these preliminary findings point to the incorporation of HYCOM into SSM as a reasonable alternative.

Our next analysis involved quantifying the SSM response to the HYCOM-based OBC. SSM performance was measured by RMSE and bias and improved slightly with HYCOM-based OBC for temperature. In terms of salinity and DO, HYCOM maintained and slightly improved the correlation coefficient respectively. However, it also increased the bias and RMSE. As shown in Table D2, the relative error (RE) of the model with and without HYCOM were nearly equivalent for all parameters. Certain areas within SSM may be more sensitive to the addition of HYCOM, something that will be explored in the future.

Table D2. Goodness of fit statistics for 2014 SSM with (a) and without (b)HYCOM.

Parameter	R		RMSE		RE[1]		Bias		N[2]
Temperature	0.95[a]	0.94[b]	0.78[a]	0.90[b]	0.06[a]	0.07[b]	-0.23[a]	-0.42[b]	97687
Salinity	0.82[a]	0.82[b]	0.84[a]	0.82[b]	0.02[a]	0.02[b]	-0.44[a]	-0.39[b]	97487
DO	0.83[a]	0.82[b]	0.99[a]	0.92[b]	0.11[a]	0.10[b]	-0.43[a]	-0.26[b]	96152
Chla[3]	0.52[a]	0.52[b]	3.42[a]	3.40[b]	0.71[a]	0.71[b]	-0.11[a]	-0.13[b]	87671
NO23	0.84[a]	0.83[b]	0.07[a]	0.07[b]	0.15[a]	0.15[b]	0[a]	-0.01[b]	1934
NH4	0.35[a]	0.36[b]	0.02[a]	0.02[b]	0.58[a]	0.57[b]	0[a]	0[b]	1595
PAR	0.61[a]	0.61[b]	6.00[a]	5.99[b]	0.78[a]	0.78[b]	-0.81[a]	-0.80[b]	82178

[1]Relative Error; [2]Sample Number
[a] Model run with HYCOM; [b] Model run Without HYCOM

Appendix E – Scenario 4 Methods

Scenario 4 was limited to evaluating increases in effluent flows from all U.S. wastewater treatment plants (WWTPs) within the model domain to reflect estimated increases in population by 2040. As population increases, the amount of wastewater being generated and treated will also increase, assuming all other factors remain constant. While there are a total of 99 marine point sources included in the Salish Sea Model (SSM), including 11 industrial facilities and nine WWTPs in Canada, for this scenario, flows were increased only for the 79 WWTPs in the U.S.

Scenario 4 is not a true 'future' scenario because it does not include other changes that the Puget Sound region will experience by 2040, such as: (1) climate change prediction and its influences on the ocean boundary and river hydrology, (2) development and land use as a result of population growth, and/or (3) management of that growth, or watershed nutrient management activities. While these factors are important to evaluate, they were beyond the scope of the 'Year 1' Optimization Scenarios.

We selected 2014 as the baseline year for all scenario 4 future 2040 wastewater simulations. This year was chosen since it is the most recent hindcast year we have simulated to date. Except for flows for municipal WWTPs in the U.S., scenario 4 runs were exactly the same as the 2014 baseline scenario. This means that Scenario 4 had:

- 2014 meteorological forcing and ocean boundary conditions.
- 2014 watershed flows and nutrient concentrations for all rivers and streams in the model domain.
- 2014 flows and nutrient concentrations for all marine point sources in Canada.
- 2014 flows and nutrient concentrations at all industrial facilities.
- 2014 nutrient concentrations for effluent from all U.S. WWTPs, i.e. this scenario assumes that there are no changes to wastewater treatment methods from 2014 through 2040 (with the exception of three facilities, described in more detail below).
- 2040 future effluent flows from all 79 U.S. WWTPs based on projected future population.

Population estimates were acquired from the Office of Financial Management's (OFM) forecasting division[3], who are required to develop these projections. OFM provides both historic population estimates (at an annual interval based on interpolation between each 10-year census) as well as population forecasts and projections for individual cities and counties in the State of Washington as part of the Growth Management Act.

Future population estimates are available at the county level and are updated every five years as part of the Growth Management Act requirements. The latest update was in 2017 and includes projected population for each year through 2040. Roberts et al., (2014) previously used the 2012 projections to estimate future wastewater loads for a prior version of the SSM. More detail on the population projection methods and assumptions can be found in OFM (2018).

[3] https://www.ofm.wa.gov/washington-data-research/population-demographics

For Scenario 4, two model runs were conducted – one using the 'Low' population growth projection, and a second using the 'High' population growth projection.

Future 2040 wastewater flows at all U.S. municipal wastewater facilities were estimated as follows:

- 2014 population estimates and 2040 projected population estimates (for both 'Low' and 'High' alternatives) for each county in the SSM domain were compiled from OFM.
- A 'flow scalar' (Table E1) was calculated for each county as follows:

$$\textbf{\textit{Flow Scalar}} = \frac{2040\ projected\ population}{2014\ population}$$

- Monthly 2014 wastewater flows for each U.S. WWTP were multiplied by the flow scalar associated with the county in which each facility is located to estimate the 2040 wastewater flows. This method to estimate 2040 wastewater flows assumes the following:
  - Each wastewater facility's service area population experiences the same growth as the county in which it is located.
  - The per capita wastewater flow does not change during 2014 through 2040.
  - The relative effect of population growth on wastewater flows is proportional year-round (in reality, there would be a proportion of the existing wet weather flows that are influenced by inflow and infiltration, and would not be influenced by population growth, but in this simplified approach, this is not taken into account).
  - A model input file that represented this scaled 2040 wastewater flows was developed for the SSM.

Table E1. Population estimates for 2014, projections for 2040 (Low and High), and calculated flow scalars for each county included in the Salish Sea Model (SSM) domain.

County	2014 Population	Low 2040 Pop. Projection	High 2040 Pop. Projection	Low 2040 Flow Scaler	High 2040 Flow Scaler
Clallam*	72,500	65,741	93,763	0.9068	1.2933
Island*	80,000	73,240	127,581	0.9155	1.5948
Jefferson*	30,700	29,402	50,850	0.9577	1.6564
King	2,017,250	2,439,025	3,118,353	1.2091	1.5458
Kitsap	255,900	255,945	420,094	1.0002	1.6416
Mason	62,000	70,013	99,664	1.1292	1.6075
Pierce	821,300	927,797	1,211,501	1.1297	1.4751
San Juan*	16,100	15,132	25,990	0.9399	1.6143
Skagit	119,500	138,164	206,280	1.1562	1.7262
Snohomish	741,000	905,221	1,263,840	1.2216	1.7056
Thurston	264,000	312,061	438,789	1.1820	1.6621
Whatcom	207,600	240,495	342,477	1.1585	1.6497

*These counties are all projected to experience a *decrease* in population under the 'Low' 2040 alternative, but an increase under the 'High' 2040 alternative.

During the process of developing future WWTP flows for 2040, we asked the permit writers of each of the 79 WWTPs whether:

- Any facilities had already experienced changes to their treatment methods or discharge location since 2014 that should be incorporated into Scenario 4 – three facilities had experienced changes, which are described below.
- Any facilities had *known or anticipated* future changes (post-2019) that would influence their flows or discharge location, which should be reflected in Scenario 4. No permit writers responded 'yes' to this question.

The three facilities have had changes to their operations since 2014, including:

- **Port Gamble WWTP** (SSM ID #541): this facility was decommissioned in 2017. A new Port Gamble Facility was built to treat wastewater, but the effluent discharges to the ground. Discharge from this facility was therefore set to zero for Scenario 4 (but exists in the existing 2014 scenario).
- **Oak Harbor RBC** (SSM ID #553) - the City of Oak Harbor used to operate this facility, but it has not been in operation since September 2010. During this period, the city was sending its wastewater flows to the nearby Oak Harbor Lagoon (which handles waste from the U.S. Navy Military Base), which discharges to Crescent Bay. However, starting in December 2018, the city started sending its wastewater to the newly built Oak Harbor Clean Water Facility (CWF) that discharges to Oak Harbor.
- **Oak Harbor Lagoon** (SSM ID #552) – this facility handles waste from the U.S. Navy Military Base, but has also been treating wastewater flows from the City of Oak Harbor since September 2010. However, it significantly scaled down its operations in December 2018 (from a 2.5 mgd plant to a 0.57 mgd plant) when the city stopped sending its wastewater to them. The permit used to be co-managed between Ecology and EPA, but is now solely managed by EPA.

To accurately represent the two Oak Harbor facilities in Scenario 4, we updated their effluent concentrations in the model to reflect the most recent data available from their discharge monitoring reports (DMRs). At the time this analysis was conducted, monthly flow and concentration for both facilities were available from December 2018–October 2019. These data were used to develop a year-long monthly time-series of flows and concentrations for each facility that best represented calendar year 2019. Since we did not yet have data for the last two months of 2019, we used October 2019 effluent data to also characterize November 2019 discharge, as well as December 2018 effluent data to represent December 2019 discharge.

Both facilities had concentration data for the following parameters: ammonia, total nitrogen, nitrate + nitrite, phosphorus, and BOD5. Other parameters needed by the SSM were calculated using stoichiometry (organic nitrogen, organic phosphorus, and dissolved organic carbon) or using previous methods as described in Mohamedali et al. (2011).

When estimating future 2040 flows for these two facilities, which are both located in Island County, we used 2019 (instead of 2014) as the base year to calculate the flow scalers, since this is the first full year reflected by their new operations. Therefore, OFM population data for the year 2019 for Island County was used to calculate the flow scalers (Table E2).

Table E2. Island County population estimates for 2019, projections for 2040 (Low and High), and calculated flow scaler used to scale the flows for the two Oak Harbor facilities.

County	2019 Population	Low 2040 Pop. Projection	High 2040 Pop. Projection	Low 2040 Flow Scaler	High 2040 Flow Scaler
Island County	84,820	73,240	127,581	0.8635	1.5041

2040 Wastewater Nutrient Loads

Future nutrient loads were calculated by multiplying future flows by existing concentrations. Figure E1, Table E3, and Figure E2 compare TN and TOC nutrient loads into different regions of WA waters under the 2040 'low' and 2040 'high' projections, relative to 2014 loads.

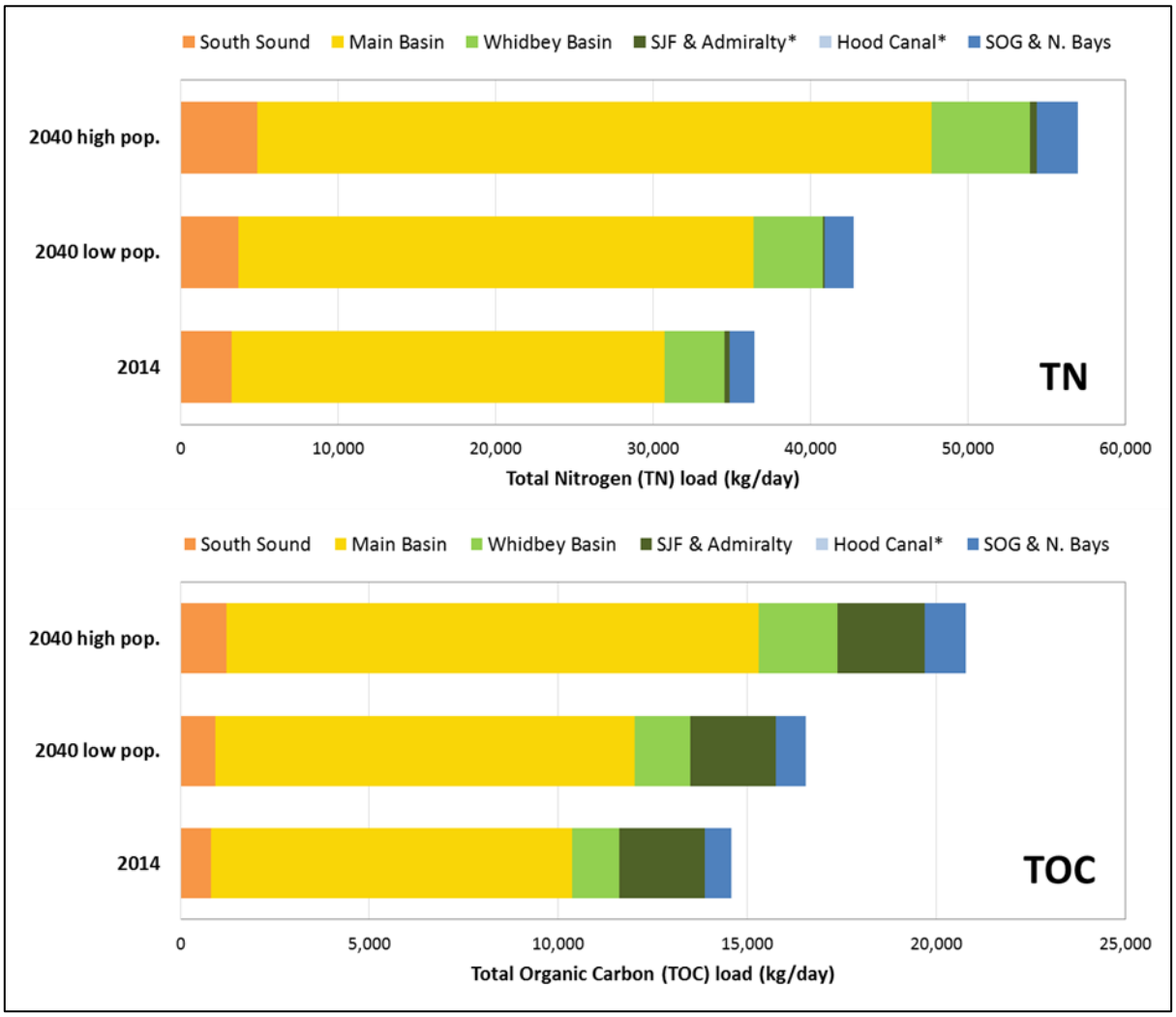

*Hood Canal has a very small TOC and TN load of less than 2 kg/day, SJF & Admiralty has a small annual DIN load of less than 500 kg/day for all scenarios (2014, 2040 low and 2040 high), and is therefore not easily visible in the plot above. The same is true for Hood Canal, which has loads of less than 1 kg/day.

Figure E1. Comparison of 2014 and 2040 (high and low) annual average total nitrogen (TN, top) and total organic carbon (TOC, bottom) loading from facilities discharging into different basins of WA waters of the Salish Sea.

Table E3. Percent increase in annual average dissolved inorganic nitrogen (DIN) and total organic carbon (TOC) loads under Scenario 4, relative to 2014 loads.

Nutrient Load	Percent increase from 2014 with 'Low' projection	Percent increase from 2014 with 'High' projection
WWTP DIN load	17%	56%
Total DIN load (River + WWTP)	7.9%	26%
WWTP TOC load	14%	43%
Total TOC load (River + WWTP)	0.6%	2.0%

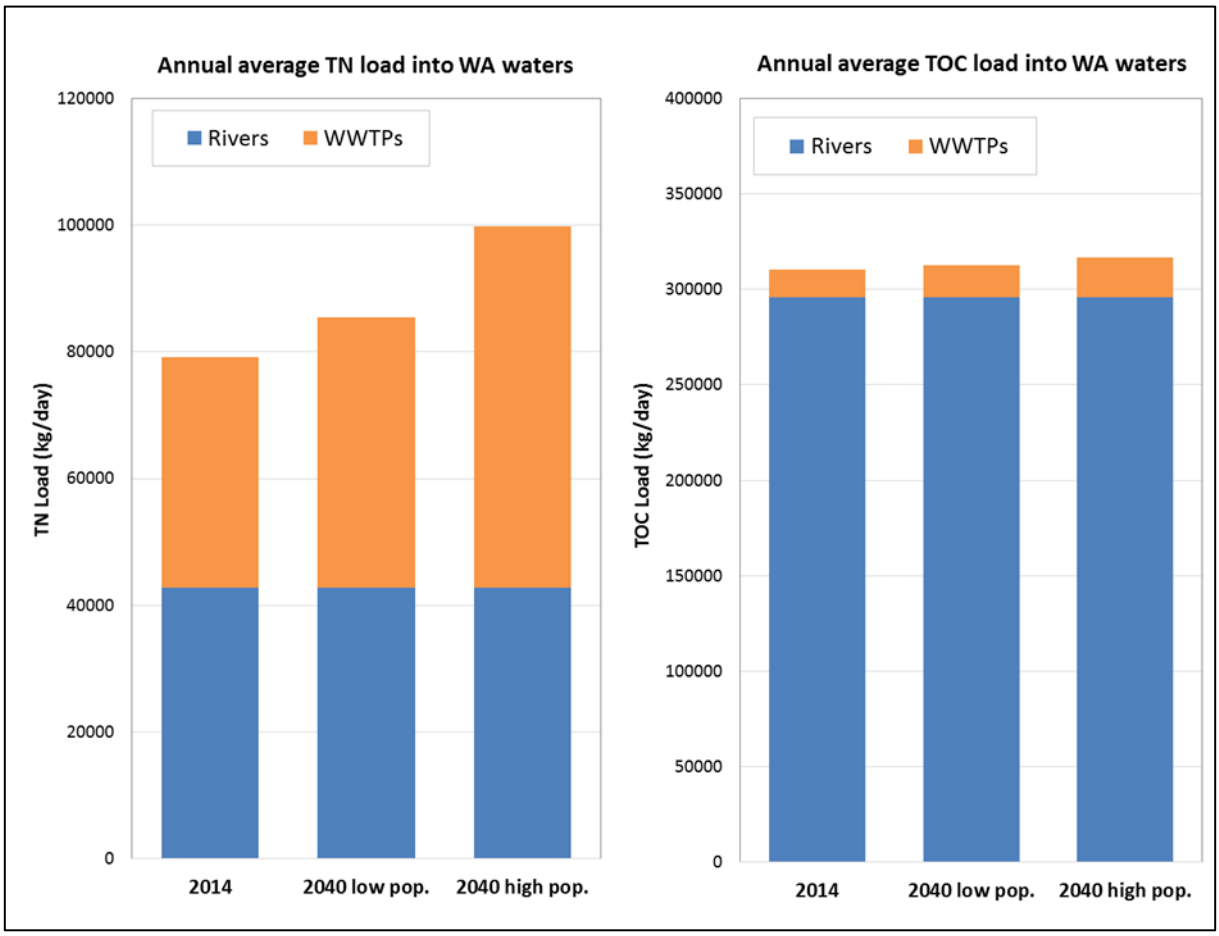

Figure E2. Comparison of annual average river (blue) and wastewater (orange) dissolved inorganic (DIN) and total organic carbon (TOC) loading into the WA waters of the Salish Sea under the 2014 scenario and future 2040 High and Low flow projections.

Comparison to Design Flows

When contacting permit writers, we also asked them to provide us with the design flows for each facility that they manage. This information was used only to compare the estimated annual average and maximum monthly future 2040 flows to design flows, but it did not influence scenario 4 model inputs. The results of this comparison are provided in Table E4. Some facilities currently have excess capacity, while others are already operating close to their design limits. By 2040, a number of facilities are exceeding, or getting close to exceeding, their design capacity under both the 2040 Low and High flow projections (25% of facilities under the Low projection, and 56% of facilities under the high based on the max annual flow).

Table E4. Table of all U.S. municipal wastewater facilities included in the SSM as well as each facility's design flow (Q max-month) and the estimated future 2040 flows (annual mean and maximum monthly) for both 'Low' and 'High' population growth alternatives.

Shaded cells with bold numbers indicate that the estimated future 2040 flow value is greater than the permitted design flow value. Numbers in bold (without shading) indicate that the estimated future flow is within 10% of the permitted design flow value. Facilities are organized alphabetically by county, and then by size (design flow).

SSM Name	Permit No.	County	Design Flow/max monthly flow (mgd)	Mean Annual Flow 2040 Low (mgd)	Max Annual Flow 2040 Low (mgd)	Mean Annual Flow 2040 High (mgd)	Max Annual Flow 2040 High (mgd)
Port Angeles	WA0023973	Clallam	10.8	2.263	3.990	3.226	5.688
Sequim	WA0022349	Clallam	1.67	0.391	0.548	0.557	0.782
Makah	WA0023213	Clallam	0.94	0.229	0.351	0.327	0.500
Sekiu	WA0024449	Clallam	0.145	0.063	0.105	0.090	**0.150**
Clallam Bay POTW	WA0039845	Clallam	0.12	0.032	0.045	0.045	0.065
Clallam DOC	WA0024431	Clallam	0.12	**0.119**	**0.160**	**0.170**	**0.228**
Oak Harbor RBC	WA0020567	Island	3.2	1.678	1.994	**2.923**	**3.474**
Whidbey Naval Station	WA0003468	Island	0.85	0.243	0.341	0.423	0.595
Oak Harbor Lagoon	WAS026611	Island	0.57	0.398	**0.768**	**0.693**	**1.337**
Coupeville	WA0029378	Island	0.44	0.162	0.211	0.282	0.368
Langley	WA0020702	Island	0.15	0.063	0.073	0.110	0.127
Penn Cove	WA0029386	Island	0.1	0.030	0.046	0.053	0.080
Port Townsend	WA0037052	Jefferson	2.05	0.766	0.893	1.325	1.545
Port Ludlow	WA0021202	Jefferson	0.32	0.164	0.239	0.284	**0.412**
West Point	WA0029181	King	215	115.188	186.588	147.265	**238.514**
South King	WA0029581	King	144	87.008	125.100	111.247	**159.953**
Lakota	WA0022624	King	10	6.153	7.842	7.868	**10.029**
Midway	WA0020958	King	9	5.292	7.806	6.765	**9.981**
Salmon Creek	WA0022772	King	8.1	3.102	5.293	3.967	6.767
Miller Creek	WA0022764	King	7.1	4.335	**6.957**	5.543	**8.895**
Redondo	WA0023451	King	5.6	3.605	**6.354**	4.609	**8.123**
Vashon	WA0022527	King	0.52	0.154	0.267	0.197	0.341
Bremerton	WA0029289	Kitsap	11/15[4]	5.356	8.568	8.792	**14.064**

[4] This facility has a Q max-month flow of 11 mgd during May-Sept and 15 mgd during Oct-Apr.

SSM Name	Permit No.	County	Design Flow/max monthly flow (mgd)	Mean Annual Flow 2040 Low (mgd)	Max Annual Flow 2040 Low (mgd)	Mean Annual Flow 2040 High (mgd)	Max Annual Flow 2040 High (mgd)
Central Kitsap	WA0030520	Kitsap	6	3.566	4.437	**5.854**	**7.283**
Port Orchard	WA0020346	Kitsap	4.2	1.841	2.378	3.021	**3.903**
Bainbridge Island City	WA0020907	Kitsap	1.2	0.506	0.707	0.831	**1.160**
Manchester	WA0023701	Kitsap	0.46	0.190	0.280	0.311	**0.460**
Suquamish	WA0023256	Kitsap	0.4498	0.242	**0.432**	0.397	**0.709**
Kitsap Co Kingston	WA0032077	Kitsap	0.292	0.114	0.144	0.187	0.237
Bainbridge Kitsap Co 7	WA0030317	Kitsap	0.28	0.095	0.148	0.157	0.243
Messenger House	WA0023469	Kitsap	0.016	0.004	0.004	0.006	0.007
Port Gamble	WA0022292	Kitsap	N/A	facility decommissioned in 2017			
Shelton	WA0023345	Mason	4.41	2.251	**4.031**	3.204	**5.738**
Hartstene	WA0038377	Mason	0.186	0.091	**0.174**	0.129	**0.247**
Rustlewood	WA0038075	Mason	0.057	0.049	**0.079**	**0.069**	**0.113**
Alderbrook	WA0037753	Mason	0.04	0.022	0.029	0.031	**0.042**
Tacoma Central	WA0037087	Pierce	36	25.673	**42.681**	**33.524**	**55.737**
Chambers Creek	WA0039624	Pierce	25.48	22.071	**30.425**	**28.820**	**39.714**
Puyallup	WA0037168	Pierce	8.094	5.142	**9.011**	6.716	**11.768**
Tacoma North	WA0037214	Pierce	6.8	5.172	**8.582**	**6.754**	**11.207**
Fort Lewis	WA0021954	Pierce	6.3	2.475	5.195	3.232	**6.783**
Gig Harbor	WA0023957	Pierce	2.4	1.031	1.243	1.346	1.624
McNeil Is	WA0040002	Pierce	0.45	0.066	0.109	0.086	0.143
Taylor Bay	WA0037656	Pierce	0.029	0.003	0.008	0.004	0.011
Friday Harbor	WA0023582	San Juan	0.69	0.261	0.423	0.448	**0.727**
Eastsound Water District	WA0030571	San Juan	0.16	0.086	0.124	**0.148**	**0.213**
Roche Harbor	WA0021822	San Juan	0.1296	0.024	0.038	0.042	0.066
Rosario Utilities	WA0029891	San Juan	0.071	0.020	0.047	0.034	**0.081**
Fisherman Bay	WA0030589	San Juan	0.053	0.023	0.029	0.040	**0.050**
Eastsound Orcas Village	WA0030911	San Juan	0.015	0.003	0.005	0.005	0.008
Mt Vernon	WA0024074	Skagit	15	4.722	6.487	7.049	9.684
Anacortes	WA0020257	Skagit	4.5	2.455	3.572	3.666	**5.334**
La Conner	WA0022446	Skagit	0.52	0.348	0.431	**0.519**	**0.644**
Skagit County 2 Big Lake	WA0030597	Skagit	0.35	0.174	0.212	0.260	**0.316**
Swinomish	WA0024422	Skagit	0.1848	**0.208**	**0.306**	**0.311**	**0.457**
Brightwater	WA0032247	Snohomish	40.9	21.013	28.576	29.336	**39.897**
Everett Snohomish	WA0024490	Snohomish	40.3	14.335	25.038	20.012	34.944
OF100[5]	N/A	Snohomish	N/A	13.854	22.448	19.343	31.338
Marysville	WA0022497	Snohomish	12.7	3.818	7.621	5.331	10.641

[5] This outfall takes combined effluent from Everett Snohomish WWTP and Marysville WWTP. The flows of the individual WWTPs were scaled before being diverted to the OF100 outfall; it therefore does not have a design flow.

SSM Name	Permit No.	County	Design Flow/max monthly flow (mgd)	Mean Annual Flow 2040 Low (mgd)	Max Annual Flow 2040 Low (mgd)	Mean Annual Flow 2040 High (mgd)	Max Annual Flow 2040 High (mgd)
Edmonds	WA0024058	Snohomish	11.8	5.732	8.945	8.004	**12.489**
Lynnwood	WA0024031	Snohomish	7.4	5.412	**7.527**	**7.557**	**10.508**
Alderwood	WA0020826	Snohomish	6	4.050	**11.163**	**5.654**	**15.587**
Lake Stevens 002	WA0020893	Snohomish	5	3.187	4.099	4.450	**5.722**
Snohomish	WA0029548	Snohomish	2.8	1.731	**3.357**	2.417	**4.688**
Mukilteo	WA0023396	Snohomish	2.61	1.429	1.931	1.995	**2.696**
Stanwood	WA0020290	Snohomish	1.5	0.698	1.075	0.975	**1.500**
Tulalip	WA0024805	Snohomish	0.372	0.281	**0.364**	**0.392**	**0.508**
Warm Beach Campground	WA0029904	Snohomish	0.15	0.022	0.057	0.030	0.080
LOTT	WA0037061	Thurston	28	12.189	17.276	17.138	24.285
Tamoshan	WA0037290	Thurston	0.166	0.027	0.040	0.039	0.056
Boston Harbor	WA0040291	Thurston	0.039	**0.035**	**0.131**	**0.050**	**0.184**
Seashore Villa	WA0037273	Thurston	0.034	0.013	0.017	0.018	0.023
Carlyon	WA0037915	Thurston	0.022	**0.024**	**0.031**	**0.034**	**0.044**
Bellingham	WA0023744	Whatcom	18.6	14.422	**21.425**	**20.537**	**30.516**
Birch Bay	WA0029556	Whatcom	1.2	1.001	**1.264**	**1.425**	**1.799**
Lummi Goose Pt	WA0025666	Whatcom	0.482	0.310	**0.500**	**0.442**	**0.712**
Blaine	WA0022641	Whatcom	0.32	**0.743**	**1.098**	**1.058**	**1.563**
Lummi Sandy Pt	WA0025658	Whatcom	0.1643	0.141	**0.230**	**0.201**	**0.327**
Larrabee State Park	WA0023787	Whatcom	0.0052	0.004	**0.006**	**0.005**	**0.009**

Several facilities are served by combined (sewage plus stormwater) collection systems. Combined sewer overflows (CSOs), which represent wet-weather flows that exceed the peak hydraulic capacity of the WWTP and discharge from designated CSO outfalls, are not included in the SSM. All CSO systems are required to control overflows to a maximum of one untreated discharge per year per outfall. By 2040, construction of these controls should be completed. One of the control strategies is capture and storage of the combined sewage and stormwater for treatment at the wastewater facility. Similarly, municipalities without combined sewers may still have a significant amount of stormwater coming into their sewage collection system through leaking pipes and older direct connections. In both of these situations, scaling flows by population growth may not be accurate because the future amount of stormwater in the system is not directly proportional to population. It may go up with combined sewage treatment, or down with infiltration repairs in the collection system, or change due to rainfall patterns.

Appendix F – DO Assessment of Water Quality Standard

The aquatic life criteria in Puget Sound vary from 4 to 7 mg/ L, depending on the designated use locations with lower values in the terminal ends of some inlets and bays. The allowed cumulative anthropogenic impact or human limit is a depletion of 0.2 mg/L.

Every grid cell in SSM has ten vertical layers of differing thickness (Figure F1). We test whether Part A or Part B of the standard is met using the daily minima at each grid-cell-layer, as described below.

The following procedure was followed to assess water quality standard compliance for DO for the optimization scenarios:

1. Starting with the model output representing the predicted marine DO reference condition, calculate the daily minimum DO value for each grid-cell-layer within the model domain.
2. Compare that daily minimum DO reference condition value for each grid-cell-layer with the numeric criteria in Part A and Part B.
   a. If the daily minimum value for the reference condition for each grid cell-layer ($DO_{reference}$ DMin) is greater than the DO aquatic life criteria plus the human limit, then the part of the standard that is tested next is Part A (refer to Step 4).
   b. If the $DO_{reference}$ DMin is less than or equal to the DO aquatic life criteria plus the human limit, then the part of the standard that is tested next is Part B.
3. Using the model output representing the predicted marine DO response to existing conditions or any other scenario condition being tested, calculate the daily minimum DO value ($DO_{existing}$ DMin) for each grid-cell-layer within the model domain.
4. Test whether Part A of the standard is met for each grid-cell-layer:
   a. Compare each $DO_{existing}$ DMin to the Part A location specific DO concentration requirement or threshold which is the aquatic life criteria designated for each location (grid cell).
   b. If the predicted $DO_{existing}$ DMin is greater or equal to the designated aquatic life criteria, then the grid-cell-layer meets Part A of the DO water quality standard.
   c. If the predicted $DO_{existing}$ DMin is less than the designated aquatic life criteria, then the grid-cell layer does not meet Part A of the DO water quality standard.
5. Test whether Part B of the standard is met for each grid-cell-layer:
   a. The total anthropogenic depletion equals $DO_{existing}$ DMin minus the $DO_{reference}$ DMin. However, to account for the cumulative anthropogenic impact in the Part B portion of the standard, calculate a Part B threshold value (or DO concentration requirement):

      $$DO_{Part\ B} = DO_{reference}\ DMin - 0.2\ mg/\ L.$$

   b. If the predicted $DO_{existing}$ DMin is greater or equal to $DO_{Part\ B}$, then the grid-cell-layer meets Part B of the DO water quality standard.
   c. If the predicted $DO_{existing}$ DMin is less than $DO_{Part\ B}$, then the grid-cell-layer does not meet Part B of the DO water quality standard.
6. Compile the magnitudes of predicted DO noncompliances for all corresponding grid-cell-layers where either Part A or Part B of the standard is predicted not to be met, and compute the largest of the daily noncompliance magnitude for each grid cell.

7. Round the magnitude of predicted noncompliances to the nearest tenth. This precludes any noncompliance between -0.05 mg/L and zero. Values more negative than -0.05 mg/L are rounded to -0.1 mg/L.

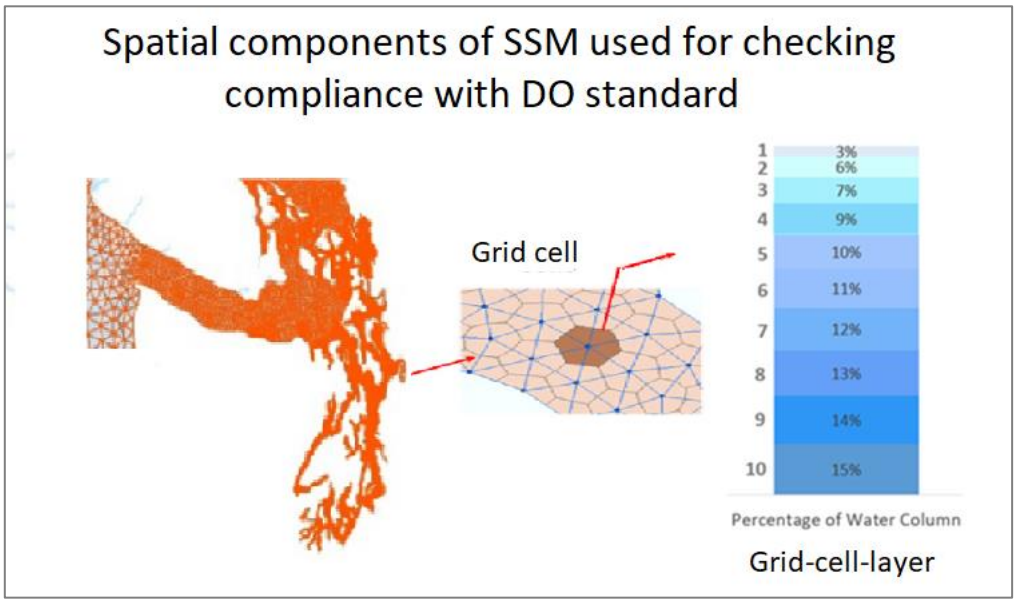

Figure F1. Grid cell and grid cell layers in SSM.

How is the DO determination for meeting water quality standards procedure for the Optimization scenarios different from that for the Bounding scenarios?

Two main differences exist between how predicted noncompliances with DO standards were computed and plotted in the Bounding Scenarios report (Ahmed et al. 2019) and how they are computed for the Optimization Scenarios. These differences are related to (1) changes in the testing algorithm to explicitly calculate the Part A and Part B thresholds referenced above for each grid-cell-layer and to include rounding of noncompliance magnitudes to 0.1 mg/l DO and (2) changes in scale for plan view maps and tables.

With respect to rounding, Ahmed et al. (2019) did not incorporate a rounding scheme, whereas in the current work, we are showing predicted noncompliances rounded to 0.1 mg/l. For example in the Bounding Scenarios Report, a 0.21 mg/L depletion has a magnitude of noncompliance of -0.01 mg/l (0.20 - 0.21 mg/l). However, in this technical memorandum, a 0.21 mg/L depletion is rounded to 0.2 mg/L, and is therefore not predicted to be in noncompliance of the criteria.

With respect to the presentation of results in the plan view maps and tables, Ahmed et al. (2019) showed the absolute magnitude of DO depletions leading to predicted noncompliances. For increased clarity in the present work, the magnitude of the predicted noncompliances relative to the water quality standard are shown instead. For Part B of the DO standard, the difference between plan view maps shown in Ahmed et al. (2019) and in this memorandum is the explicit inclusion of the human limit for lowering DO (0.20 mg/L). For example, in this memorandum, instead of presenting the full magnitude of predicted DO depletion of 0.26 mg/L, which, after rounding, leads to a predicted noncompliance due to Part B of -0.10 mg/L, the value of predicted noncompliance shown in plan view maps is -0.1 mg/L.

Appendix G – Additional Results Tables and Figures

Summary of Noncompliance Across all Scenarios

Table G1 and Table G2 summarize noncompliant days, area, and magnitude aggregated to WA waters of the Salish Sea for all modeled scenarios for the years 2006 and 2014, respectively. The tables present the absolute values for each scenario, the change in noncompliance relative to baseline or existing conditions, as well as the percent change in days and area. Negative values indicate a reduction in noncompliance (i.e. an improvement in dissolved oxygen).

Table G1. Noncompliant days, area, and DO magnitudes in WA waters of the Salish Sea under each model scenario for the year 2006, as well as well as percent changes relative to baseline levels.

Scenario	Normalized noncompliant days*	Change in normalized noncompliant days* from baseline	Percent change in normalized noncompliant days* from baseline	Noncompliant area (km2)	Change in noncompliant area from baseline (km2)	Percent change in noncompliant area from baseline (km2)	Largest magnitude of noncompliance (mg/L DO)	Change in largest magnitude of noncompliance from baseline
Scen1 South Sound Wtshds @Ref	42.4	-24.0	-36.1%	384.8	-96.7	-20.1%	-1.3	0.6
Scen1 Main Wtshds @Ref	45.8	-20.5	-31.0%	381.9	-100	-20.7%	-1.8	0.1
Scen1 Hood Wtshds @Ref	59.1	-7.27	-11.0%	436.3	-45.2	-9.4%	-1.9	0.0
Scen1 Whidbey Wtshds @Ref	45.2	-21.1	-31.8%	315.8	-166	-34.4%	-1.9	0.0
Scen1 SJF & Admiralty Wtshds @Ref	64.3	-2.09	-3.2%	470.3	-11.18	-2.3%	-1.9	0.0
Scen1 SOG & N. Bays Wtshds @Ref	63.7	-2.68	-4.0%	460.1	-21.4	-4.4%	-1.9	0.0
Scen2 South Sound @Ref	54.4	-11.9	-18.0%	443.9	-37.5	-7.8%	-1.7	0.2
Scen2 Main WWTPs @Ref	13.0	-53.3	-80.4%	177.0	-304	-63.2%	-1.7	0.2
Scen2 Hood WWTPs @Ref	66.3	-0.02	0.0%	481.5	0.00	0.0%	-1.9	0.0
Scen2 Whidbey WWTPs @Ref	53.4	-12.9	-19.5%	405.2	-76.3	-15.8%	-1.9	0.0
Scen2 SJF & Admiralty WWTPs @Ref	65.7	-0.63	-0.9%	480.0	-1.45	-0.3%	-1.9	0.0
Scen2 SOG & N. Bays WWTPs @Ref	65.7	-0.69	-1.0%	471.8	-9.68	-2.0%	-1.9	0.0
Scen3 BNR-All (annual)	19.9	-46.5	-70.0%	206.6	-275	-57.1%	-1.7	0.2
BNR-All (seasonal)	33.0	-33.4	-50.3%	302.1	-179	-37.2%	-1.8	0.1
BNR-1000 (seasonal)	39.2	-27.1	-40.9%	347.2	-134	-27.9%	-1.8	0.1
BNR-8000 (seasonal)	46.2	-20.2	-30.4%	394.1	-87.3	-18.1%	-1.9	0.0
Scen5a 15% Wtshds, BNR8	14.0	-49.1	-77.8%	142.6	-338	-70.3%	-1.5	0.5
Scen5b 40% Wtshds, BNR8	7.3	-55.9	-88.4%	60.8	-419	-87.3%	-1.2	0.8
Scen5c 40% Wtshds, BNR balanced	6.2	-57.0	-90.1%	47.6	-433	-90.1%	-1.2	0.8
Scen5d 40% Wtshds, BNR3	4.9	-58.3	-92.2%	27.8	-452	-94.2%	-1.1	0.9
Scen5e 65% Wtshds, BNR3	3.3	-59.9	-94.8%	14.1	-466	-97.1%	-0.7	1.3

Table G2. Noncompliance in days, area, and magnitudes in WA waters of the Salish Sea under each model scenario for the year 2014, as well as percent changes relative to baseline levels.

Scenario	Normalized noncompliant days*	Change in normalized noncompliant days* from baseline	Percent change in normalized noncompliant days* from baseline	Noncompliant area (km2)	Change in noncompliant area from baseline (km2)	Percent change in noncompliant area from baseline (km2)	Largest magnitude of noncompliance (mg/L DO)	Change in largest magnitude of noncompliance from baseline
Scen1 South Sound Wtshds @Ref	32.2	-18.0	-35.8%	276.6	-69.7	-20.1%	-1.0	1.0
Scen1 Main Wtshds @Ref	35.3	-15.0	-29.8%	275.4	-70.8	-20.5%	-1.9	0.1
Scen1 Hood Wtshds @Ref	46.8	-3.41	-6.8%	280.1	-66.1	-19.1%	-2.0	0.0
Scen1 Whidbey Wtshds @Ref	34.8	-15.4	-30.6%	248.4	-97.9	-28.3%	-1.9	0.1
Scen1 SJF & Admiralty Wtshds @Ref	49.9	-0.31	-0.6%	344.6	-1.63	-0.47%	-2.0	0.0
Scen1 SOG & N. Bays Wtshds @Ref	48.4	-1.87	-3.7%	305.9	-40.4	-11.7%	-1.9	0.1
Scen3 BNR-All (annual)	12.9	-37.3	-74.3%	142.5	-204	-58.8%	-1.8	0.2
BNR-All (seasonal)	24.2	-26.1	-51.9%	206.7	-140	-40.3%	-1.9	0.1
BNR-1000 (seasonal)	29.2	-21.0	-41.8%	234.7	-112	-32.2%	-1.9	0.1
BNR-8000 (seasonal)	39.8	-10.5	-20.9%	294.1	-52.1	-15.1%	-1.9	0.1
Scen5a 15% Wtshds, BNR8	7.7	-42.3	-84.6%	93.1	-247	-72.7%	-1.3	0.6
Scen5b 40% Wtshds, BNR8	3.7	-46.3	-92.5%	26.2	-314	-92.3%	-1.0	0.9
Scen5c 40% Wtshds, BNR balanced	3.0	-47.0	-93.9%	17.4	-323	-94.9%	-0.9	1.0
Scen5d 40% Wtshds, BNR3	2.7	-47.3	-94.7%	13.0	-328	-96.2%	-0.8	1.1

Figure G1 presents bar plots of percent reductions in noncompliant area and noncompliant days in different regions for all 2014 scenarios.

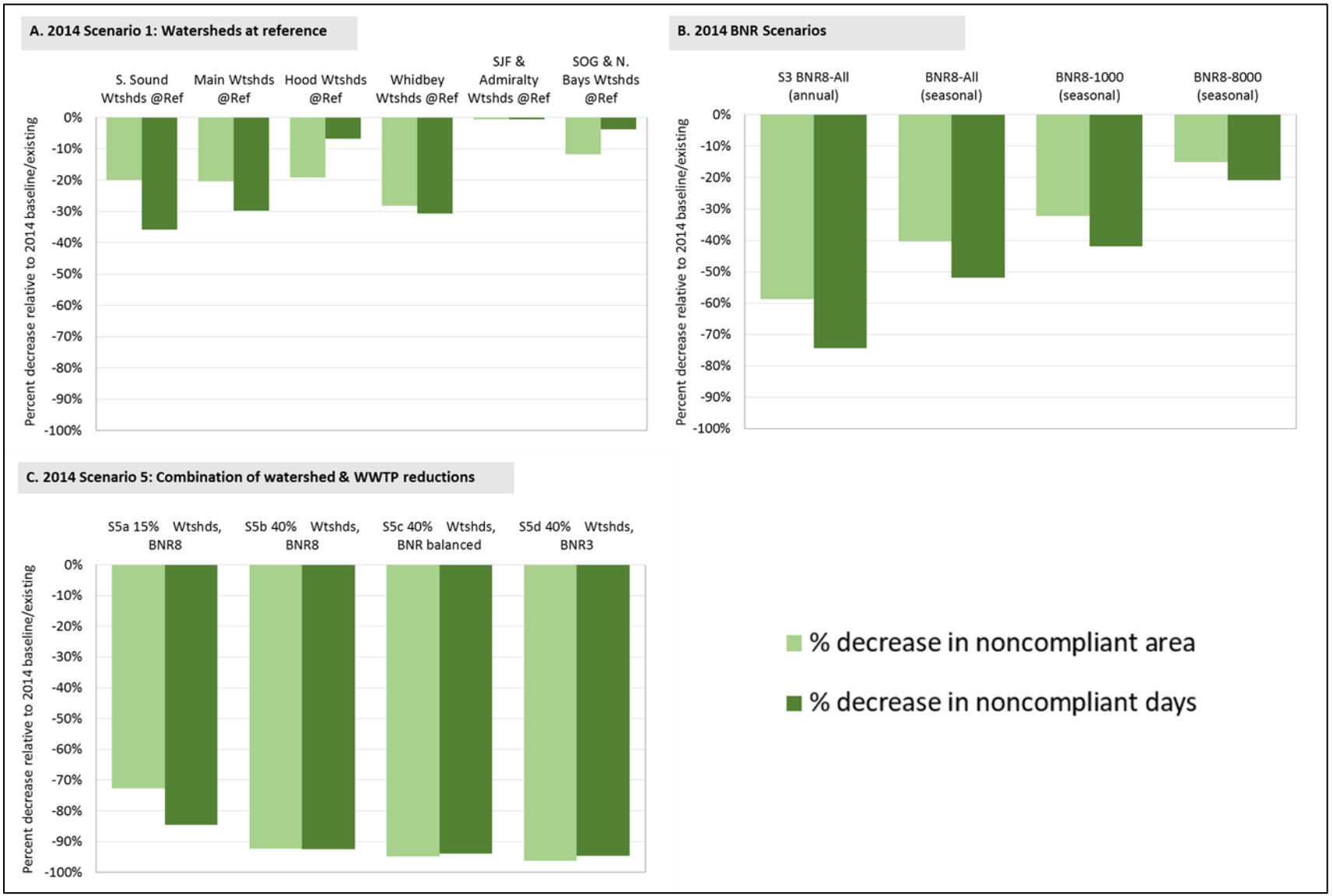

Figure G1. Percent change (decreases shown as negative values) in noncompliant days and area in WA waters of the Salish Sea from all Optimization and BNR scenarios, relative to 2014 conditions.

Scenario 1 and Scenario 2

The plan view maps for Scenario 1 in 2006 and 2014 (Figures G2, G3, and G4) show the spatial extent of the magnitude of predicted DO noncompliance under existing conditions and also when watersheds in different regions are set at reference conditions. Strait of Juan de Fuca/Admiralty Inlet, Strait of Georgia/Northern Bays, and Hood Canal regions see full reductions in predicted DO noncompliance within their boundaries when each is set to reference conditions. In all other regions, the magnitude and extent of predicted noncompliances are reduced, but not eliminated, when watersheds in that region are set to reference. The remaining predicted noncompliances in these regions persist largely due to influences from outside the focus region.

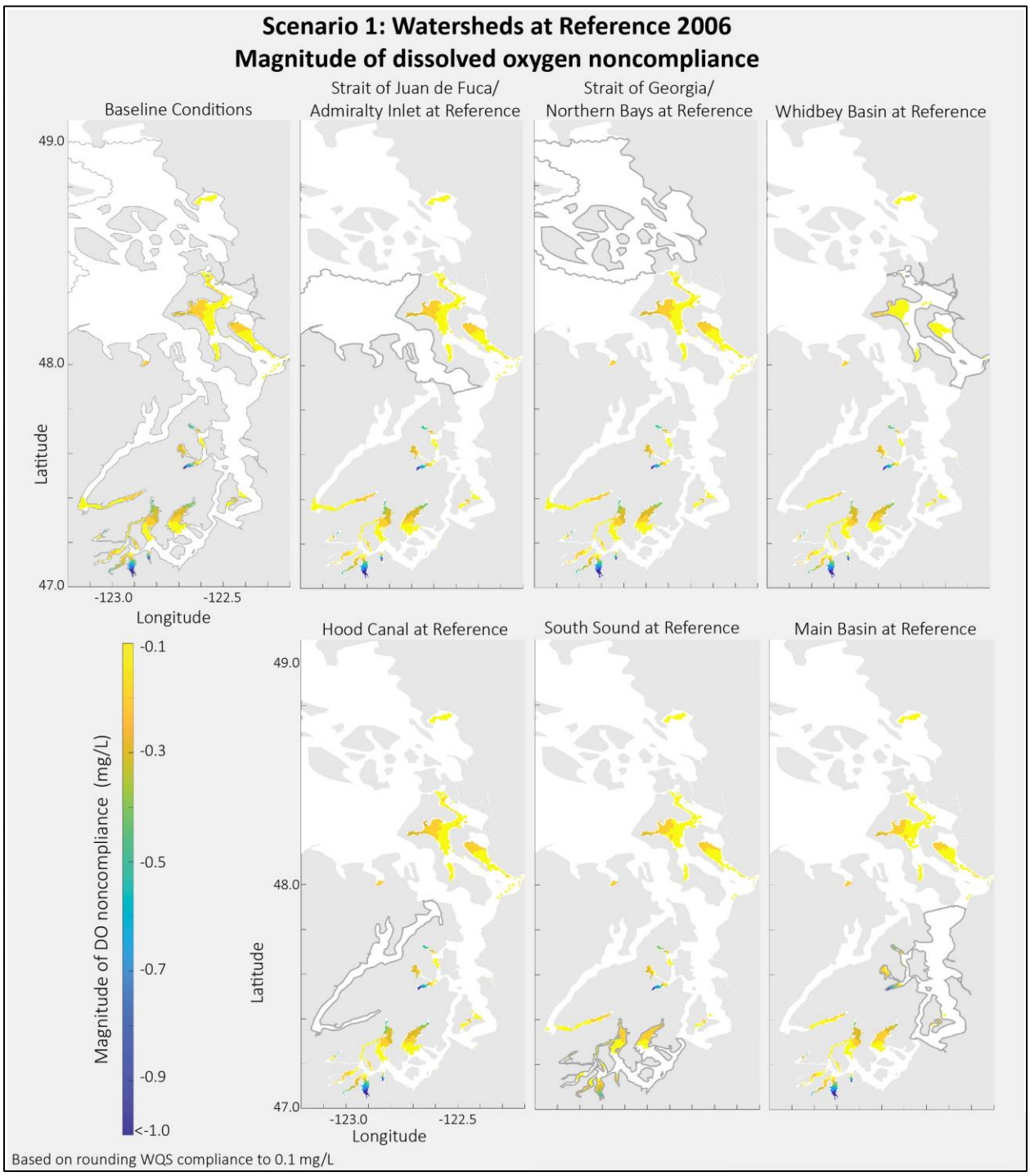

Figure G2. Plan view maps of magnitude of predicted DO noncompliance during Scenario 1 model runs (2006) with watersheds at reference conditions in different regions.

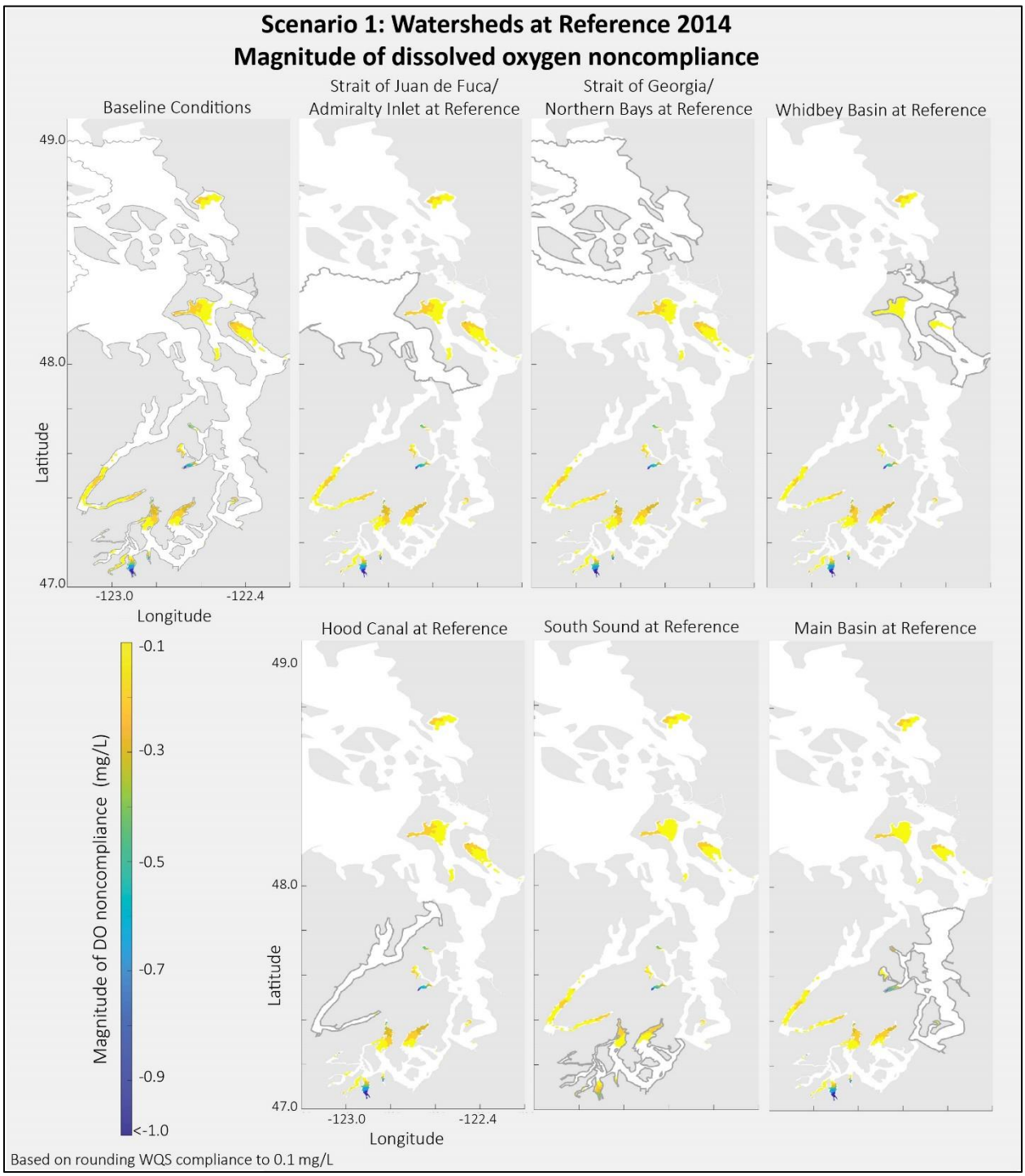

Figure G3. Plan view maps of magnitude of predicted DO noncompliance during Scenario 1 model runs (2014) with watersheds at reference conditions in different regions.

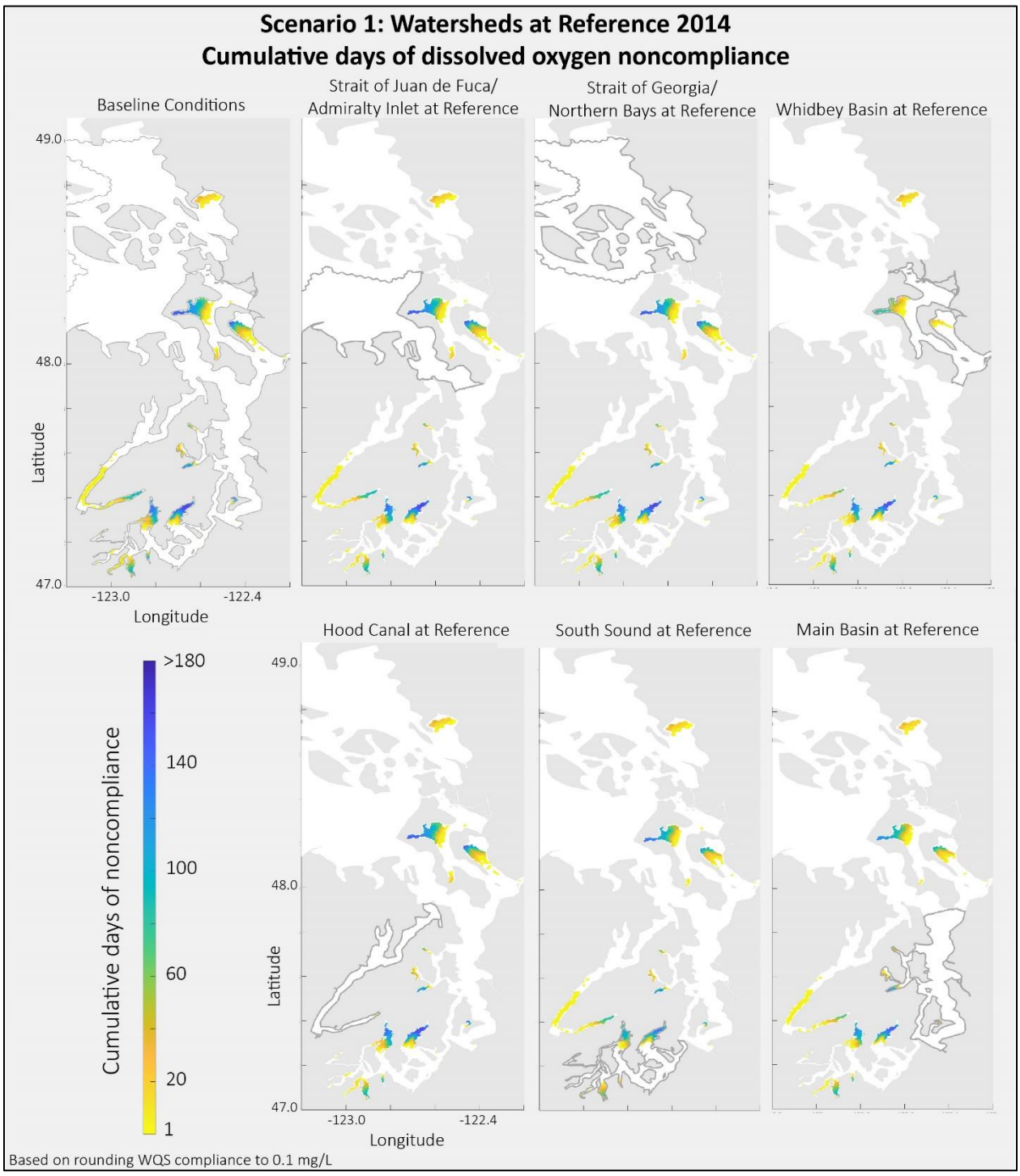

Figure G4. Plan view maps of predicted cumulative days of noncompliance during Scenario 1 model runs (2014) with watersheds at reference conditions in different regions.

The plan view maps for Scenario 2 (Figure G5) show the spatial extent of the magnitude of predicted DO noncompliance under existing conditions, when WWTPs in different regions are set at reference conditions in 2006. The largest spatial extent of reductions in DO noncompliance magnitude throughout Puget Sound is observed when the WWTPs in the Main Basin are set at reference conditions. There is not a strong spatial difference in the magnitude of predicted DO noncompliance when WWTPs in the following regions are set to reference conditions: Strait of Juan de Fuca/Admiralty Inlet, Strait of Georgia/Northern Bays, and Hood Canal.

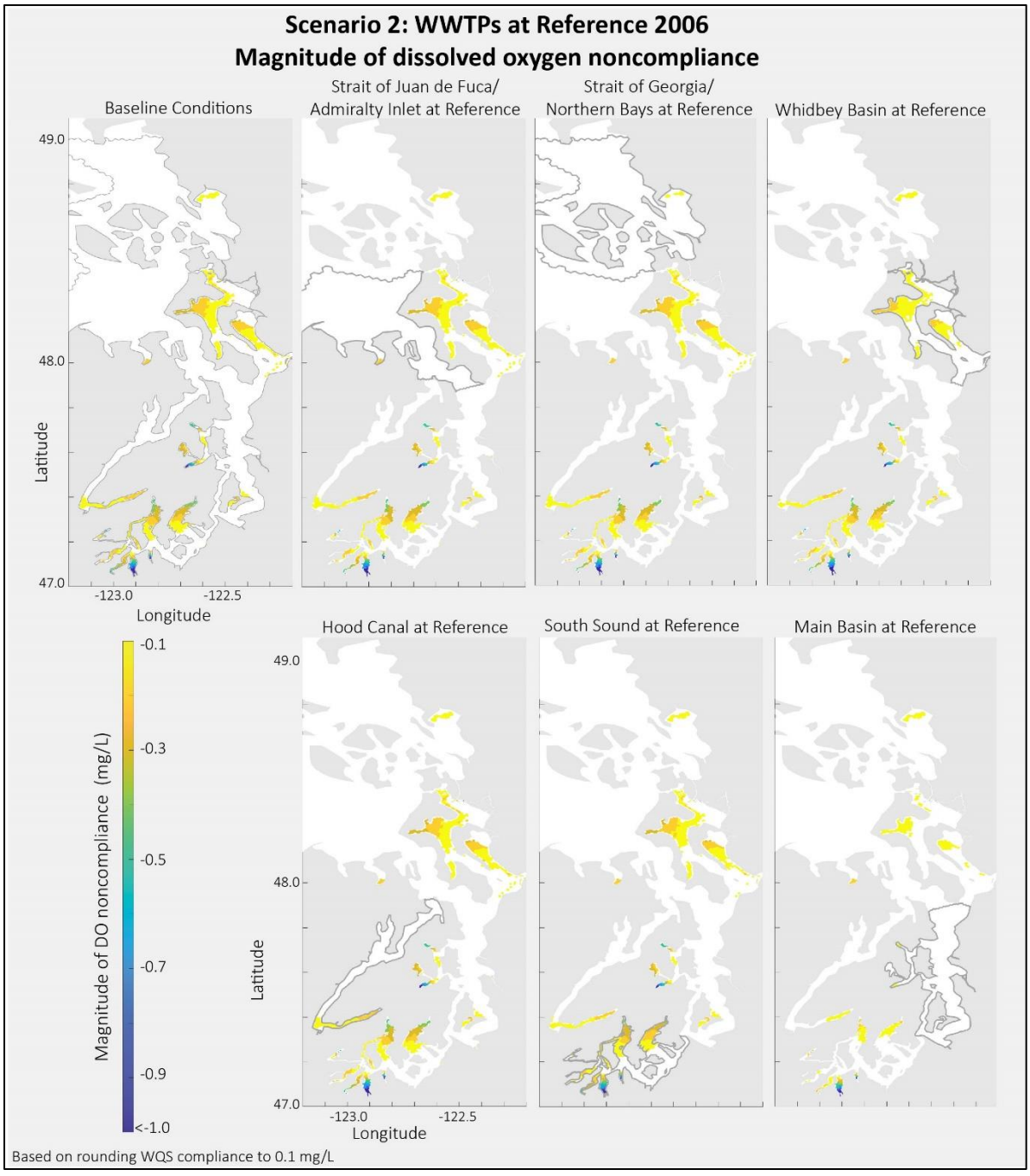

Figure G5. Plan view maps of magnitude of predicted DO noncompliance during Scenario 2 model runs (2006) with WWTPs at reference conditions in different regions.

Figures G6 shows results of Scenario 1 in terms of percentage decrease (relative to 2014 baseline levels) in predicted noncompliant days and area *within* each of the six regions with respect to all others. The more negative the magnitude of the percent decrease in predicted noncompliance, the greater the improvement. Similar to the 2006 Scenario 1 results, these figures show that watershed nutrient reductions in Main Basin, South Sound, and Whidbey Basin influence predicted compliance outside of their respective regions, but watershed reductions in Hood Canal, SJF & Admiralty, and SOG and N. Bays primarily only influence predicted compliance within the regions where nutrients are reduced.

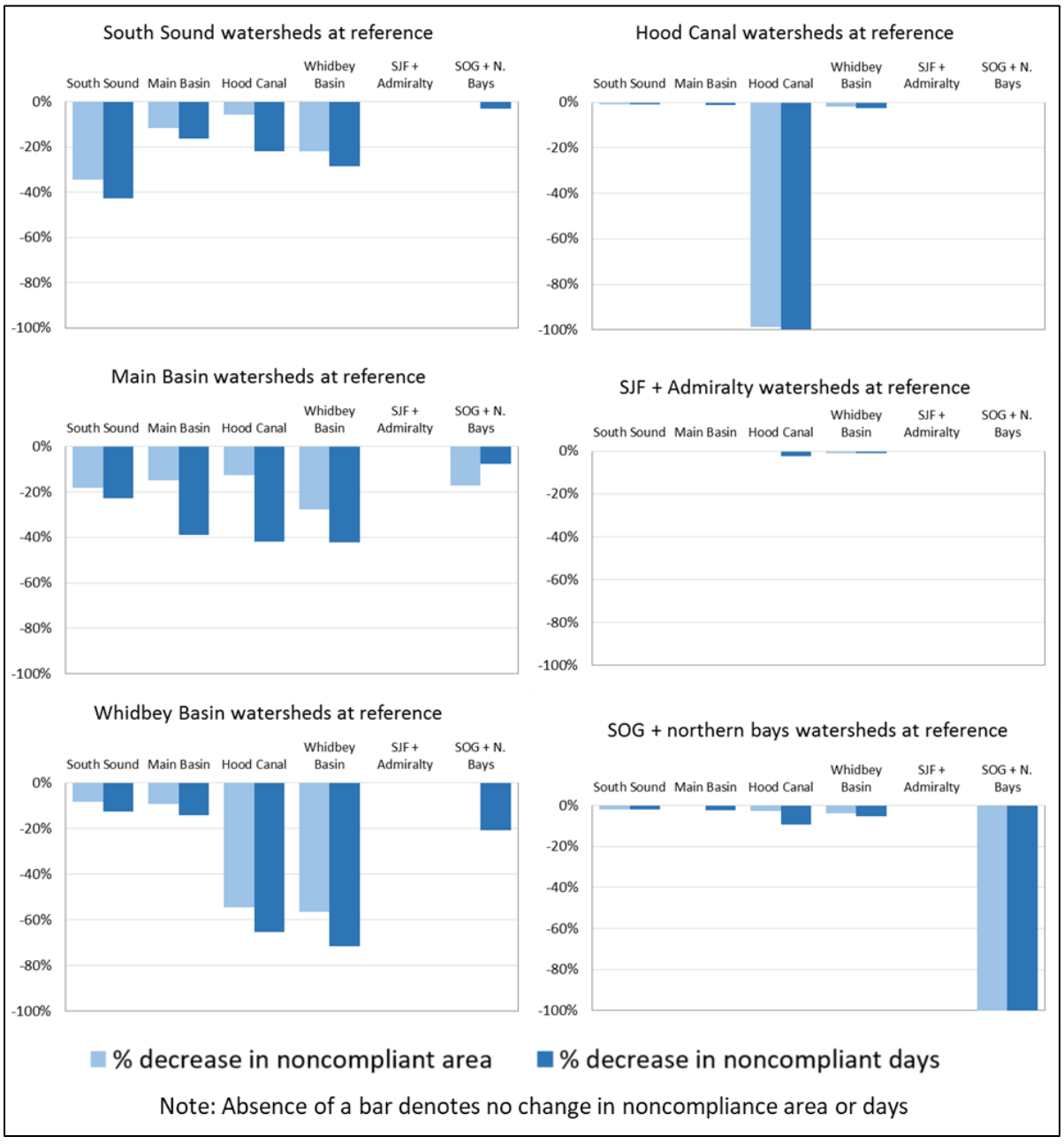

Figure G6. Percent change (decreases shown as negative values) in predicted noncompliant days and area within each region from Scenario 1 runs, when watersheds each of the six regions are set to reference conditions in 2014.

Setting *watershed* nutrient loads to reference levels in South Sound and Whidbey Basin result in reductions in the peak (or worst) magnitude of noncompliance predicted in these regions in both 2006 and 2014. Setting watershed loads to reference in SJF & Admiralty and SOG & N. Bays eliminates predicted noncompliance within these locations in both years (blue bars in Figure G6 and Figure G7).

The peak magnitude of predicted noncompliance in Main Basin is not reduced by watershed reductions to the Main Basin in 2006, and only slightly reduced in 2014 (blue bar in plot for Main Basin in Figure G7 and G8). However, this peak is reduced significantly when WWTPs nutrient loads in this basin are set to reference levels in 2006 (see orange bar in center left plot for Main Basin in Figure G7). Such a large improvement in predicted magnitude of compliance is most likely due to reductions from local sources *within* embayments.

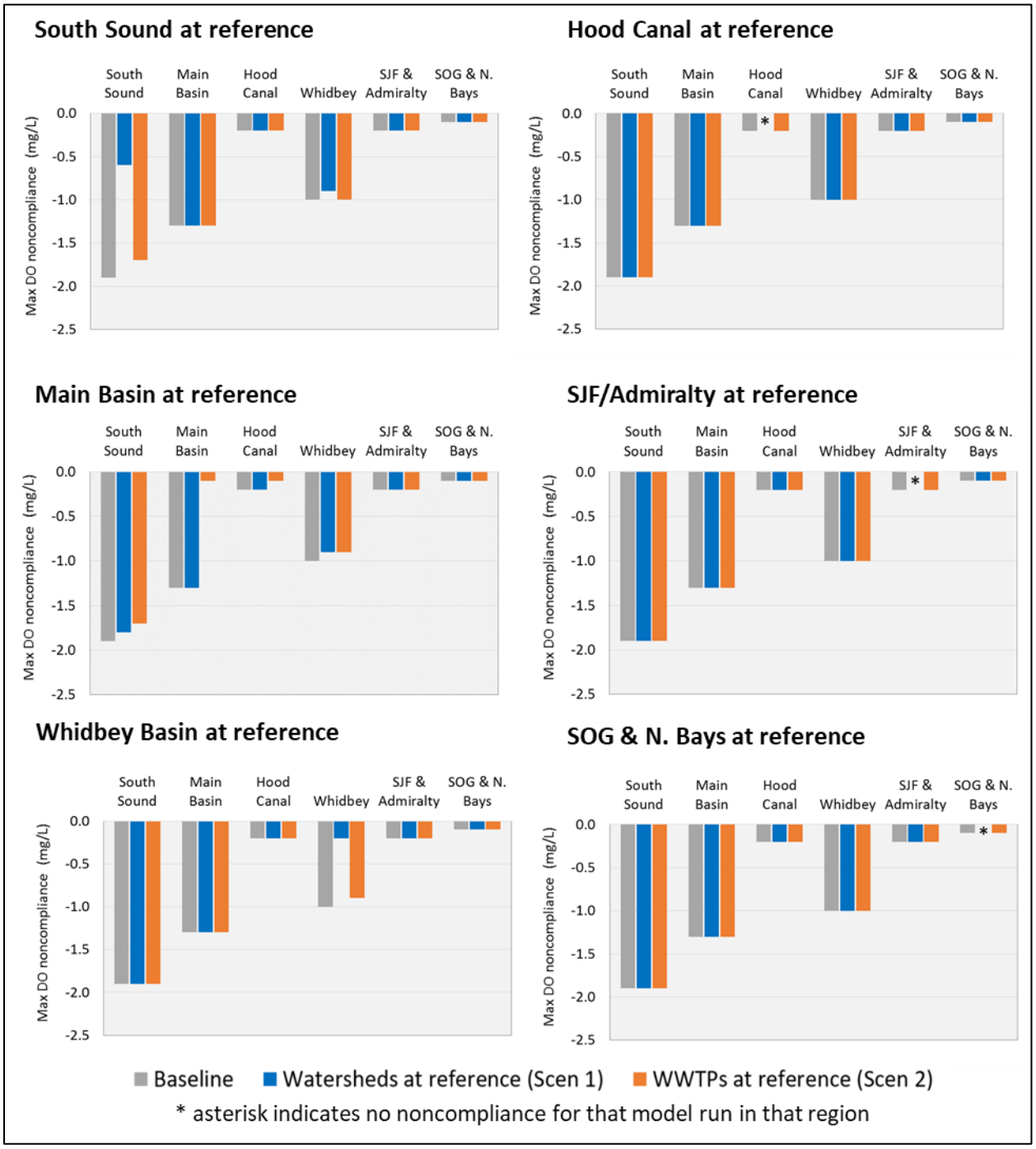

Figure G7. Maximum predicted noncompliance magnitude in each region in 2006 as a response to setting anthropogenic nutrient loads in watersheds to reference (blue) and WWTP to reference (orange) in different regions, compared to baseline noncompliance (grey).

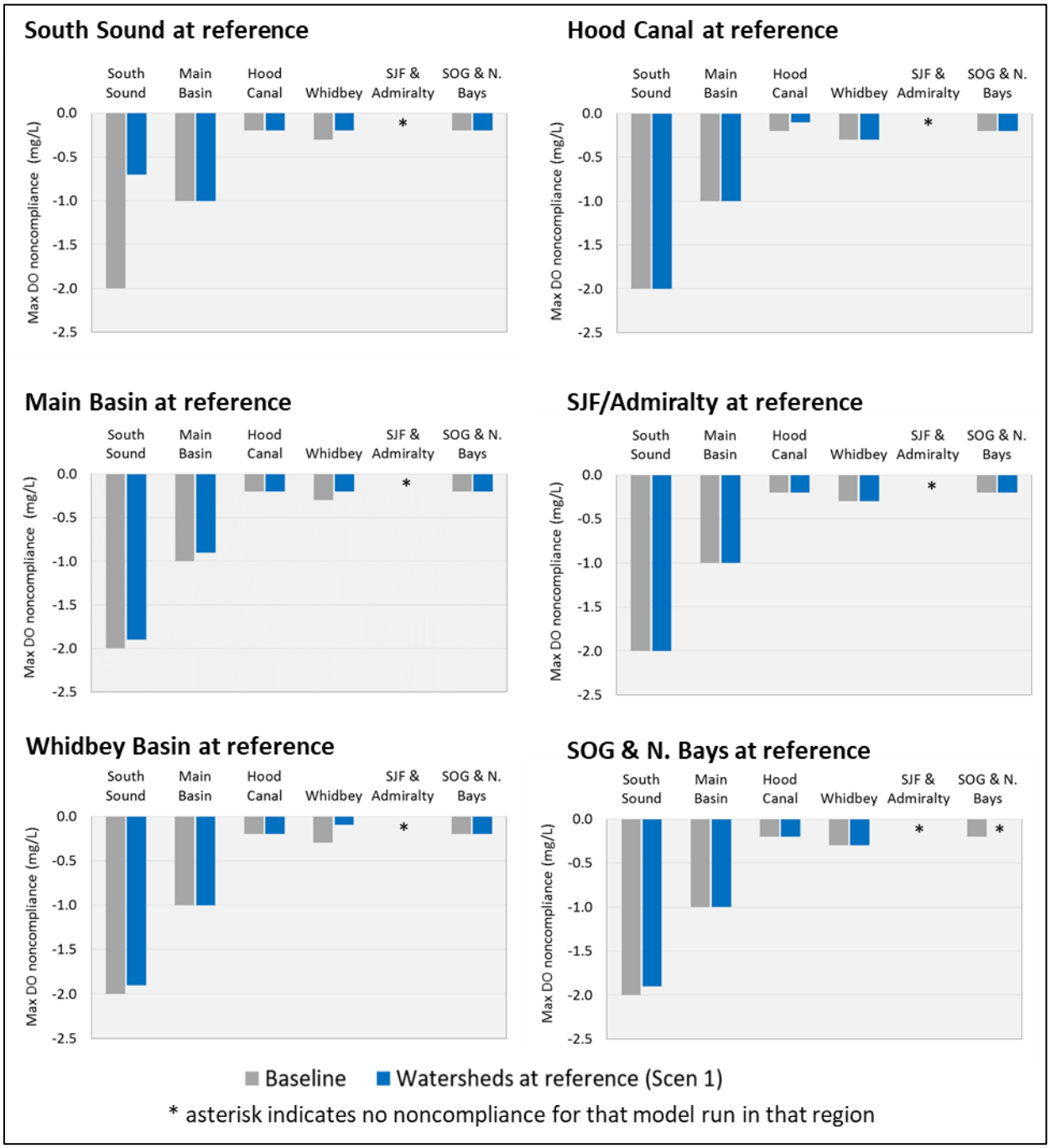

Figure G8. Maximum predicted noncompliance magnitude in each region in 2014 as a response to setting anthropogenic nutrient loads in watersheds to reference (blue) within different regions, compared to baseline noncompliance (grey).

BNR Scenarios

The plan view maps show the spatial results from Scenario 3 during 2006 and 2014 (Figures G9 and G10, respectively). The largest reductions in both cumulative days of noncompliance and magnitude of DO noncompliance are observed when BNR is applied annually at all WWTPs. These reductions are most prominent in Whidbey Basin, Main Basin, South Sound, and Hood Canal.

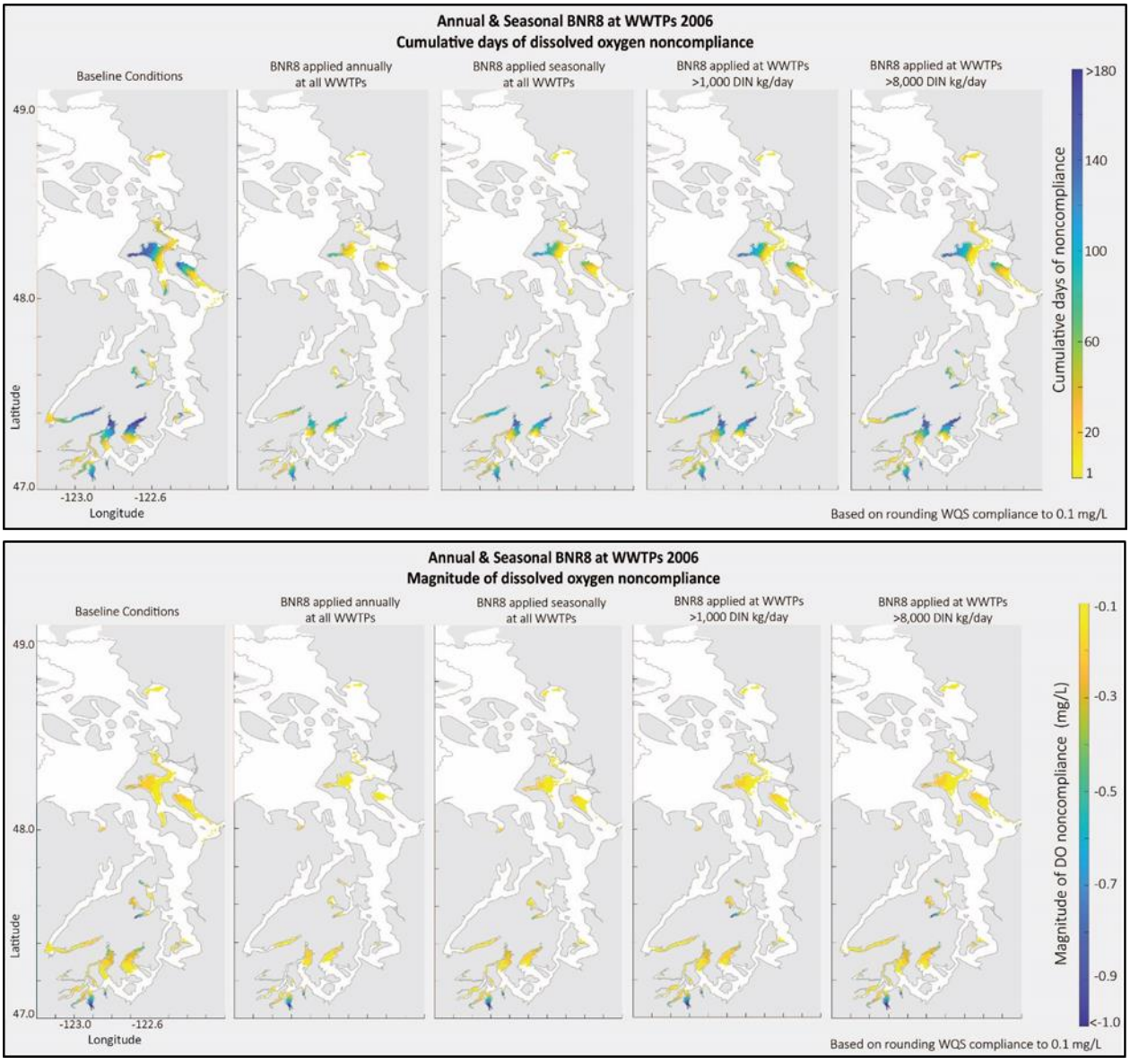

Figure G9. Plan view maps of cumulative days of predicted DO noncompliance (above) and magnitude of DO noncompliance (below) during Scenario 3 runs (2006).
Seasonal BNR is applied April–October.

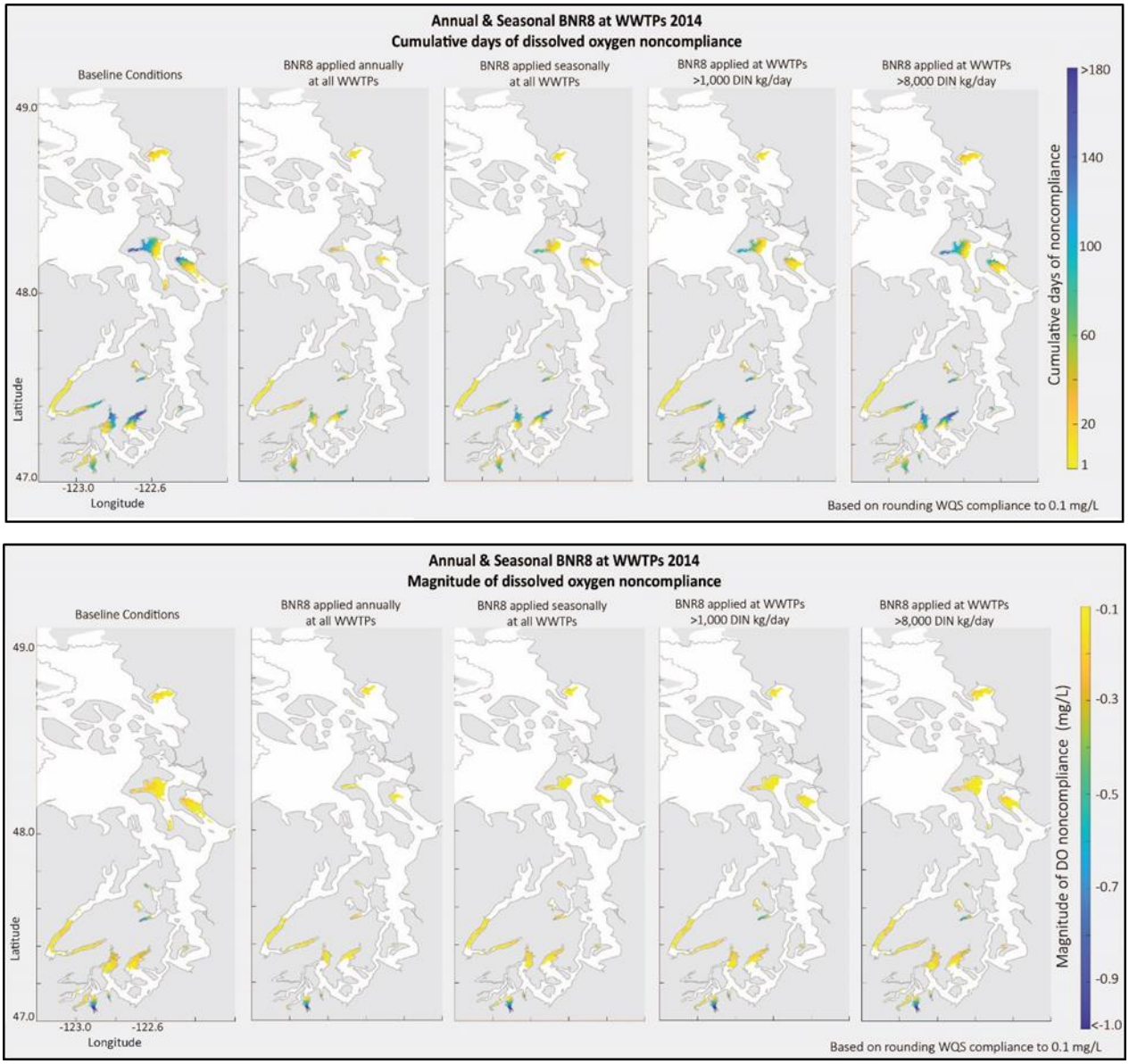

Figure G10. Plan view maps of cumulative days of predicted DO noncompliance (above) and magnitude of DO noncompliance (below) during Scenario 3 runs (2014).
Seasonal BNR is applied April–October.

Scenario 4: Effect of Future Wastewater Flows

Figure G11 shows plan view results of DO noncompliance days and magnitude under Scenario 4, compared to 2014 conditions. An increase in wastewater flows and corresponding nutrient loads result in an increase in the number of predicted noncompliant days, the magnitude of predicted noncompliance, and expand the predicted areas noncompliance. These increases are greater in under the '2040 high WWTP flows' scenario than in the '2040 low WWTP flows' scenarios.

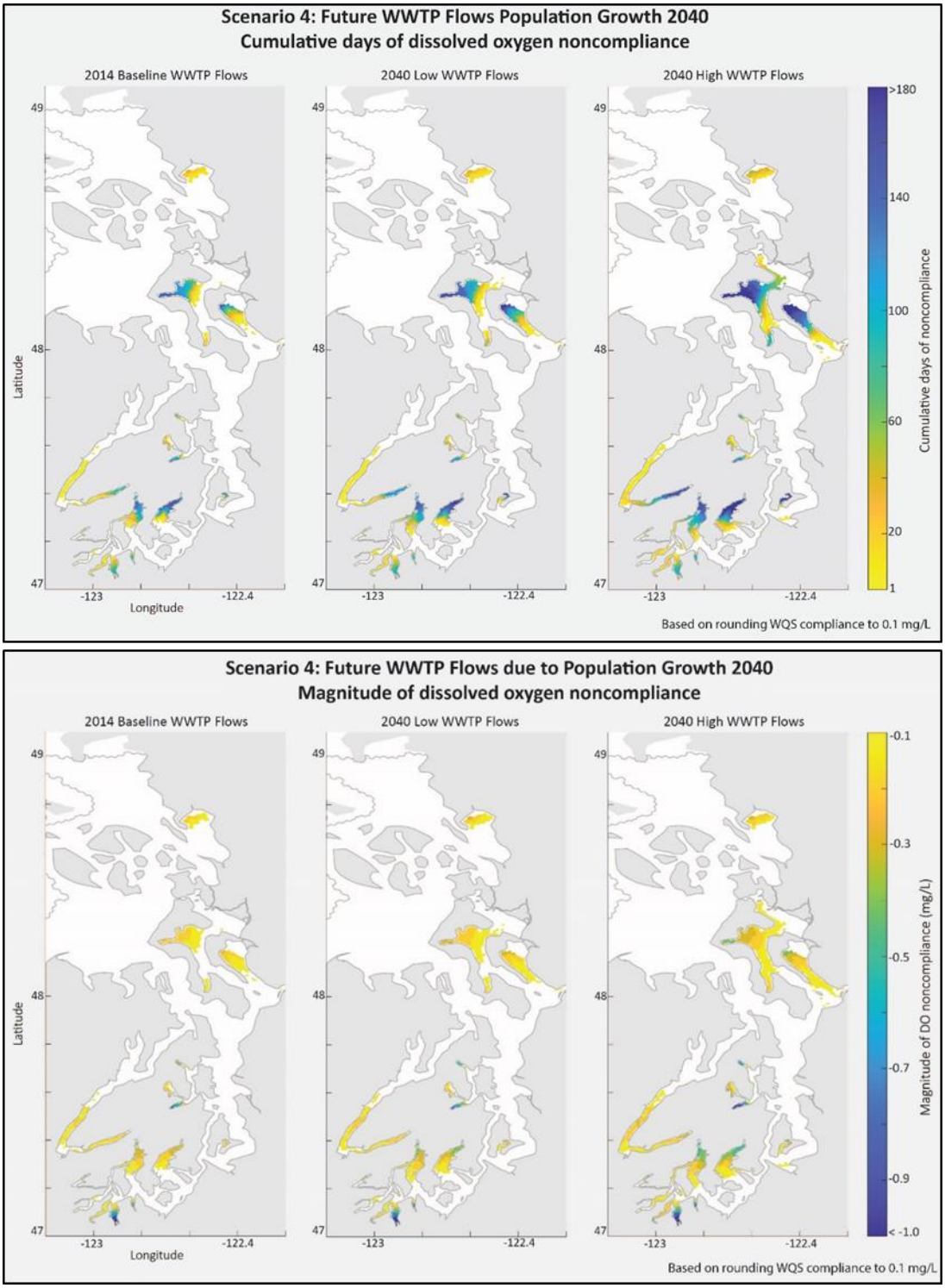

Figure G11. Plan view maps of cumulative days of predicted DO noncompliance (top) and predicted magnitude of DO noncompliance (bottom) during Scenario 4 future WWTP flows due projected future wastewater flows in 2040.

Appendix H – Water Quality Binders

Appendix H (H1-H4) is available as a separate file, a 325-page pdf

- Appendix H1 – Marine Station Locations and Changes to Observed Database
- Appendix H2 – How to Read Time-Depth Plots
- Appendix H3 – WQ Binders 2006
- Appendix H4 – WQ Binders 2014

References

Ahmed, A., G. Pelletier, M. Roberts, and A. Kolosseus. 2014. South Puget Sound Dissolved Oxygen Study: Water Quality Model Calibration and Scenarios. Publication 14-03-004. Washington State Department of Ecology, Olympia. https://apps.ecology.wa.gov/publications/SummaryPages/1403004.html.

Ahmed A., C. Figueroa-Kaminsky, J. Gala, T. Mohamedali, G. Pelletier, and S. McCarthy. 2019. Puget Sound Nutrient Source Reduction Project, Volume 1: Model Updates and Bounding Scenarios. Publication 19-03-001. Washington State Department of Ecology, Olympia. https://apps.ecology.wa.gov/publications/SummaryPages/1903001.html

Arndt, S., B.B. Jørgensen, D.E. LaRowe, J.J. Middelburg, R.D. Pancost, and P. Regnier. 2013. Quantifying the degradation of organic matter in marine sediments: A review and synthesis. Earth-Science Reviews. Vol. 123 (August 2013), pp. 53-86. https://doi.org/10.1016/j.earscirev.2013.02.008.

Bakun, Coastal Upwelling Indices, West Coast of North America, 1946-1971,NOAA Technical Report, June, 1973

Bennett, K.E., Werner, A.T. and Schnorbus, M., 2012. Uncertainties in hydrologic and climate change impact analyses in headwater basins of British Columbia. *Journal of Climate*, *25*(17), pp.5711-5730.

Chassignet, E.P., Smith, L.T., Halliwell, G.R. and Bleck, R., 2003. North Atlantic simulations with the Hybrid Coordinate Ocean Model (HYCOM): Impact of the vertical coordinate choice, reference pressure, and thermobaricity. *Journal of Physical Oceanography*, *33*(12), pp. 2504-2526.

Chassignet, E.P., Hurlburt, H.E., Smedstad, O.M., Halliwell, G.R., Hogan, P.J., Wallcraft, A.J., Baraille, R. and Bleck, R., 2007. The HYCOM (hybrid coordinate ocean model) data assimilative system. *Journal of Marine Systems*, *65*(1-4), pp. 60-83.

Cummings, J.A. and Smedstad, O.M., 2013. Variational data assimilation for the global ocean. In *Data Assimilation for Atmospheric, Oceanic and Hydrologic Applications (Vol. II)* (pp. 303-343). Springer, Berlin, Heidelberg.

Davenne, E. and Masson, D., 2001. Water Properties in the Straits of Georgia and Juan de Fuca (British Columbia, Canada).). *Institute of Ocean Sciences*.

Déry, S.J., Hernández-Henríquez, M.A., Owens, P.N., Parkes, M.W. and Petticrew, E.L., 2012. A century of hydrological variability and trends in the Fraser River Basin. *Environmental Research Letters*, *7*(2), p. 024019.

Figueroa-Kaminsky, C., 2018. Predicting Puget Sound's organic carbon—and why we need enhanced monitoring, presentation at the Salish Sea Ecosystem Conference. Washington State Department of Ecology, Olympia.

Hedges, J. I., R. G. Keil, and R. Benner. 1997. What happens to terrestrial organic matter in the ocean? Org. Geochem. Vol. 27, No. 5/6, pp. 195-212.

Hickey, B.M. and Banas, N.S., 2003. Oceanography of the US Pacific Northwest coastal ocean and estuaries with application to coastal ecology. *Estuaries*, *26*(4), pp. 1010-1031.

Hickey, B., Banas, N., & MacCready, P. (2013). Marine spatial planning report: November 1, 2012- June 30, 2013. Retrieved from https://www.msp.wa.gov/wpcontent/uploads/2013/07/UWOceanography_FinalReport.pdf

Hopkins, B. 2021. Personal communication with C. Figueroa-Kaminsky. Washington State Department of Ecology, Olympia.

Kang, D.H., Shi, X., Gao, H. and Déry, S.J., 2014. On the changing contribution of snow to the hydrology of the Fraser River Basin, Canada. *Journal of Hydrometeorology*, *15*(4), pp. 1344-1365.

Khangaonkar, T., B. Sackmann, W. Long, T. Mohamedali, and M. Roberts. 2012. Simulation of annual biogeochemical cycles of nutrient balance, phytoplankton bloom(s), and DO in Puget Sound using an unstructured grid model. Ocean Dynamics 62(9): 1353–1379.

Khangaonkar, T., W. Long, and W. Xu. 2017. Assessment of circulation and inter-basin transport in the Salish Sea including Johnstone Strait and Discovery Islands pathways, Ocean Modelling, 109:11-32. doi: 10.1016/j.ocemod.2016.11.004

Khangaonkar, T., A. Nugraha, W. Xu, W. Long, L. Bianucci, A. Ahmed, T. Mohamedali, and G. Pelletier. 2018. Analysis of hypoxia and sensitivity to nutrient pollution in Salish Sea. Journal of Geophysical Research: Oceans 123: 4735–4761. https://doi.org/10.1029/2017JC013650.

Lavtar, K., Bezak, N. and Šraj, M., 2020. Rainfall-Runoff Modeling of the Nested Non-Homogeneous Sava River Sub-Catchments in Slovenia. *Water*, *12*(1), p. 128.

Loukas, A., and L. Vasiliades. 2014. Streamflow simulation methods for ungauged and poorly gauged watersheds. Natural Hazards and Earth System Sciences 14, no. 7 (2014): 1641.

Mays, L.W., 2010. *Water resources engineering*. John Wiley & Sons, pp. 286.

McCarthy, S. 2019. Puget Sound Nutrient Synthesis Report, Part 2: Comparison of Watershed Nutrient Load Estimates. Publication 19-03-019. Washington State Department of Ecology, Olympia. https://apps.ecology.wa.gov/publications/SummaryPages/1903019.html

Metzger, E.J., Smedstad, O.M., Wallcraft, A.J., Posey, P.G., and Franklin, D.S., 2013. *An Update on the 1/12 deg Global HYCOM Effort*. NAVAL RESEARCH LAB STENNIS DETACHMENT STENNIS SPACE CENTER MS.

Metzger, E.J., Helbert, R., Hogan, P., Posey, P., Thoppi, P., Townsend, T., Wallcraft, A., Smedstad, O., Franklin, D.l., Zamudo_Lopez, L., Phelps, M., 2017. Global Ocean Forecast System 3.1 Validation Testing, Naval Research Laboratory Report, United States Navy, NRL/MR/7320--17-9722

Mohamedali, T., M. Roberts, B. Sackmann, and A. Kolosseus, 2011. Puget Sound dissolved oxygen model nutrient load summary for 1999–2008. Publication 11-03-057. Washington State Department of Ecology, Olympia. https://apps.ecology.wa.gov/publications/SummaryPages/1103057.html

Moriasi, D.N., Arnold, J.G., Van Liew, M.W., Bingner, R.L., Harmel, R.D. and Veith, T.L., 2007. Model evaluation guidelines for systematic quantification of accuracy in watershed simulations. *Transactions of the ASABE*, *50*(3), pp.885-900

NOAA, web site accessed 2/25/2021 https://oceanwatch.pfeg.noaa.gov/products/PFELData/upwell/monthly/upindex.mon

Office of Financial Management (OFM). 2018. County Growth Management Population projections by Age and Sex: 2010-40. https://ofm.wa.gov/sites/default/files/public/dataresearch/pop/GMA/projections17/GMA_2017_county_pop_projections.pdf

Oudin, L., C. Michel, and F. Anctil, 2005. Which potential evapotranspiration input for a lumped rainfall-runoff model: Part 1—Can rainfall-runoff models effectively handle detailed potential evapotranspiration inputs? J. Hydrol., 303(1–4), 275–289.

Pike, R.G. 1998. Current limitations of hydrologic modeling in BC: An examination of the HSPF, TOPMODEL, UBCWM and DHSVM hydrologic simulation models, BC Data Resources and Hydrologic-Wildfire Impact Modeling. PhD diss., University of Victoria.

Pitcher, G.C., Figueiras, F.G., Hickey, B.M., and Moita, M.T., 2010. The physical oceanography of upwelling systems and the development of harmful algal blooms. *Progress in oceanography*, *85*(1-2), pp.5-32.

Roberts, M., T. Mohamedali, B. Sackmann, T. Khangaonkar, and W. Long (PNNL). 2014. Puget Sound and the Straits Dissolved Oxygen Assessment: Impacts of Current and Future Human Nitrogen Sources and Climate Change through 2070. Publication 14-03-007. Washington State Department of Ecology, Olympia. https://apps.ecology.wa.gov/publications/SummaryPages/1403007.html

Roberts, M., Pelletier, G., Ahmed, A., 2015. Deschutes River, Capitol Lake, and Budd Inlet Total Maximum Daily Load Study: Supplemental Modeling Scenarios. Publication 15-03-002. Washington State Department of Ecology, Olympia. https://apps.ecology.wa.gov/publications/SummaryPages/1503002.html

Sackmann, B., 2011. Deschutes River Continuous Nitrate Monitoring. Publication 11-03-030. Washington State Department of Ecology, Olympia. https://apps.ecology.wa.gov/publications/SummaryPages/1103030.html

Simenstad, C. A., R. C. Wissmar, 1985. $\delta^{13}C$ evidence of the origins and fates of organic carbon in Lavtar, K., Bezak, N. and Šraj, M., 2020. Rainfall-Runoff Modeling of the Nested Non-Homogeneous Sava River Sub-Catchments in Slovenia. *Water*, *12*(1), p.128.

Wise, D.R., and H.M. Johnson. 2013. Application of the SPARROW model to assess surface-water nutrient conditions and sources in the United States Pacific Northwest. U.S. Geological Survey Scientific Investigations Report 2013–5103. http://pubs.usgs.gov/sir/2013/5103/.

Xu, J., Lowe, R., Ivey, J. Pattiaratchi, C., Jones, N. and Brinkman R.(2013) Dynamics of the summer shelf circulation and transient upwelling off Ningaloo Reef, Western Australia, Journal of Geophysical Research , Oceans, Vol. 118, 1099-1125.

Acronyms

BNR	biological nitrogen removal
DFO	Department of Fisheries and Oceans Canada
DIN	dissolved inorganic nitrogen
DO	dissolved oxygen
DOC	dissolved organic carbon
Ecology	Washington State Department of Ecology
et al.	and others
HYCOM	Hybrid Coordinate Ocean Model
MLLW	mean lower low water
NOAA	National Oceanic and Atmospheric Administration
OBC	ocean boundary condition
OFM	Office of Financial Management
POC	particulate organic carbon
PSNSRP	Puget Sound Nutrient Source Reduction Project
SJF	Strait of Juan de Fuca
SOG	Strait of Georgia
SSM	Salish Sea Model
TN	total nitrogen
TOC	total organic carbon
WA	Washington State
WQS	water quality standard
WWTP	wastewater treatment plant